MICRODYNAMICS OF STRUCTURED SOLIDS

by

© MARTIN OSTOJA-STARZEWSKI

A thesis submitted to the Faculty of Graduate Studies and Research in partial fulfillment of the requirements for the degree of Doctor of Philosophy

Micromechanics Research Laboratory
Department of Mechanical Engineering
McGill University
Montreal, Canada

February, 1983

MICRODYNAMICS OF STRUCTURED SOLIDS

by

Martin Ostoja-Starzewski

Department of Mechnical Engineering
McGill University
Montreal, Canada

Ph.D. Thesis
February 1983

ABSTRACT

In this thesis a microdynamics theory of structured solids is formulated on the basis of probabilistic functional analysis. The theory which is developed on the principles of probabilistic micro-mechanics, introduces from the onset spatial and temporal scales relevant in the dynamic analysis. A general formulation of the micro-dynamics of a three-dimensional solid is given in terms of an abstract dynamical system; the analysis is then specialized to the kinematic subspace of the general state space, whereby the former is found to possess the topological structure of a Hilbertian-Sobolev space.

The abstract dynamical system in the microdynamics theory is developed explicitly for the wave propagation in a semi-infinite bar of a polycrystalline solid with an arbitrary cross-section. The micr-structure of the solid is taken to consist of cubic grains with random physical properties. The existence of an internal and a macroscopic time is postulated, which permits the formulation of the evolution of the wave motion first in a one-dimensional solid by means of a four parametric Markovian operator having a semi-group property. This model of the cubic solid structure is shown to be asymptotically equivalent to a "generalized wave equation" of the continuum theory. A more general model of the wavefront evolution for a three-dimensional solid is then given in terms of a super-martingale (parametrized by the macro-

time) on a generalized random field.

It is shown that numerical results for the wave propagation in a discrete solid in accordance with the new microdynamics theory can be obtained by the application of the Monte-Carlo simulation method. A comparison of these results with known classical and random continuum theories is given.

SOMMAIRE

Dans cette thèse, la théorie de microdynamique des solides à structure organisée est formulée d'après les fondements de l'analyse fonctionelle probabilite. La théorie, developpée sur les principes de la micromécanique probabilite, établit dès le début les échelles spatiales et temporelles qui sont pértinentes à l'analyse dynamique. La formulation générale de la microdynamique par un solide tri-dimensionel est presentée par un système dynamique abstrait. Enfin, l'analyse est introduite au sous-espace cinématique de l'espace générale d'état, dont la première se révèle d'être d'une structure topologique d'un espace Hilbert-Sobolev.

Le système dynamique abstrait de la théorie de la microdynamique est developpé sans forme explicite pour la propagation des ondes dans un solide polycrystallin avec une section arbitraire. On attribue à la microstructure du solide des grains cubiques avec des propriétés physiques aléatoires. L'existence d'un temps interne et d'un temps macroscopique est postulée, ce qui permet la formulation de l'évolution d'ondes, tout d'abord dans un solide uni-dimensionel grâce à un opérateur Markovien possédant la propriété d'un semi-groupe. Ce modèle d'un solide à structure cubique se révèle d'être équivalent à l'asymptote de l'équation généralisée d'onde de la théorie d'un continu. Un modèle plus générale de l'évolution du front d'onde, dans un solide tri-dimensionel, est exprimée grâce à une sur-martingale (avec le macro-temps comme paramètre) dans un champs aléatoire généralisé.

On a démontré que les résultats numériques pour la propagation des ondes dans un solide discret en accord avec la nouvelle théorie

de microdynamique, peuvent être obtenus en appliquant la méthode de simulation de Monte-Carlo. Une comparaison entre les résultats connus de la théorie classique et de ceux de la théorie aléatoire du continu, est fournie.

ACKNOWLEDGEMENTS

The author would like to express his sincere thanks to his research director Professor D.R. Axelrad for the guidance, numerous discussions and continuous encouragement throughout the course of this work.

The author would also like to express his appreciation to Mr. B.K. Biswas for the assistance given to him in the execution of the Monte Carlo computer simulation and to Dr. K. Rezai for his help in the graphical representation of the results. He also wishes to thank Mr. J. Turski for many critical discussions concerning some of the mathematical aspects of this thesis.

The author also benefited in the early stage of the research, from discussions with Professor I. Kunin, University of Houston, and Professor A. Chudnovski, Case Western Reserve University.

Special thanks are due to the Natural Sciences and Engineering Research Council of Canada and the Michael Markiewicz Memorial Scholarship Fund which made the work presented in this thesis possible.

Finally, the author would like to thank Mr. A. Taras for the help in preparing the French version of the abstract and Miss J. Armour for the typing of the manuscript.

TABLE OF CONTENTS

LIST OF SYMBOLS

Latin Letters

c	wave propagation velocity
c_L, c_T	propagation velocity of longitudinal, transverse waves
d	crystal size
$\underset{\sim}{e}$	unit vector in the direction of motion
i	subscript denoting the incident wave quantities
i	superscript denoting the internal quantities at a microscale
$p(\cdot)$	probability density
$\underset{\sim}{p}$	unit vector in the direction of propagation
r	bond distance
r	subscript denoting the reflected wave quantities
s	generalized time
s	superscript denoting the surface quantities at a microscale
t	time, internal time
$\bar{t}$	macroscopic time (macro-time)
t_m	microscopic time at the atomic scale
t_r	subscript denoting the transmitted wave quantities
$\underset{\sim}{u}$	deformation
$\underset{\sim}{v} \equiv \dot{\underset{\sim}{u}}$	deformation rate (wave velocity vector)
$C(\cdot)$	space of continuous functions
$C(\cdot)$	transmission operator
C_r, C_{tr}	reflection and transmission coefficients
E	event set
$^{\alpha}E$	Young's modulus
$E\{\cdot\}$	mathematical expectation (average, mean)

G	shear modulus
$H^m(X)$	Hilbertian-Sobolev space on X
I	identity operator
L	subscript or superscript denoting the longitudinal wave quantities
M	macroscopic body domain
M	material operator
P	probability or probability distribution
P	pressure pulse
S_k	sequences in M $(k=1,\ldots,K)$
T	transformation on the state space
T	subscript or superscript denoting the transverse (shear) wave quantities
$^1T(\bar{t})$	semi-group operator on the $C(\mathcal{D}_L)$ space
$^2T(t)$	semi-group operator on the $C(\bar{V})$ space
$W_p^m(X)$	Sobolev space on X
(X_1, X_2, X_3)	external reference frame
(Y_1, Y_2, Y_3)	internal reference frame fixed at the center of mass of a microelement α

Greek Letters

α	as a superscript denotes random quantities at a microscale
α, β, γ	microelements
$\overset{\alpha\beta}{\delta}$	distance between grains α and β (deformed configuration)
ε	nondimensional parameter characterizing small fluctuations
$\underset{\approx}{\varepsilon}$	strain tensor
θ	angle in the grain boundary due to the shear motions

$\underset{\sim}{\chi}$	kinematic state vector
λ	wavelength, also Lamé constant
μ	average value, also Lamé constant
ρ	mass density
σ	standard deviation
$\underset{\sim}{\sigma}$ or $\underset{\approx}{\sigma}$	stress state vector or stress tensor
${}^{\alpha}\tau$	passage (sojourn) time
τ_L, τ_T	dispersion time of longitudinal, transverse waves
${}^{\alpha\beta}\chi \equiv \chi$	impedance ratio
ω	outcome in the probability space, also the frequency
${}^{\alpha\beta}\Delta$	distance between grains α and β (undeformed configuration)
Σ	stress space
Φ	interatomic potential
Ω	probability space
$\mathcal{M}$	mesodomain or superscript of the meso-scale quantities

Mathematical Symbols

$\dot{\sim}$	denotes vector quantity
$\dot{\approx}$	denotes tensor quantity
ϵ	element of
$\subset$	contained in
$\cup$	union
$\cap$	intersection
$\rightarrow$	mapping, convergence
$\{\cdot,\ldots,\cdot\}$	system
$\lvert\cdot\rvert$	absolute value, magnitude
$\lVert\cdot\rVert$	norm

$\nabla^2 \equiv \Delta$	Laplace operator
$\langle \cdot \rangle$	average value
$\mathbb{R}^n$	n-dimensional real space
$\mathbb{Z}^+$	natural numbers
$\square$	end of proof
$\mathcal{F}$	σ-algebra
$\mathcal{T}$	topology, time domain
$\mathcal{P}$	probability measure
$\mathcal{X}$	state space
$\mathcal{K}$	kinematic space
$\mathcal{V}$	velocity space
$\mathcal{W}$	general velocity space
$O(\cdot)$	small order term

CHAPTER 1

REVIEW OF THE ANALYSIS OF WAVE PROPAGATION IN SOLIDS

1.1 Introduction

With the advance of science and technology in the 19th century it became increasingly obvious, that the rigid body concept was not a sufficient basis for the mechanical models of matter. It was recognized, that dynamic effects become important, if the characteristic time of loading at any given point of a finite dimensional body, is of the same order of magnitude as the ratio of the largest distance from this point to the propagation velocity of the disturbance (load). The latter quantity remained rather undefined until it was formally established on the assumption, that an elastic solid can be treated as an elastic "aether". Indeed it was the notion of a solid being an "elastic continuum", that not only initiated the wave propagation analysis, but also led to its development in the form of a rigorous mathematical theory known as "elastodynamics".

Great discoveries in physics at the end of the 19th century clearly indicated that all matter (solid, liquid, gaseous) is composed of particles. The very large number of particles of which a solid medium is composed justified an idealization, that led to mechanical models on the basis of a "continuum". Since mechanics is a rigorous science, it had to be built on mathematical principles and concepts. The calculus of continuous functions was then the main body of mathematics whilst the discrete functions analysis has been developed only in recent time. The idea of a physical quantity

as a continuous function of the space coordinates accorded many advantages in the past and continues to be important to the present time. This is reflected in the more recent advances in differentiable manifold theory.

Although continuum mechanics generally provides a very successful tool in the study of the mechanical behaviour of materials, it has been recognized in the last decade, that it supplies only a first order approximation. This is so, because many phenomena encountered in engineering and applied sciences deny the applicability of a continuum hypothesis for the inclusion of the great variety of microstructural effects. Although the physical properties of materials have been studied extensively from an experimental and theoretical point of view, a rigorous formulation of the mechanics and especially of dynamic problems, that would include the existing microstructure evades us still. Since the dynamic case is the most general part of mechanics, the availability of such a formulation is crucial in the study of a multitude of technological and applied science problems. Hence, such a formulation has been the goal of most approaches in the past two decades. Although many of these attempts go beyond the classical continuum approach, they still rely essentially on the continuum hypothesis. Several other theories have been tried on the principles of statistical mechanics, but the ensuing analyses do not reflect the discreteness of real materials and more importantly fail to establish "evolution laws". A brief account of these main trends in the mechanical wave propagation theory will be given in the following sections of this chapter. This will then supply the motivation and the layout of the present thesis program.

1.2 The Elastic, Isotropic and Homogeneous Solid

As already mentioned earlier, the elastic-light propagation theory initiated the mechanical wave propagation theory, which we now recognize as the isothermal linearized elastodynamics of a homogeneous isotropic medium. The history of these developments as well as the formulation of the governing equations and the then-available methods are given in Love's well-known treatise (1926). Further research on small deformation dynamics of an elastic solid has mainly continued on the same assumption of a homogeneous isotropic medium. Hence, the analyses were primarily concerned with the mathematical methods of solution already known from the classical formulation.

Kolsky's book written thirty years ago became a classical exposition of the theory and experiments on stress waves in elastic and anelastic solids. The state of the art was then the differential and integral calculus. The most advanced analytical tools were restricted to the use of the complex variable technique and the integral transform method applicable to the solution of two-dimensional and three-dimensional problems, respectively (see also the Chapter on "Dynamical Problems" by Sneddon and Berry in Encyclopedia of Physics, 1958). A measure of the progress that has been made later in the analysis of wave propagation, can be given by a number of reports, reviews and conference proceedings such as Sneddon and Hill (1960) and Miklowitz (1966). Thus we can cite Lindholm (1968) that "the effort in the sixties was expended towards the generation of both experimental data on the dynamic mechanical response of

materials as well as the formulation of realistic constitutive theories". Although much attention was devoted at that time to dislocation mechanism as a means of explaining other than purely elastic dynamic phenomena, the theoretical models including microscopic effects were crude, based on the continuum hypothesis and deterministic.

A comprehensive study of wave propagation relations from a deterministic continuum standpoint exclusively, along with a great number of analytical techniques is given by Achenbach (1973), whilst a more rigorous mathematical presentation of elastodynamics is due to Eringen and Suhubi (1974).

The above remarks point to the developments in the theory of wave propagation in elastic isotropic homogeneous solids. Hence, at this stage we give the fundamental equations governing the motion of such a body:

- the stress equations of motion $\sigma_{ij,j} + \rho f_i = \rho \ddot{u}_i$ (1.1)
- Hooke's law $\sigma_{ij} = \lambda \varepsilon_{kk} \delta_{ij} + 2\mu \varepsilon_{ij}$ (1.2)
- the strain displacement relations $\varepsilon_{ij} = \frac{1}{2}(u_{i,j} + u_{j,i})$ (1.3)

Substitution of relation (1.3) into (1.2) and (1.1) yields the well-known displacement equations of motion as follows:

$$\mu u_{i,jj} + (\lambda+\mu) u_{j,ji} + \rho f_i = \rho \ddot{u}_i \,, \qquad (1.4)$$

which can subsequently be decomposed into two wave equations governing the longitudinal and transverse wave motion in such a solid, respectively, :

$$\nabla^2 \varphi = \frac{1}{c_L^2} \ddot{\varphi} \,, \qquad (1.5)$$

$$\nabla^2 \underset{\sim}{\psi} = \frac{1}{c_T^2} \ddot{\underset{\sim}{\psi}}, \qquad (1.6)$$

where we have assumed that $\nabla \cdot \underset{\sim}{\psi} = 0$ and φ and $\underset{\sim}{\psi}$ represent two wave potentials.

These relations (1.5, 1.6) were usually subject to advanced calculus techniques mentioned before. However, only recently considerations have been given to more rigorous methods of solution of three-dimensional problems, whereby the modern tools of functional analysis and variational calculus are more fully employed (see for instance, Stakgold, 1979).

1.3 Behaviour of Anisotropic Non-Homogeneous Solids

Although some media can be modelled successfully in terms of the linearly elastic isotropic homogeneous solid, a growing range of media encountered in engineering sciences require the development of less restrictive mechanical theories. The earliest studies of this type of media date back to the nineteenth century (see also Love 1926), when the foundation for the wave propagation analysis in anisotropic homogeneous bodies has been established. However, further developments in the field took place only after the second World War; these studies can be generally classified into two major groups, namely wave mechanics in crystals and wave mechanics in macroscopic bodies.

The first group, i.e. the wave mechanics in crystals, encompasses two kinds of approaches, the deterministic and the probabilistic one. The deterministic approach is based on the classical work of

Brillouin (1953) and is directed mainly at the understanding of the passage from the acoustic to the optical lattice vibrations (see for instance Smith (1961)) and the determination of the "effective elastic" coefficients for crystals. On the other hand, the probabilistic approach is important in the analysis of crystals with imperfections (see Chow and Keller, 1972). We have to note, that these wave mechanics models are good at the crystal level, but do not apply to polycrystalline solids. An original outgrowth of lattice dynamics is the non-local elasticity theory (see Eringen, 1972, and Kunin, 1968) which, however, omits the intermittent scale in the passage from the atomistic to the global level, e.g. considerations of dislocations, grain boundaries, etc.

The second group of studies on wave propagation in anisotropic non-homogeneous solids deals, in general, with macroscopic media that have a random microstructure. Interestingly, from the mathematical point of view, two major trends can also be distinguished: the deterministic and the probabilistic one. The deterministic approach is based on the assumption, that one can safely take ensemble averages over the random microstructure in order to establish the mean field response (see for instance Datta, 1977). Why this approach is fundamentally erroneous is dealt with in Section 2.1 of the present thesis. In the probabilistic approach one can distinguish two kinds of theories depending on the type of the model chosen, i.e., continuous random media and discrete random media. Theories of wave propagation in continuous random media have been initiated by the work of Chernov (1960), and put on a firm mathematical basis by Kampé de Fériet during the sixties (1962 and 1966). A number of mathematical techniques

developed in this area comprise especially the wave formalism and the ray formalism (Frisch, 1968). The latter approach is based on geometrical optics and applies to the case of very short wavelengths only. It gives the statistics of the rays and the wave fluctuations, but not their evolution in time (see also Keller, 1962). The formulation of the wave motion, that applies to the problem when the wavelength is larger than the correlation range of the random inhomogeneities, usually contains all the random characteristics of the medium in the index of refraction which enters in the classical Helmholtz equation. Wave propagation in continuous random media is a rapidly developing field, since it can be used for a number of problems and is particularly successful in the analysis of the scattering of sound waves by turbulent gases, scintillation of stellar images and scattering of waves by tropospheric turbulence (see Uscinski, 1977). However, it is essentially a phenomenological approach and hence not appropriate for the present study.

On the other hand, the microscopic approach is adopted in the wave propagation theories for discrete random media. Since in this case the physical properties and field quantities are described by discontinuous random functions, it is necessarily a much harder approach than in the continuous random problem and thus presents formidable mathematical difficulties. Various existing theories are usually restricted to the problem of scattering of a wave by the randomly distributed inhomogeneities that are usually embedded in a continuum matrix and therefore referred to as multiple scattering problem. Almost invariably these theories rely on the averaged

statistical field quantities and make a passage to the continuum in order to use the classical wave equation (see Ishimaru, 1978, Uscinski, 1977, and Sobczyk, 1976). The successful applications of these theories include the molecular scattering of light, the theory of dielectrics and problems associated with radiative transfer. To the best of our knowledge there has not been developed a strictly probabilistic theory concerning the wave propagation in a discrete random medium and in particular for the mechanical wave propagation in such media. It is the main aim of this thesis to develop such a probabilistic theory.

1.4 Motivation of Research, Layout of the Thesis

The brief review of the theories of wave propagation in solids given above indicates that the existing theoretical models are of the phenomenological type and take at best, only part of the true structure of the solid into account. It becomes apparent that there is a need for a more comprehensive theory for the dynamical behaviour of solids which have a discrete random microstructure.

The proposed theory in this thesis, being the first one of this nature, will restrict its scope to the isothermal and small deformation motions with the primary goal of the inclusion in the theory of random micro-scale effects. These micro-scale effects shall comprise the non-conservative grain boundary phenomena and the conservative (elastic) intra-grain phenomena. The basic considerations that are given at the beginning of Chapter II will be adapted to a microdynamics theory on a rigorous mathematical basis. Thereafter,

we give a discussion of the essential properties of the microstructure of a solid and the statement of the fundamental problem of this thesis. Subsequent to the three-dimensional formulation of the probabilistic micro-dynamics in terms of an abstract dynamical system we specialize the analysis to the kinematic space as a probabilistic function space.

Chapter III is devoted to the determination of the transition operator of the abstract dynamical system. This is accomplished after the existence of an internal and a macroscopic time has been postulated. The evolution of the wave propagation process in the one-dimensional model of the solid is formulated on the basis of a four-parameter transition operator on the Markov random field. Subsequently, a general stochastic model is developed for the wavefront propagation in the three-dimensional medium, where the interactions between contiguous microelements of the structure are represented in terms of interatomic potentials. Finally, an asymptotic equivalence of the proposed probabilistic microdynamics theory to the deterministic continuum theory is established, whereby it is shown that the average time of the random wave propagation process becomes idential to the macroscopic time.

Chapter IV is devoted to the comparison of the classical theories to the microdynamics theory. The results of the latter are obtained through the Monte-Carlo simulation method and reveal some interesting characteristics.

Concluding remarks with some proposals for future research and comments on the contribution to the theoretical mechanics by the author of this thesis are given in Chapter V.

CHAPTER II

MICRODYNAMICS OF STRUCTURED SOLIDS

2.1 Introduction: Determinism versus Probability

It has been pointed out in the first chapter that there is a need for a general theory of the dynamical behaviour of solids possessing a discrete microstructure. The main objective of this study is the formulation of the relations that govern the dynamic response of a discrete medium such as a polycrystalline solid, although it is expected that the proposed theory might readily be modified to model other classes of structured solids (e.g. fibrous, composite). Furthermore, the attention in this work is focused on the transient wave propagation, which is considered to be of fundamental importance in the analysis of the steady-state motions that occur later.

It is well known that the microstructure of any solid exhibits random configurational and physical characteristics, which manifest themselves through the arrangement and properties of individual microelements (e.g. crystals). It is therefore a matter of logical deduction to conclude that the field quantities which describe the mechanical states of the medium, will be random functions. Hence, the evolution of the physical processes involved is to be treated in a probabilisitc rather than deterministic manner. An approach of this kind should naturally include the finiteness of the microelements with its relation to the overall size of the macroscopic body domain, as well as the interaction effects at the internal surfaces in the medium. Thus a probabilistic problem in mechanics can be stated in

a very general way as follows:

find a solution of the random equation

$$T(\omega)\, x(t) = y(t,\omega)\,, \tag{2.1}$$

in which y is a known function, $T(\omega)$ a random operator from $\Omega \times \mathfrak{X}$ into $\mathfrak{Y}$ and where Ω is a probability space and $\mathfrak{X}$ and $\mathfrak{Y}$ are generally Banach spaces.

The prevailing view amongst most researchers in engineering, and applied sciences in general, and those concerned with wave motion analyses, in particular, is that one can work with the average values of the field quantities. This implies that the random quantities in equation (2.1) can be replaced by their expected values and thus solving the deterministic operator equation only, i.e.:

$$\langle T \rangle \langle x(t) \rangle = y(t) \tag{2.2}$$

However, it is one of the fundamental facts in the theory of random equations, that the expected solution of equation (2.1) and the solution of equation (2.2) are not equal, except for simple forms of $T(\omega)$ or $y(t,\omega)$, so that in general:

$$E\{x(t)\} \neq \langle x(t) \rangle \tag{2.3}$$

For a detailed discussion of this and related aspects of random fixed point theorems see for instance Bharucha-Reid (1972).

The above observation explains why the results obtained from the classical deterministic wave equation can not yield desired results, even if one is concerned with the average values only. Interestingly, the averaging procedure symbolized by equation (2.2)

involves usually the smearing out of the internal effects between the microelements uniformly throughout the entire medium which further restricts the physical theory.

It is important to point out at this stage, that the approach taken in the random continuum theories, discussed in section 1.3 and subsequently in 4.3 of this thesis, preserves the randomness of the medium to a certain extent by admitting the physical characteristics and state variables as random functions, that are continuous in space and hence excluding an appropriate treatment of the effects at internal surfaces.

A theory which was formulated from the outset to include the essential discreteness of a structured solid along with its random properties in the global governing equations is the probabilistic micromechanics theory conceived by Axelrad, 1963. This random theory of the mechanical behaviour of discrete media has been successfully applied by Axelrad and his coworkers to a number of problems of complex and diverse nature, and especially to quasi-static phenomena in polycrystalline and fibrous materials (see Axelrad, 1978 and references there). This theory has also been used in a somewhat modified form to model fracture and fatigue phenomena (Provan, 1977). However, a rigorous generalization to the dynamics of such solids is attempted for the first time in the present study.

2.2 Fundamental Concepts, Physics, Wave Characteristics

2.2.1 Postulates of probabilistic micromechanics

It was pointed out in the foregoing section that the probabilistic micromechanics theory naturally allows for the inclusion of the discreteness of a solid along with its random character in the derivation of the governing equations. This theory is based on four fundamental postulates (Axelrad, 1978 and 79), which we briefly re-state here and comment upon in light of their relevance in the micro-dynamics theory.

Postulate 1:

Three measuring scales are used in which the smallest refers to a "microelement" of the structure, an intermediate one called "mesodomain" containing a statistical ensemble (Gibbsian) of micro-elements, and finally a finite number of non-intersecting mesodomains that form the macroscopic material body.

Postulate 2:

All field quantities pertaining to a microelement are random variables or functions of such variables.

Postulate 3:

Stresses, strains, rates of strain, etc. are generalized so that the response of a microelement includes interaction forces between elements. Such forces are derivable from a bond or interaction potential.

Postulate 4:

A material functional or operator is used that contains in its argument characteristics of the specific material under consideration, giving a connection between stresses and deformations.

The above postulates provide a basis for the ensuing mathematical formulation and shall be referred to at various steps in this chapter. It is however important to point out at this stage that it becomes necessary to introduce one more postulate for the dynamic theory regarding the "multidimensional time concept". We defer the formulation of this postulate until a later, more appropriate stage.

2.2.2 Basic physical considerations

It is well known from solid state physics that all sound waves are composed of phonons, i.e. quanta of energy. However, consideration of a mechanical wave from a quantum point of view is only necessary at a very high frequency range, which means that a continuum approximation for the perfect crystal lattice is valid for frequencies below $10^{11} \div 10^{12}$ Hz. This roughly means for wavelengths larger than 10^{-8} m (see Kittel, 1968). Since the acoustic range covers wavelengths from 10^{-8} m up, which may be less than the typical crystal size in a polycrystalline solid, we can, in general, distinguish the following three cases:

a) $\lambda < \alpha d$ - very high frequency

b) $\lambda \simeq \alpha d$ - high frequency

c) $\lambda > \alpha d$ - low frequency

where λ is the wavelength.

Considering that the crystal size ${}^{\alpha}d$ may in general vary in polycrystalline solids between 0.1 mm and 5.0 mm, and for a wave propagation velocity between $2 \div 7.10^3$ m/s, elementary calculations show that case b) will correspond to frequencies of the order of 10^6 to 10^7 Hz. We note that this high frequency range is characterized by a strong scattering. This phenomenon has been well explained by the very fact, that the wavelength is of the same order as the scatterer's size (see Mason (1958)). Thus by choosing to work in the so-called low frequency range, i.e. case c), we still cover most of the frequencies normally encountered in mechanical engineering applications.

Following the above discussion we now give the following definition:

Definition 1:

A single microelement α (grain or crystal) is taken as an elastic continuum which is characterized by:

- two elastic constants, e.g. ${}^{\alpha}E$ (elastic modulus) and ${}^{\alpha}G$ (shear modulus)
- its mass density ${}^{\alpha}\rho$

} constant throughout the body of α

- its geometric shape and size in a 3-D space, all of which are random and described by their respective distributions, as for example $P({}^{\alpha}\rho)$.

A two dimensional view of typical microelements within the microstructure of the solid is schematically shown in Fig. 2.1. It is seen that the interior body domain of the crystal α is denoted by

${}^{\alpha}\mathcal{D}$, which is a simply connected, open subset of the $\mathbb{R}^3$-Euclidean space*. The grain boundary $\partial^{\alpha}\mathcal{D}$ is a two-dimensional surface in $\mathbb{R}^3$ and the entire body domain of α is ${}^{\alpha}\bar{\mathcal{D}} = {}^{\alpha}\mathcal{D} \cup \partial^{\alpha}\mathcal{D}$. We conclude that according to Definition 1 the properties of a structured solid are described by random functions with discrete realizations (piecewise continuous), which, with reference to Postulate 1, are considered to be space homogeneous within a certain mesodomain.

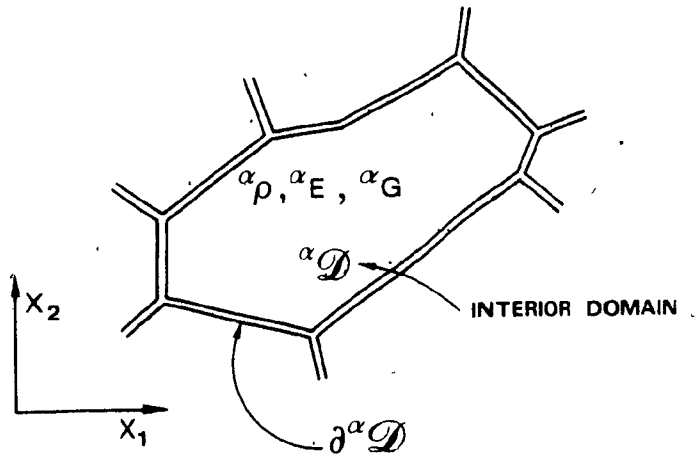

FIG. 2.1 PLANE VIEW OF A MICROELEMENT IN A POLYCRYSTALLINE SOLID.

---

* The choice of ${}^{\alpha}\mathcal{D}$ as an open set in the $\mathbb{R}^3$-topology is arbitrary since no physical reality corresponds perfectly to the notion of a point belonging to the boundary of the grains.

As was mentioned earlier, the attention in this work is focused on the transient wave propagation, whereby a specific initial form of the given pulse does not have to be deterministic, since the whole analysis is conducted in the language of probability theory. We recognize, however, that due to the random physical properties ${}^{\alpha}E$, ${}^{\alpha}G$ and ${}^{\alpha}\rho$ and the random geometric shape of the microelements, a multiple scatter of even the simplest initial pulses will take place throughout the whole microstructure. It is evident that the random geometry of the grain boundaries will give rise to the rather complicated phenomena of waves splitting at these interfaces and later overlapping inside the microelements. However, it is considered that the random geometry of the $\partial^{\alpha}\mathcal{D}$ surfaces represents only a secondary effect with respect to the role played by the randomness of the physical properties. Hence, in order to make an initial formulation possible, we simplify the problem by assuming all microelements to have identical shapes of a cube (dxdxd) and to be arranged in a perfect lattice-like structure. Furthermore, with reference to Fig. 2.2 we adopt an external reference frame (X_1, X_2, X_3) with its axes parallel to the edges of the microelements and consider propagation of the plane waves whose propagation vector is parallel to X_1, X_2 or X_3, respectively. Although it is evident, that a perfect plane wave generated at any boundary of the macroscopic body domain will immediately begin to loose its perfect form due to the interactions between the microelements, it will continue to propagate as a macro-disturbance in the same direction for a considerable time before diffusing completely throughout the entire body. It is the evolution of such a disturbance, which is of main interest to us in this thesis.

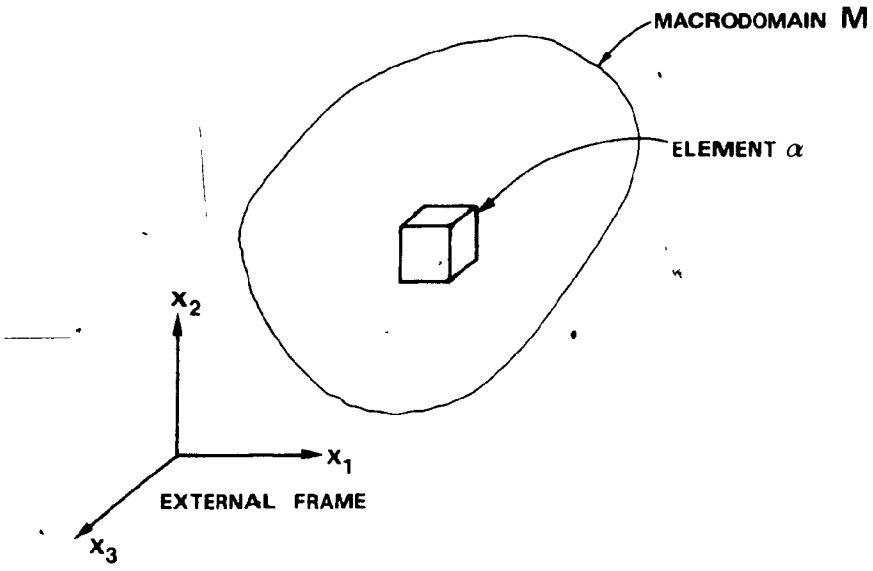

FIG. 2.2 CUBIC STRUCTURAL ELEMENT.

As is well known from elastodynamics (Achenbach, 1973), in the case of a plane wave propagation (longitudinal or transverse) we have for the occurring deformation the following relation:

$$\underset{\sim}{u}(\underset{\sim}{X},t) = f(\underset{\sim}{X}\cdot\underset{\sim}{p} - ct)\,\underset{\sim}{e}\,, \tag{2.4}$$

which is a general 3-D space-time description, and where

$\underset{\sim}{p}$ is the direction of propagation, i.e. a unit vector, and

$\underset{\sim}{e}$ is the direction of motion, (also a unit vector);

the propagation velocity is:

$$\left.\begin{aligned} c &= c_L \text{ - longitudinal wave, when } \underset{\sim}{p} \parallel \underset{\sim}{e} \\ c &= c_T \text{ - transverse wave, when } \underset{\sim}{p} \perp \underset{\sim}{e} \end{aligned}\right\} \quad (2.5)$$

Obviously, the representation in (2.4) is inadequate for the microdynamics theory and can at best be used at a micro-scale only. Indeed, we will now study the wave propagation across the intercrystalline interfaces, where specific phenomena necessitate the introduction of new field quantities not employed in the continuum mechanics theory.

2.2.3 Wave propagation across the intercrystalline boundaries

It is a well known fact in metal physics that the presence of many grain boundaries in the polycrystalline solid increases its overall strength on the one hand and causes an energy dissipation on the other. In general, grain boundaries are best considered as regions of "bad crystals" (Martin and Doherty, 1976, and Christian, 1965). However, there is still little known about them, and in particular about their behaviour under dynamic loads. It appears therefore that a possible approach is to generalize the kinematic model for the quasi-static interactions developed earlier by Axelrad and Provan (1972), which is based on Bollman's geometrical theory of coincidence lattices (1970).

Figure 2.3a presents the kinematics of two contiguous micro-elements α and β under the action of a general plane wave containing both longitudinal and transverse components, where the propagation vector is parallel to the X_1 axis. As is usual in micromechanics, a

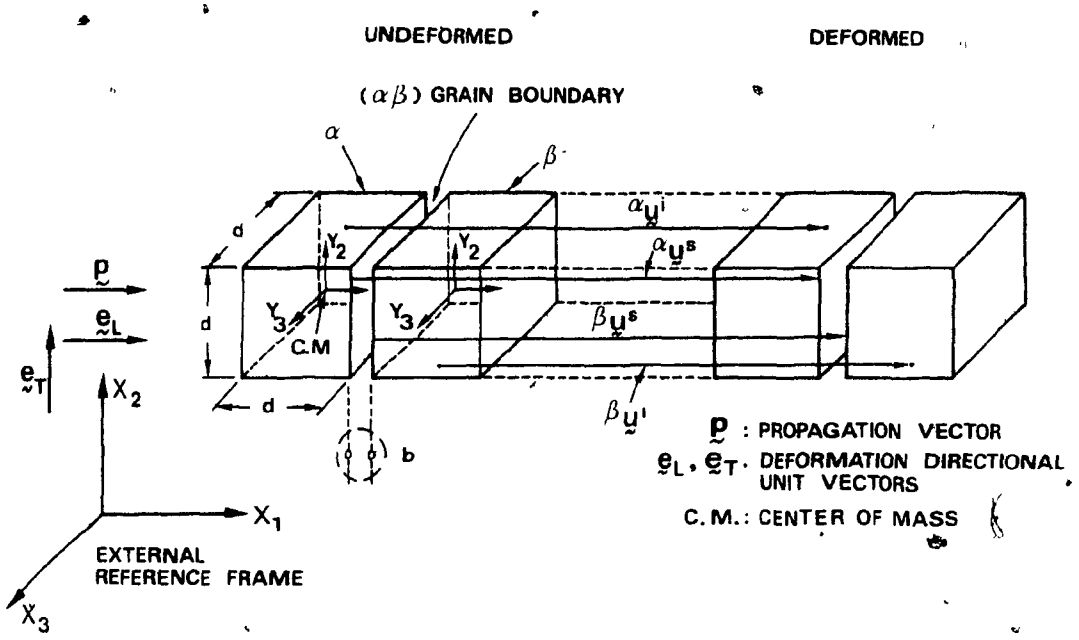

(a) ONE-DIMENSIONAL MODEL .

(b) GRAIN BOUNDARY UNIT CELL MODEL , AXELRAD , 1978 .

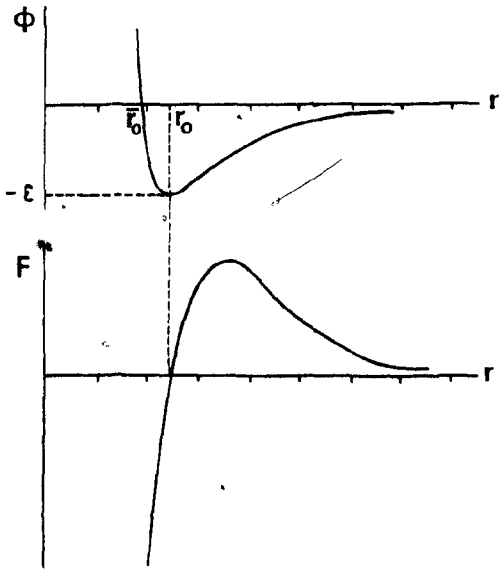

(c) GENERAL FORCE - POTENTIAL SCHEMATICS .

FIG. 2.3 DEFORMATION KINEMATICS (1-D MODEL)

local coordinate frame (Cartesian) is fixed at the centre of mass of each crystal (see Axelrad 1978). The internal and surface deformations are describable by the $\underset{\sim}{u}^i$ and $\underset{\sim}{u}^s$ vector fields, respectively. This distance between the grains α and β is denoted by ${}^{\alpha\beta}\underset{\sim}{\Delta}$ in the undeformed configuration and by ${}^{\alpha\beta}\underset{\sim}{\delta}$ in the deformed one. It is seen that the deformation in the grain boundary can be expressed by:

$$ {}^{\alpha\beta}\underset{\sim}{d} = {}^{\alpha\beta}\underset{\sim}{\delta} - {}^{\alpha\beta}\underset{\sim}{\Delta} \tag{2.6} $$

and where ${}^{\alpha\beta}\underset{\sim}{d}$ is also

$$ {}^{\alpha\beta}\underset{\sim}{d} = {}^{\beta}\underset{\sim}{u}^s - {}^{\alpha}\underset{\sim}{u}^s \tag{2.7} $$

This distance has been taken as the relative displacement between two "coincidence cell points" at the surfaces of the crystal lattices of both grains α, β (Fig. 2.3b). On the assumption that at certain points within surface area d^2 perfect bonding exists, the initial thickness of the grain boundary will become identical to the interatomic distance at equilibrium r_0, i.e.:

$$ \left| {}^{\alpha\beta}\underset{\sim}{\Delta} \right| = r_0 \tag{2.8} $$

which corresponds to a minimum potential energy between the atomic layers. The relationship between the potential energy ϕ and force F at a distance r is given from physics by:

$$ \underset{\sim}{F}_e = -\frac{\partial \phi}{\partial r} \tag{2.9} $$

in the case of a conservative surface effect. The nonconservative contribution can be assumed to be representable by a rate dependent "dissipative potential", giving a dissipative surface force:

$$\underset{\sim}{F}_d = \frac{\partial \phi}{\partial \dot{r}} \tag{2.10}$$

where $\dot{r}$ here is a time rate of change of the bond distance r in the boundary zone between 2 coincidence lattice points in perfect bonding.

We see that the total surface interaction force between two coincidence cell points can be expressed by:

$$\underset{\sim}{F} = \underset{\sim}{F}_e + \underset{\sim}{F}_d \tag{2.11}$$

This force is a discrete quantity since the both component forces as given in (2.9) and (2.10) are also discrete quantities. Assuming that there are N interatomic bonds per surface area d^2 of the boundary zone between two cubic crystals α and β, it follows that on the average the surface interaction force in this zone is:

$$^{\alpha\beta}\underset{\sim}{F} = N \cdot \underset{\sim}{F} \tag{2.12}$$

Furthermore, on the assumption that the bonds are uniformly distributed in space, we can obtain the surface traction at a point on the grain boundary surface by taking a limit in the Cauchy sense as follows:

$$^{\alpha\beta}\underset{\sim}{T} = \lim_{\Delta s \to 0} \frac{^{\alpha\beta}\underset{\sim}{F}}{\Delta s} = \frac{N\underset{\sim}{F}}{d^2} \tag{2.13}$$

According to the Definition 1, the forward going plane wave in the crystal α may be described in the continuum sense (see relations (2.4) and (2.5)) as follows:

$$^{\alpha}\underset{\sim}{u}(X_1, t) = f(X_1 - {}^{\alpha}c\, t) \tag{2.14}$$

where the propagation is assumed in the positive X_1 direction as in Fig. 2.3a and the direction of motion may either be $\underset{\sim}{e}_L$ - longitudinal or $\underset{\sim}{e}_T$ -transverse wave. We shall later find it more convenient to

develop the stochastic theory in terms of wave velocity vector, i.e. the deformation rate, so that we can also describe such a plane wave as follows:

$$ {}^{\alpha}\dot{\underset{\sim}{u}} = \frac{\partial}{\partial t} f(X_1 - {}^{\alpha}c\,t)\,\underset{\sim}{e} = \bar{f}(X_1 - {}^{\alpha}c\,t)\,\underset{\sim}{e} \equiv {}^{\alpha}\dot{\underset{\sim}{u}}_i \qquad (2.15) $$

This wave will be identified with the incident wave ${}^{\alpha}\dot{\underset{\sim}{u}}_i$. The wave will traverse the microelement α in a certain finite time, which is embedded in the real time. To clarify this, we use the following definition:

Definition 2:

> The sojourn or passage time is the micro-time ${}^{\alpha}\tau \overset{df}{=} \frac{{}^{\alpha}d}{{}^{\alpha}c}$ (2.16) of passing of a wavefront through an element α, where ${}^{\alpha}d$ is the size of this element in the direction of wave propagation, and ${}^{\alpha}c$ is the wave propagation velocity.

It is assumed that the probability distribution of the random variable ${}^{\alpha}\tau$ is obtainable from appropriate experiments on single crystals.

From the causality principle we know that a wavefront incident upon an interface between two crystals α and β will produce a reflected wavefront (into α) and a transmitted wavefront (into β). Both these wavefronts are directed away from the interface, so that:

$$ \left.\begin{aligned} {}^{\alpha}\dot{\underset{\sim}{u}}_r &= g(X_1 + {}^{\alpha}c\,t)\,\underset{\sim}{e} \qquad (a) \\ {}^{\beta}\dot{u}_{tr} &= h(X_1 - {}^{\beta}c\,t)\,\underset{\sim}{e} \qquad (b) \end{aligned}\right\} \qquad (2.17) $$

It is apparent, that in the above relations, the amplitude functions g and h are unknown and undetermined. It becomes necessary therefore in the analysis to introduce two conceptually new coefficients, that

will link the above relations with the actual incident velocity in the crystal . Thus, we give the following definition:

Definition 3:

The reflection coefficient $C_r \overset{df}{=} \frac{{}^{\alpha}\dot{\underset{\sim}{u}}_r}{{}^{\alpha}\dot{\underset{\sim}{u}}_i}$,

The transmission coefficient $C_{tr} \overset{df}{=} \frac{{}^{\beta}\dot{\underset{\sim}{u}}_{tr}}{{}^{\alpha}\dot{\underset{\sim}{u}}_i}$,

where ${}^{\alpha}\dot{\underset{\sim}{u}}_i$, ${}^{\alpha}\dot{\underset{\sim}{u}}_r$ and ${}^{\alpha}\dot{\underset{\sim}{u}}_{tr}$ are the incident, reflected and transmitted wave vectors, respectively.

It is evident, that due to the random physical properties of the microstructure these coefficients will be random functions of the coefficients and it becomes necessary to determine their explicit forms for a given medium. Whilst it is assumed that the probability distributions of C_r and C_{tr} are obtainable from appropriate experiments on bi-crystals, we make here an attempt to derive them analytically.

Since a connection between the wave velocities in contiguous crystals α, β and the effect of the presence of the grain boundary is sought, it is important to note the relevant kinematic condition, i.e.:

$$ {}^{\beta}\dot{\underset{\sim}{u}}^s - {}^{\alpha}\dot{\underset{\sim}{u}}^s = {}^{\alpha\beta}\dot{\underset{\sim}{d}}, \tag{2.18} $$

where the surface velocities are respectively

$$ \left.\begin{aligned} {}^{\alpha}\dot{\underset{\sim}{u}}^s &= {}^{\alpha}\dot{\underset{\sim}{u}}_i - {}^{\alpha}\dot{\underset{\sim}{u}}_r \qquad (a) \\ {}^{\beta}\dot{\underset{\sim}{u}}^s &= {}^{\beta}\dot{\underset{\sim}{u}}_{tr} \qquad (b) \end{aligned}\right\} \tag{2.19} $$

Introducing the above into (2.18) and making use of Definition 3, we obtain the following important relation:

$$ {}^{\alpha\beta}\underset{\sim}{d} = (C_{tr} + C_r - 1)\, {}^{\alpha}\underset{\sim}{\dot{u}}_i \qquad (2.20) $$

In order to eliminate C_r from the above we now invoke the "stress condition" of surface forces in the boundary, i.e.:

$$ {}^{\alpha}\underset{\approx}{\sigma}^{s} = {}^{\beta}\underset{\approx}{\sigma}^{s} \qquad (2.21) $$

where the surface stresses are given in terms of the stresses involved in the travelling waves, i.e.:

$$ \left.\begin{aligned} {}^{\alpha}\underset{\approx}{\sigma}^{s} &= {}^{\alpha}\underset{\approx}{\sigma}_i + {}^{\alpha}\underset{\approx}{\sigma}_r \qquad (a) \\ {}^{\beta}\underset{\approx}{\sigma}^{s} &= {}^{\beta}\underset{\approx}{\sigma}_{tr} \qquad (b) \end{aligned}\right\} \qquad (2.22) $$

It is known from elastodynamics that for the plane waves travelling in the X_1 direction, the components of the stress tensor are related to the components of the velocity vector in the following way:

$$ \sigma_{11} = -\rho c_L \dot{u}_1 \qquad \text{in the longitudinal motion} \qquad (2.23) $$

and

$$ \left.\begin{aligned} \sigma_{12} &= -\rho c_T \dot{u}_2 \\ \sigma_{13} &= -\rho c_T \dot{u}_3 \end{aligned}\right\} \text{ in the transverse motion} \qquad (2.24) $$

Thus returning to (2.21) and employing (2.22a,b) we can write, in general, that:

$$ {}^{\alpha}\rho\, {}^{\alpha}c\, {}^{\alpha}\dot{u}_i + {}^{\alpha}\rho\, {}^{\alpha}c\, {}^{\alpha}\dot{u}_r = {}^{\beta}\rho\, {}^{\beta}c\, {}^{\beta}\dot{u}_{tr} \qquad (2.25) $$

Making use of Definition 3 again, we obtain a relation between the transmission and reflection coefficients as follows:

$$ C_r = \chi C_{tr} - 1 \qquad (2.26) $$

where

$$ \chi = \frac{{}^{\beta}\rho\, {}^{\beta}c}{{}^{\alpha}\rho\, {}^{\alpha}c} \qquad (2.27) $$

is referred to as the impedance ratio. We note that χ is a new random variable whose mean is equal to unity if it is assumed that the statistics of the physical properties are space homogeneous. Eliminating C_r from (2.26) and (2.20) we arrive at a key relation between the transmission coefficient, the incident wave velocity and the grain boundary displacement rate, i.e.:

$$\overset{\alpha\beta}{\underset{\sim}{\dot{d}}} = {}^{\alpha}\underset{\sim}{\dot{u}}_i \left[C_{tr}(\chi+1) - 2\right] \tag{2.28}$$

It is important to note that $\overset{\alpha\beta}{\underset{\sim}{\dot{d}}}$ in the above form is directly related to the time rate of the bond distance r through some kinematic condition:

$$\overset{\alpha\beta}{\underset{\sim}{\dot{d}}} = \varphi[\dot{r}] = \varphi\left[\frac{\partial r}{\partial t_m}\right] \tag{2.29}$$

The above relation indicates that r is varying in the "microtime t_m", which is a time scale involved in the interatomic phenomenon. In general, although this microtime t_m is embedded in the real time t, the phenomena taking place in t_m are characterized by very high frequencies ($10^{14} \div 10^{15}$ Hz), which is in contrast to the passage time ${}^{\alpha}\tau$ of a mechanical wave through a microelement which is of the order of $10^{-6} \div 10^{-8}$s. From equation (2.29) we see that $\overset{\alpha\beta}{\underset{\sim}{\dot{d}}}$ is also taken with respect to t_m, so that (2.28) implies that C_{tr} is a function of the microtime t_m, viz:

$$C_{tr} = C_{tr}(t_m) \tag{2.30}$$

It follows then, that in order to determine C_{tr} from the relation (2.28), one has to determine the long time behaviour of $\overset{\alpha\beta}{\underset{\sim}{\dot{d}}} \equiv \frac{\partial \overset{\alpha\beta}{\underset{\sim}{d}}}{\partial t_m}$. Thus, one has to establish the variation of the bond distance r on

the real time scale t first, and only later infer the functional form of C_{tr}.

Thus from equation (2.29) we have:

$$\frac{\partial r}{\partial t_m} = \varphi^{-1}\left({}^{\alpha\beta}\underset{\sim}{\dot{d}}\right)$$

which upon substituting (2.28) becomes:

$$\frac{\partial r}{\partial t_m} = \varphi^{-1}\left\{{}^{\alpha}\underset{\sim}{\dot{u}}_i \left[C_{tr}\,(\chi+1) - 2\right]\right\} \tag{2.31}$$

In general, the component of the surface stress ${}^{\beta}\underset{\approx}{\sigma}^{s}$ which is relevant in the particular type of wave motion is related to the surface traction ${}^{\alpha\beta}\underset{\sim}{T}$ in the $(\alpha\beta)$ boundary as follows (see also Fig. 2.5 on page 31)

$${}^{\beta}\sigma^{s}_{ik} = {}^{\alpha\beta}\underset{\sim}{T}\cdot\cos\left({}^{\alpha\beta}\underset{\sim}{T}, {}^{\alpha\beta}\underset{\sim}{d}\right), \quad k = 1,2,3. \tag{2.32}$$

Making use of one of the relations (2.23) or (2.24) for the transmitted wave and recalling (2.13) we can write:

$$-C_{tr}\,{}^{\alpha}\dot{u}_{k_i}\,{}^{\beta}\rho\,{}^{\beta}c = {}^{\alpha\beta}T\cdot\cos\left({}^{\alpha\beta}\underset{\sim}{T}, {}^{\alpha\beta}\underset{\sim}{d}\right) = \frac{NF}{d^2}\cdot\cos\left({}^{\alpha\beta}\underset{\sim}{T}, {}^{\alpha\beta}\underset{\sim}{d}\right)$$

Substituting C_{tr} from the above into (2.31) we obtain the general equation governing the behaviour of the bond distance with respect to the microtime t_m, i.e.:

$$\frac{dr}{dt_m} = \varphi^{-1}\left\{{}^{\alpha}\dot{u}_{k_i}\left[\frac{-NF\cdot\cos\left({}^{\alpha\beta}\underset{\sim}{T}, {}^{\alpha\beta}\underset{\sim}{d}\right)}{{}^{\alpha}\dot{u}_{k_i}\,{}^{\beta}\rho\,{}^{\beta}c\,d^2}(\chi+1) - 2\right]\right\} \tag{2.33}$$

It is seen that the force F depends on r and $\frac{dr}{dt_m}$ according to (2.9) and (2.10). Further (2.33) represents an autonomous nonlinear differential equation of the first order. Thus, in order to determine

the global behaviour of r on the real time scale t one has to consider specific forms of the conservative and nonconservative parts of the potential under the specific type of wave motion.

The elastic contribution in the grain boundary zone can be taken generally (applies to face centered cubic, body-centered cubic and other crystal structures) as a Lennard-Jones potential, i.e.:

$$\Phi = 4\varepsilon\left[\left(\frac{\bar{r}_0}{r}\right)^{12} - \left(\frac{\bar{r}_0}{r}\right)^{6}\right], \qquad \frac{r_0}{\bar{r}_0} = 1.09, \tag{2.34}$$

where $\bar{r}_0$ is the zero energy distance, i.e. $\Phi(\bar{r}_0) = 0$ (Kittel, 1976). Hence, it follows from (2.9) that:

$$F = 24\varepsilon\left[2\frac{\bar{r}_0^{12}}{r^{13}} - \frac{\bar{r}_0^{6}}{r^{7}}\right] \tag{2.35}$$

The rate dependent dissipative potential is assumed as negligibly small in the present model, so that according to (2.10) the dissipative surface force is negligible too.

For the plane wave propagation in a cubic microstructure, which is assumed here for simplicity of the analysis, we can recognize four cases of interaction of a wave with the boundary. Thus with reference to Fig. 2.4 we have:

case (1) L-wave propagating normal to boundary

case (2) L-wave propagating parallel to boundary

case (3) T-wave propagating normal to boundary

case (4) T-wave propagating parallel to boundary

It is seen that a similar kind of motion is involved in cases (1) and (4) (direction of motion normal to the boundary), as well as in cases (2) and (3) (direction of motion parallel to the boundary). However, only cases (1) and (3) represent propagation of a given wave across

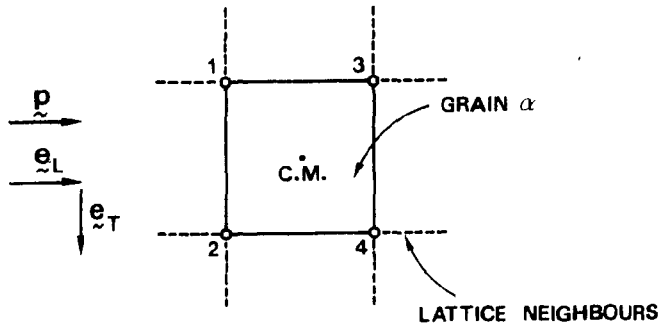

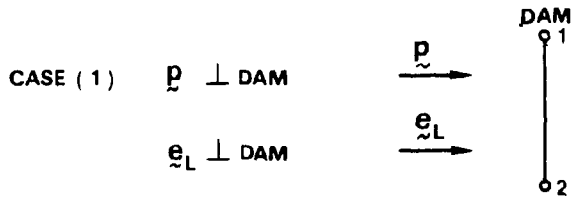

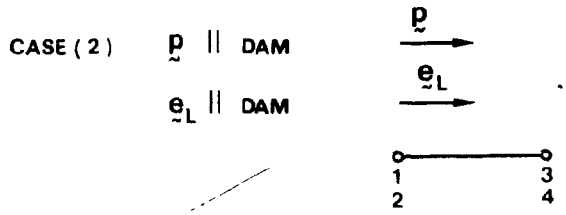

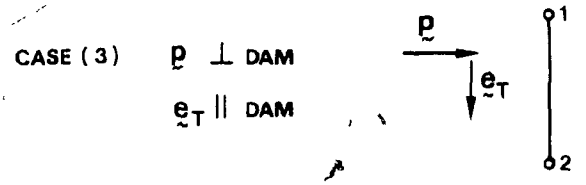

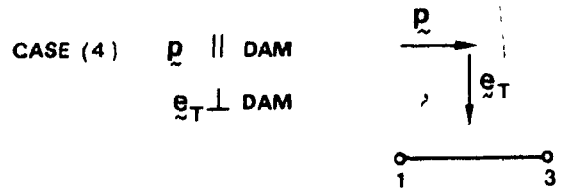

p : PROPAGATION VECTOR

e_L , e_T : DEFORMATION DIRECTIONAL UNIT VECTORS

FIG. 2.4 SCHEMATICS OF WAVE MOTION IN CUBIC MICROSTRUCTURE .

the grain boundary, which is the subject matter of this section. Hence, we shall now consider these two cases separately, assuming that the results will be equally indicative for the wave propagation parallel to the grain boundary, i.e. case (2) and (4).

(A) Motion perpendicular to the boundary ($\alpha\beta$):

The relative displacement between atomic surface layers is only the difference between the initial thickness ${}^{\alpha\beta}\underset{\sim}{\Delta}$ in the undeformed configuration and the thickness ${}^{\alpha\beta}\underset{\sim}{\delta}$ in the deformed one, i.e. following (2.6) and (2.8) we can write (Fig. 2.5a)

$$ {}^{\alpha\beta}\underset{\sim}{d} = {}^{\alpha\beta}\underset{\sim}{\delta} - {}^{\alpha\beta}\underset{\sim}{\Delta} \cong r - r_0 \qquad (2.36) $$

It follows then that the rate of change of ${}^{\alpha\beta}\underset{\sim}{d}$ in the microtime is simply:

$$ \frac{d\,{}^{\alpha\beta}\underset{\sim}{d}}{dt_m} = \frac{dr}{dt_m} \qquad (2.37) $$

Noting that the stress condition (2.32) takes the form of:

$$ {}^{\beta}\sigma_{11}^{s} = {}^{\alpha\beta}T $$

and substituting (2.35) and (2.37) into (2.33) we obtain:

$$ \frac{dr}{dt_m} = {}^{\alpha}\dot{u}_i \left[\frac{-(\chi+1)N}{{}^{\alpha}\dot{u}_i\, \rho_\beta\, \rho_c\, d^2}\, 24\varepsilon \left(2\,\frac{\bar{r}_0^{12}}{r^{13}} - \frac{\bar{r}_0^{6}}{r^{7}} \right) - 2 \right] \qquad (2.38) $$

A global analysis of this nonlinear differential equation can be avoided in the first approximation, if we note that in case of the external forces acting along the axis of the elastic interatomic bond, the response time will be very short on the t_m -time scale. Thus, the bond distance r will vary extremely fast on the real time scale

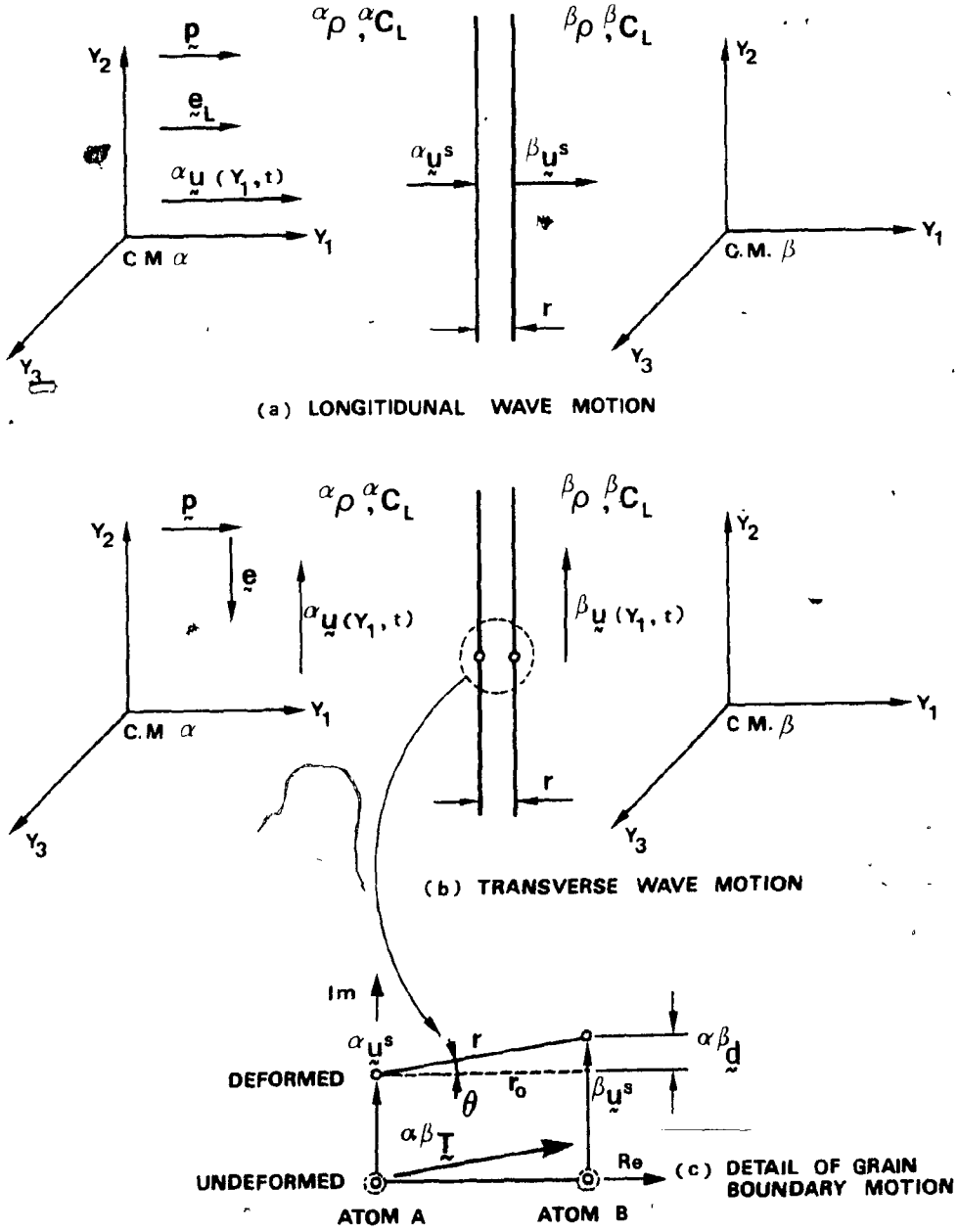

C.M.: CENTER OF MASS

FIG. 2.5 TRANSFER OF WAVE MOTION IN GRAIN BOUNDARIES

remaining around a certain constant value very close to the equilibrium* bond distance, so that the expected value is given by:

$$E\{r(t_m)\} \cong r_0 \tag{2.39}$$

Hence, we may conclude that

$$E\left\{\frac{dr}{dt_m}\right\} = \lim_{t'_m \to \alpha\tau/2} \frac{1}{2t'_m} \int_{-t'_m}^{+t'_m} \frac{dr}{dt_m}\, dt_m = 0 \tag{2.40}$$

To verify the above convergence a numerical model has been investigated (see Appendix A).

Now, considering (2.40) and (2.31), it can be seen that:

$$^{\perp}C_{tr} = \frac{2}{1+\chi} \tag{2.41}$$

$$^{\perp}C_{r} = \frac{\chi-1}{\chi+1} \tag{2.42}$$

This means that in the case of grain boundaries perpendicular to the direction of wave motion the boundaries may be considered as rigid, i.e. the transmission coefficient will be given only in terms of the random impedance ratio χ.

(B) Motion parallel to the boundary ($\alpha\beta$)

With reference to Fig. 2.5b, we assume both atoms of the bond to be moving on the parallel straight lines separated by the equilibrium distance r_0 of the bond. Thus adopting a complex plane coordinate system we can write the position equation as follows:

---

* It should be noted that in a crystal lattice the equilibrium bond distance is smaller than the equilibrium bond distance in an isolated bond due to the presence of other neighbours of the lattice.

$$i\,{}^{\alpha\beta}d + r_o = r e^{i\theta}$$

and by differentiating we obtain the velocities condition as

$$i\,{}^{\alpha\beta}\dot{d} = \dot{r} e^{i\theta} + r i\omega e^{i\theta} \qquad (2.43)$$

which is equivalent to

$$\dot{r}\cos\theta - r\omega\sin\theta = 0 \qquad (2.43')$$

and

$$\dot{r}\sin\theta + r\omega\cos\theta = {}^{\alpha\beta}\dot{d} \qquad (2.43'')$$

From (2.43') and (2.43") we arrive at the explicit form of the kinematic condition (2.29) in this type of motion, i.e.

$${}^{\alpha\beta}\dot{d} = \varphi(\dot{r}) = \dot{r}\left(\sin\theta + \operatorname{ctg}\theta\cdot\cos\theta\right), \qquad (2.44)$$

where with reference to Fig. 2.5c we have introduced the angle θ such that

$$\theta = \arccos\frac{r_o}{r}$$

Now, the explicit form of the surface stress condition (2.32) is here:

$${}^{\beta}\sigma^{s}_{1k} = {}^{\alpha\beta}T\sin\theta\,, \quad k = 2,3$$

so that the equation governing the behaviour of the bond distance r on the microtime scale t_m becomes:

$$\frac{dr}{dt_m} = {}^{\alpha}\dot{u}_i \sin\theta\left[\frac{-(\chi+1)N\sin\theta}{{}^{\alpha}\dot{u}_i\,{}^{\beta}\rho\,{}^{\beta}c}\,24\varepsilon\left(\frac{\bar{r}_o^{12}}{r^{13}} - \frac{\bar{r}_o^{6}}{r^{7}}\right) - 2\right] \qquad (2.45)$$

This is an even more complex nonlinear differential equation than that in (2.38). It is beyond the presently available experimental techniques to assess the range of variation of θ. We therefore assume that this angle will vary about the mean zero value and note that the characteristic time response will still be very short

compared to the global time scale of mechanical waves. Thus it becomes possible to assume the same asymptotic behaviour as in the perpendicular type of motion*, namely that:

$$E\{r(t_m)\} \cong r_0 \tag{2.46}$$

and hence

$$E\left\{\frac{dr}{dt_m}\right\} = \lim_{t'_m \to \alpha\tau/2} \frac{1}{2t'_m} \int_{-t'_m}^{+t'_m} \frac{dr}{dt_m}\, dt_m = 0 \tag{2.47}$$

It follows then from the above that in the case of grain boundaries parallel to the direction of wave motion, the boundaries may also be considered as rigid interfaces. The equivalent forms of the transmission coefficient resulting from (2.31) will be as follows:

$$\|C_{tr} = \frac{2}{1+\chi} \tag{2.48}$$

and that of the reflection coefficient will be according to (2.26)

$$\|C_r = \frac{\chi-1}{\chi+1} \tag{2.49}$$

It is to be noted that the case of the convergence indicated in (2.47) has been assessed using a computer model and is reported in Appendix I.

The above analysis shows that for wave propagation parallel to the grain boundary with the direction of motion either parallel to it (case (2)) or normal (case (4)), the same rigid bond and hence the rigid interface model may be assumed. However, in this case, the concept of the transmission and reflection coefficient has to be

---

* As before, we note that the crystal lattice spacing is smaller than the equilibrium bond distance in an isolated bond.

generalized to an operator in order to account for the interaction of a given wave with the grain boundary in a finite passage time ${}^{\alpha}\tau$. The analysis of this type of interaction will be extended in sections 3.4 and 4.4.

2.3 Concept of an Abstract Dynamical System $[\Omega, \mathcal{F}, \mathcal{P}, T]$ in the Representation of the Wave Motion

According to the micromechanics theory the state of a micro-element α is described by and r-dimensional state vector

$$ {}^{\alpha}\underset{\sim}{y}(t) : {}^{\alpha}y_i(t) ; \; i = 1, 2, \ldots, r \quad , \tag{2.50} $$

where r represents the number of basic mechanical parameters (see Axelrad, 1980). These parameters may be specified in general as follows:

$$ {}^{\alpha}\underset{\sim}{y}(t) = \begin{bmatrix} {}^{\alpha}\underset{\sim}{u}^{i} \\ {}^{\alpha}\underset{\sim}{u}^{s} \\ {}^{\alpha}\dot{\underset{\sim}{u}}^{i} \\ {}^{\alpha}\dot{\underset{\sim}{u}}^{s} \\ {}^{\alpha}\underset{\approx}{\sigma}^{i} \\ {}^{\alpha}\underset{\approx}{\sigma}^{s} \\ {}^{\alpha}\underset{\sim}{f} \\ \vdots \end{bmatrix} \begin{matrix} \text{internal deformation} \\ \text{surface deformation} \\ \text{internal velocity} \\ \text{surface velocity} \\ \text{internal stress} \\ \text{surface stress} \\ \text{body force} \\ \vdots \end{matrix} \tag{2.51} $$

Noting from (2.51) that the ${}^{\alpha}y_i(t)$ parameters are of either kinematic, stress, or body force type, we introduce a following definition in the microdynamics theory:

Definition 4:

The state of the microelement α is described at any instant of time t by a "dynamic state vector" ${}^{\alpha}\underset{\sim}{y}(t)$, which in general is given by:

$$ {}^{\alpha}\underset{\sim}{y}(t) = \begin{bmatrix} {}^{\alpha}x(t) \\ {}^{\alpha}\sigma(t) \\ {}^{\alpha}f(t) \\ \vdots \end{bmatrix} \begin{matrix} \text{kinematic state vector} \\ \text{stress state vector} \\ \text{body force vector} \\ \vdots \end{matrix} $$

This dynamic state vector may be considered at any fixed time as the outcome of a trial or a random experiment. Thus, in the language of probability theory (see Rényi (1970)), the entire set of possible outcomes defines the sample space Ω.

We point out the algebraic aspect here, namely that Ω is a real vector space, i.e.

$$ \Omega = \{ V, \mathbb{R}, \vec{+}, +, \times, (\cdot) \} \tag{2.52} $$

which is a system consisting of an Abelian group $\{V, \vec{+}\}$ and a field $\mathcal{F} = \{\mathbb{R}, +, \times\}$ with an identity element e. Further $(\cdot)$ is a binary operation of the elements ${}^{\alpha}\underset{\sim}{y}, {}^{\beta}\underset{\sim}{y}, \ldots \in V$ by the elements $a, b, \ldots \in \mathbb{R}$ such that ${}^{\alpha}\underset{\sim}{y} \cdot a \in \Omega$ (scalar multiplication).

In the vector space Ω the r-dimensional open sets

$$ E = \{ {}^{\alpha}y_i : y_i < {}^{\alpha}y_i < y_i + \Delta y_i \; ; \; i = 1, 2, \ldots, r \}, \quad E \subset \Omega, $$

may be identified, as belonging to a certain topology of Ω. In general, this topology is generated by an infinitely countable topological basis $\mathcal{T}$ of the following sets:

$$ {}^{n}E = \left\{ {}^{n}\underset{\sim}{\nu} < {}^{\alpha}\underset{\sim}{\nu} < {}^{n}\underset{\sim}{\nu} + \Delta^{n}\underset{\sim}{\nu} \right\} ; \quad n \in Z^{+}, \; {}^{n}E \subset \Omega . $$

Thus $\{\Omega, \mathcal{T}\}$ becomes a topological vector space, and in case ${}^{\alpha}\nu_i$ in equation (2.50) are real valued, Ω has the familiar $\mathbb{R}^r$-topology. If $\mathcal{F}$ is a σ-algebra generated by the basis $\mathcal{T}$ we have a measurable topological space $\{\Omega, \mathcal{F}\}$ which is called an experiment $\mathcal{E}$ in probability theory. The minimal σ-algebra $\mathcal{F}$ which contains all open sets E is called the Borel σ-algebra of Ω, and the elements of $\mathcal{F}$ are called Borel sets.

However, due to experimental accuracies that can be achieved, the outcome ${}^{\alpha}\underset{\sim}{\nu}$ at a specific time of the α-th trial annot be determined exactly, but only within a certain finite range $\Delta^{s}\nu$, $s \in$ finite subset of Z^{+}. It is seen that such "window sets":

$$ {}^{s}E = \left\{ {}^{s}\underset{\sim}{\nu} < {}^{\alpha}\underset{\sim}{\nu} < {}^{s}\underset{\sim}{\nu} + \Delta^{s}\underset{\sim}{\nu} \right\} ; \quad s = 1,2,\ldots,S ; \quad S - \text{finite} $$

give rise to topology $\mathcal{T}_s$ which is weaker than $\mathcal{T}$ topology. The σ-algebra $\mathcal{F}_s$ generated by the basis $\mathcal{T}_s$ is identified as a sub-σ-algebra of $\mathcal{F}$.

While the analysis in probabilistic mechanics is usually conducted in the $\{\Omega, \mathcal{F}\}$ space it is supposed that the results (e.g. probability distributions) are congruent to the physically measurable information in $\{\Omega, \mathcal{F}_s\}$.

In accordance with the definition of the event ${}^{s}E$ we can now introduce the probability measure on $\mathcal{F}$ defined as follows:

$$ P^{\underset{\sim}{\nu}} = P\{{}^{s}E(\underset{\sim}{\nu})\} = P\left\{ {}^{s}\underset{\sim}{\nu} < {}^{\alpha}\underset{\sim}{\nu} < {}^{s}\underset{\sim}{\nu} + \Delta^{s}\underset{\sim}{\nu} \right\} ; \quad P\{\Omega\} = 1 . \qquad (2.54) $$

$P^{\underset{\sim}{\nu}}$ is readily recognized to be a σ-additive Borel measure.

The experiment $\mathcal{E}$ together with $P^{\underset{\sim}{\nu}}$ forms a triple $\{\Omega, \mathcal{F}, P^{\underset{\sim}{\nu}}\}$ or so-called space of elementary events.

We now introduce a random variable $\underset{\sim}{\xi}$ defined as an $\{\Omega, \mathcal{F}\}$ - measurable function:

$$\underset{\sim}{\xi} : \{\Omega, \mathcal{F}\} \rightarrow \{\mathfrak{X}, \mathcal{B}\}, \tag{2.55}$$

where $\mathfrak{X}$ is the state space and $\mathcal{B}$ is the Borel σ-algebra in $\mathfrak{X}$. In accordance with the micromechanics theory (see Axelrad, 1983) we consider an elementary outcome ${}^{\alpha}\underset{\sim}{\nu} \in \Omega$ to be described by the corresponding point x of the state space $\mathfrak{X}$. This means that, if $\Omega = \mathfrak{X}$, $\mathcal{F} = \mathcal{B}$, and the function $\underset{\sim}{\xi} = \underset{\sim}{\xi}(x)$ has the form $\underset{\sim}{\xi}(x) = x, x \in \mathfrak{X}$, then the random variable $\underset{\sim}{\xi}(\underset{\sim}{\nu})$ is called a directly given random variable (see Prohorov and Rozanov (1969)). Hence, it is seen why in the probabilistic micromechanics theory the state space $\mathfrak{X}$ is identified with the probabilistic function space.

We shall always suppose that our probability space may be extended to be complete whenever this is needed.

Various topologies may be defined in $\mathfrak{X}$, and we defer the consideration of this feature until the next section, where the analysis is restricted to the kinematic subspace of $\mathfrak{X}$. It can be seen, however, that the specific topology in $\mathfrak{X}$ allows an analysis in terms of continuous functions over $\mathfrak{X}$, which is in contrast to the notion of continuity in the physical domain of the material body, as assumed in the classical mechanics of solids (see the discussion in Sections 1.2 and 2.1). It is of interest to point out that in order to conduct a rigorous analysis in deterministic continuum mechanics, the topology of the state space has also to be considered

(see Knops and Wilkes (1973)). In fact, the analysis of a mechanical system and its evolution in the state space, has been introduced for the first time by Poincaré (1881), in analytical dynamics, which is strictly a deterministic treatment. Let us then recall the formulation of an abstract dynamical system in a deterministic setting:

Definition 5:

A dynamical system corresponding to a triple $(T, \mathcal{T}, \mathcal{X})$ is a set $\mathcal{B}(T, \mathcal{X})$ of functions defined on T taking values in $\mathcal{X}$ such that

(i) $\varphi_\tau \in \mathcal{B}(T, \mathcal{X})$ whenever $\varphi \in \mathcal{B}(T, \mathcal{X})$, $\tau \in \mathcal{T}$,

(ii) $\lim_{t \to 0} \varphi_\tau(t) = \varphi(\tau)$, $\varphi \in \mathcal{B}(T, \mathcal{X})$, $\tau \in \mathcal{T}$.

In the above notation T is a locally compact semi-group with identity 0, which is usually taken as $\mathbb{R}^+ \cup \{0\}$, $\mathcal{T}$ is a subset of T, and $\mathcal{X}$ an arbitrary set containing all the relevant dependent variables. Furthermore, if φ is a motion in the function space $\mathcal{B}(T, \mathcal{T})$ and φ_τ its translate, this formulation enables one to trace the motion in time along a path or trajectory in the phase space. These trajectories are fixed in the phase space, which distinguishes thus a deterministic system from a probabilistic one. Hence, in the microdynamics theory we shall work only with the probability of an outcome to be in a given set at a fixed time t_0, and thus, the evolution of this set at a later time $t_0 + \Delta t$ has to be investigated in terms of a certain transition operator. Whilst in the deterministic theory one defines invariant sets, here the consideration of an invariant measure of a set is of a fundamental importance (see Oxtoby and Ulam (1941) and Balescu (1974)).

Let us introduce a mapping $T = T[\underset{\sim}{\nu}]$ of the set Ω onto itself, and denote for each $E \subset \Omega$ by $T^{-1}[E]$ the set of those $\underset{\sim}{\nu} \in \Omega$ for which $T[\underset{\sim}{\nu}] \in E$. Thence, following Rényi (1970), we come to the following definition:

Definition 6:

The mapping $T = T[\underset{\sim}{\nu}]$ of Ω onto itself such that for each $E \subset \Omega$ one has $T^{-1}[E] \in \mathcal{F}$ and further:

$$P^{\underset{\sim}{\nu}}\{T^{-1}[E]\} = P^{\underset{\sim}{\nu}}[E] \tag{2.56}$$

is called a measure-preserving transformation of the probability space $\{\Omega, \mathcal{F}, P^{\underset{\sim}{\nu}}\}$; the probability measure $P^{\underset{\sim}{\nu}}$ is called invariant under the transformation T; the system $\{\Omega, \mathcal{F}, P^{\underset{\sim}{\nu}}, T\}$ is called an abstract dynamical system.

The principal advantage of identifying a measure perserving transformation T in the probabilistic analysis is that it allows a formulation of the physical process as a stationary random process. However, the measure preserving property is not absolutely necessary for a more general definition of an abstract dynamical system in the case of a Markov process formulation. In order to establish such a formulation (see Chapter III) we shall now specialize our general dynamical system to model the evolution in the kinematic subspace of the general state space.

2.4 Kinematic Space as a Probabilistic Function Space

Let us recall from definition 4, that the dynamic state vector can be decomposed in the following fashion:

$$ {}^{\alpha}\underset{\sim}{y} = \begin{bmatrix} {}^{\alpha}\underset{\sim}{x} \\ {}^{\alpha}\underset{\sim}{\sigma} \\ {}^{\alpha}\underset{\sim}{f} \end{bmatrix} \qquad (2.57) $$

where we have omitted the energy density and where the time dependence is assumed implicitly . The three components of the state vector may be considered to belong to their respective spaces or subspaces of $\mathfrak{X}$ as follows:

$ {}^{\alpha}\underset{\sim}{x} \in \mathcal{K}$ — kinematic space

$ {}^{\alpha}\underset{\sim}{\sigma} \in \Sigma$ — stress space

$ {}^{\alpha}\underset{\sim}{f} \in F$ — body force space,

which are disjoint subspaces of the general state space $\Omega = \mathfrak{X}$ and where:

$$ \mathcal{K} \cup \Sigma \cup F = \mathfrak{X} $$

From now on, we assume that the body forces can be neglected, i.e. that:

$$ \underset{\sim}{f} \equiv \underset{\sim}{0} \qquad (2.58) $$

for simplicity.

The general form of expression (2.51) permits without loss of generality the two remaining vector components of ${}^{\alpha}\underset{\sim}{y}$ to be written as follows:

$$
{}^{\alpha}\underset{\sim}{\chi} = \begin{bmatrix} {}^{\alpha}\underset{\sim}{u}^{i} \\ {}^{\alpha}\underset{\sim}{u}^{s} \\ {}^{\alpha}\underset{\sim}{\dot{u}}^{i} \\ {}^{\alpha}\underset{\sim}{\dot{u}}^{s} \\ {}^{\alpha}\underset{\approx}{\varepsilon}^{i} \\ {}^{\alpha}\underset{\approx}{\varepsilon}^{s} \\ \cdot \\ \cdot \\ \cdot \\ \cdot \end{bmatrix} \quad \begin{array}{ll} \text{internal deformation} ; & {}^{\alpha}\underset{\sim}{u}^{i} \in \mathcal{U}^{i} \\ \text{surface deformation} ; & {}^{\alpha}\underset{\sim}{u}^{s} \in \mathcal{U}^{s} \\ \text{internal velocity} ; & {}^{\alpha}\dot{u}^{i} \in \mathcal{V}^{i} \\ \text{surface velocity} ; & {}^{\alpha}\dot{u}^{s} \in \mathcal{V}^{s} \\ \text{internal strain} ; & {}^{\alpha}\underset{\approx}{\varepsilon}^{i} \in \mathcal{E}^{i} \\ \text{surface strain} ; & {}^{\alpha}\underset{\approx}{\varepsilon}^{s} \in \mathcal{E}^{s} \\ \text{accelerations} ; & \\ \cdot & \\ \cdot & \\ \cdot & \end{array} \Bigg\} \quad (2.59)
$$

$$
{}^{\alpha}\underset{\sim}{\sigma} = \begin{bmatrix} {}^{\alpha}\underset{\approx}{\sigma}^{i} \\ {}^{\alpha}\underset{\approx}{\sigma}^{s} \end{bmatrix} \quad \begin{array}{ll} \text{internal stress} ; & {}^{\alpha}\underset{\approx}{\sigma}^{i} \in \Sigma^{i} \\ \text{surface stress} ; & {}^{\alpha}\underset{\approx}{\sigma}^{s} \in \Sigma^{s} \end{array} \Bigg\} \quad (2.60)
$$

where in the above forms, $\mathcal{U}, \mathcal{V}, \ldots$ etc. are the corresponding subspaces of the components of these vectors.

In the above we have introduced the particular subspaces to which the components of ${}^{\alpha}\underset{\sim}{\chi}$ and ${}^{\alpha}\underset{\sim}{\sigma}$ belong, and all of which are real vector spaces contained in the Ω space (vide (2.52)).

It is seen from relations (2.59) and (2.60) that two distinct types of field variables are involved in the description of the mechanical state of a microelement, namely those concerning internal behaviour and other related to the interaction phenomena. We recall that in micromechanics (Axelrad, 1978) two types of operators are introduced:

$$
{}^{\alpha}\overset{\circ}{A} : \Sigma^{i} \to \mathcal{U}^{i} \; ; \quad {}^{\alpha\beta}B : \Sigma^{s} \to \mathcal{U}^{s}, \qquad (2.61)
$$

which relate to the internal and interaction effects, respectively. In microdynamics of discrete media such as polycrystalline solids these operators in the linear case are tensors of the third order so that we have:

$$ {}^{\alpha}\underset{\sim}{u}^{i} = {}^{\alpha}\underset{\approx}{A}\,{}^{\alpha}\underset{\approx}{\sigma}^{i} \quad , \qquad {}^{\alpha}\underset{\sim}{u}^{s} = {}^{\alpha\beta}\underset{\approx}{B}\,{}^{\alpha}\underset{\approx}{\sigma}^{s} \tag{2.62} $$

In general a microelement material operator (Axelrad, 1978) can be defined as:

$$ {}^{\alpha}M : \Sigma \to \mathcal{U} \quad \text{such that} \quad {}^{\alpha}M = {}^{\alpha}M\left({}^{\alpha}\underset{\approx}{A}, {}^{\alpha\beta}\underset{\approx}{B}\right) \tag{2.63} $$

Using the strong monotonicity condition it was found by Basu, (1975) that the operator M is invertible, i.e. that there exists a mapping:

$$ {}^{\alpha}M^{-1} : \mathcal{U} \to \Sigma \tag{2.64} $$

This implies that not only the deformation space $\mathcal{U}$ is in a one-to-one relation to the space Σ but also the strain space $E = E^{i} \cup E^{s}$.

The above discussion indicates that one can, in general, restrict the analysis to one of the subspaces $\mathcal{K}$ or Σ, since a bijection exists between the main components of $\mathcal{K}$ and the stresses. Considering that the stress states are not experimentally verifiable in contrast to the kinematic states which can be observed, we decide to work in the kinematic space from now on.

It is now important to establish a topology of the $\mathcal{K}$ space. We have to consider the continuity of the displacement and stress fields involved in the transient wave motion. We recall from elastodynamics that the wavefront is a moving surface across which some of the field variables and/or their derivatives are discontinuous. If the velocity is allowed to be discontinuous, then the stress is discontinuous too (see Bland, 1969), and we have a shock wave. However, in order to describe such waves fully, a discussion of the thermodynamics involved would be necessary and that is outside the scope of this thesis. We consider therefore surfaces only across which

the velocity and hence the stress are continuous. For this purpose we take at the mesoscale:

$$ {}^{M}\underset{\sim}{\dot{u}}^{i},\ {}^{M}\underset{\sim}{\dot{u}}^{s},\ {}^{M}\underset{\approx}{\dot{\sigma}}^{i},\ {}^{M}\underset{\approx}{\dot{\sigma}}^{s} \in C({}^{M}\bar{\mathcal{D}}),\quad {}^{M}\bar{\mathcal{D}} = \bigcup_{\alpha=1}^{\nu} {}^{\alpha}\bar{\mathcal{D}} \tag{2.65} $$

where we assume that mesodomain ${}^{M}\bar{\mathcal{D}}$ is a simply connected, domain and subset of $\mathbb{R}^3$. We note that (2.65) implies the continuity of the internal and surface deformations, viz:

$$ {}^{M}\underset{\sim}{\dot{u}}^{i},\ {}^{M}\underset{\sim}{\dot{u}}^{s} \in C({}^{M}\bar{\mathcal{D}}) \tag{2.66} $$

Moreover, by virtue of the Hookean stress-strain relations for an isotropic elastic solid (vide Def. 1) the strains are given as:

$$ {}^{M}\underset{\approx}{\dot{\varepsilon}}^{i},\ {}^{M}\underset{\approx}{\dot{\varepsilon}}^{s} \in C({}^{M}\bar{\mathcal{D}}) \tag{2.67} $$

although the accelerations may be discontinuous.

Indeed, if

$$ {}^{M}\underset{\sim}{\ddot{u}}^{i},\ {}^{M}\underset{\sim}{\ddot{u}}^{s} \in D({}^{M}\bar{\mathcal{D}}) \tag{2.68} $$

then we have an acceleration wave.

We see that we need a means for expressing the "degree of smoothness" of all these field quantities. We can do this best by employing the notion of Sobolev spaces (see Oden, 1979 and Rudin, 1973). Thus, a Sobolev space of order m, p ($m \geq 0$) denoted by $W_p^m(X)$ is defined as the function space:

$$ W_p^m(X) = \{ f \in \mathcal{D}'(X) \ : f \text{ and all of its distributional partial derivatives of order} \leq m \text{ are in } L_p(X),\ p \geq 1 \} \tag{2.69} $$

where - X is a simply connected, open subset of $\mathbb{R}^n$

- $\mathcal{D}'(X)$ is the space of distributions
- $L_p(X)$ is a Lebesque space

The distributional partial derivatives of f are defined by:

$$D^{\underset{\sim}{s}} f \equiv \frac{\partial^{\sum s_i} f}{\prod_i \partial^{s_i} x_k} \in L_p(X), \quad |\underset{\sim}{s}| = |\sum_i s_i| \leq m, \qquad (2.70)$$

$$\underset{\sim}{s} = (s_1, s_2, \ldots) \in Z^+$$

$$\underset{\sim}{x} = (x_1, x_2, \cdots, x_k, \cdots, x_n) \in \mathbb{R}^n$$

A norm in a Sobolev space is then defined by:

$$\|f\|_{W_p^m(X)} = \left\{ \int_X \sum_{|\underset{\sim}{s}| \leq m} |D^{\underset{\sim}{s}} f|^p dx \right\}^{\frac{1}{p}} = \left\{ \sum \|D^{\underset{\sim}{s}} f\|^p_{L_p(X)} \right\}^{\frac{1}{p}} \qquad (2.71)$$

Since we place no requirements on the continuity of accelerations we shall henceforth assume (2.68) to hold in general. Thus, with reference to Fig. 2.6 which represents a one-dimensional situation, we have

$$\left.\begin{aligned} &{}^M\underset{\sim}{u}^i \in H^2({}^M\mathcal{D}) \\ &{}^M\underset{\sim}{\varepsilon}^i \in H^1({}^M\mathcal{D}) \\ &{}^M\dot{\underset{\sim}{u}}^i \in H^1({}^M\mathcal{D}) \\ &{}^M\ddot{\underset{\sim}{u}}^i \in H^0({}^M\mathcal{D}) \\ &{}^M\dddot{\underset{\sim}{u}}^i \in H^{-1}({}^M\mathcal{D}) \end{aligned}\right\} \qquad (2.72)$$

where a Hilbertian Sobolev space $H^m(X)$ has been identified for the domain ${}^M\mathcal{D} \subset \mathbb{R}^1$. It is defined as follows:

$$H^m(X) \equiv W_2^m(X) \qquad (2.73)$$

Now it is natural to choose a Hilbert space of boundary functions for the surface components of the kinematic state vector ${}^M\underset{\sim}{\chi}$. We recall that if φ is a boundary function such that

$$\varphi \in L_2(\partial X) \qquad (2.74)$$

we can define the following norm:

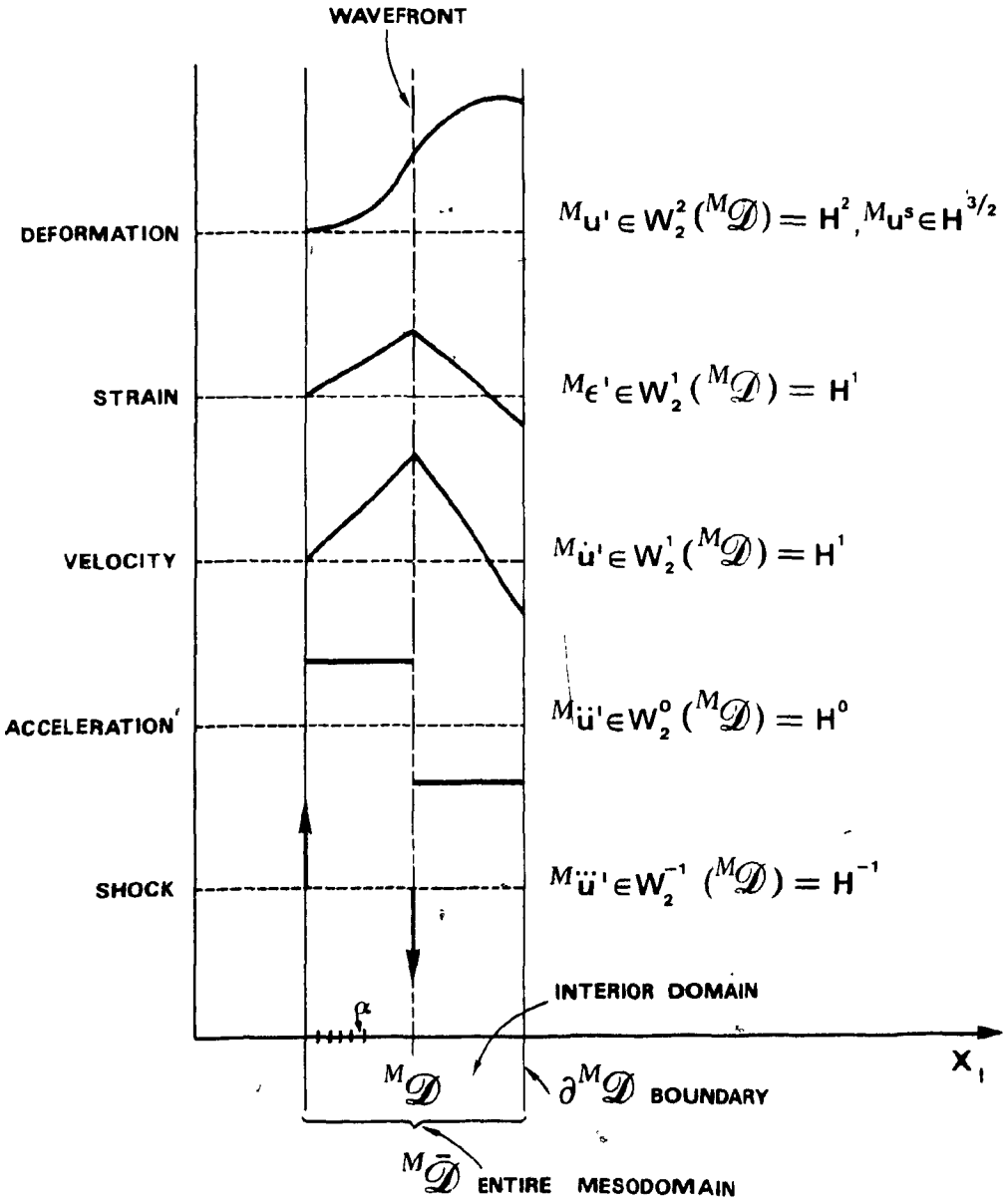

FIG. 2.6 THE ACCELERATION WAVE IN A HILBERTIAN SOBOLEV SPACE REPRESENTATION FOR AN ENSEMBLE OF MICROELEMENTS ($\alpha = 1, .., \mu$)

$$\|\varphi\|_{H^{m-j-1/2}(\partial X)} \equiv \inf_{f \in H^m(X)} \{ \|f\|_{H^m(X)} ; \varphi = \gamma_j f \} \tag{2.75}$$

where γ_j is the trace operator defined as:

$$\gamma_j f \equiv \frac{\partial^j f}{\partial n^j}\Big|_{\partial X} , \quad 0 \leq j \leq m-1$$

It follows that the completion of the $L_2(X)$ space in the norm (2.75) is a Hilbert space of boundary functions

$$H^{m-j-1/2}(\partial X), \quad 0 \leq j \leq m-1 \tag{2.76}$$

Hence, the surface components of ${}^M\underset{\sim}{x}$ in the one-dimensional case, are found to belong to the following spaces:

$$\left.\begin{aligned} &{}^M\underset{\sim}{u}^s \in H^{3/2}(\partial {}^M\mathcal{D}) \\ &{}^M\underset{\approx}{\varepsilon}^s \in H^{1/2}(\partial {}^M\mathcal{D}) \\ &{}^M\dot{\underset{\sim}{u}}^s \in H^{1/2}(\partial {}^M\mathcal{D}) \\ &{}^M\ddot{\underset{\sim}{u}}^s \in H^{-1/2}(\partial {}^M\mathcal{D}) \\ &{}^M\dddot{\underset{\sim}{u}}^s \in H^{-3/2}(\partial {}^M\mathcal{D}) \end{aligned}\right\} \tag{2.77}$$

In the two-dimensional and three-dimensional cases, that is for ${}^M\bar{\mathcal{D}} \subset \mathbb{R}^2$ and $\mathbb{R}^3$ respectively, the components of the ${}^M\underset{\sim}{x}$ vector must be placed in other spaces. For this purpose we may employ the imbedding theorem (see Sobolev, 1963) which indicates the order of the $W_p^m(X)$ space whose elements are continuous functions in $X \subset \mathbb{R}^n$. Thus for $n = 2$ or 3 and $p = 2$ the order m must satisfy the inequality $m > \frac{n}{p} = \frac{2}{2}$ or $\frac{3}{2}$ so that $m = 2$ must be chosen for the space of deformation rates in case of acceleration waves, i.e.

$${}^M\dot{\underset{\sim}{u}}^i \in H^2({}^M\mathcal{D})$$
$${}^M\ddot{\underset{\sim}{u}}^i \in H^1({}^M\mathcal{D})$$

so that

$$ {}^{M}\underset{\sim}{u}^{i} \in H^{3}({}^{M}\mathcal{D}) $$

$$ {}^{M}\underset{\approx}{\varepsilon}^{i} \in H^{2}({}^{M}\mathcal{D}) $$

It follows then that the spaces of boundary values will be:

$$ {}^{M}\underset{\sim}{u}^{s} \in H^{5/2}(\partial {}^{M}\mathcal{D}) $$

$$ {}^{M}\dot{\underset{\sim}{u}}^{s} \in H^{3/2}(\partial {}^{M}\mathcal{D}) $$

$$ {}^{M}\ddot{\underset{\sim}{u}}^{s} \in H^{1/2}(\partial {}^{M}\mathcal{D}) $$

It is seen that the imbedding theorem is to be used to determine the particular subspaces of the $\mathcal{K}$-space for the waves which are weaker than the acceleration waves.

We may note, in passing, that all these field quantities being in the Hilbert spaces are elements of a more general Banach space, which agrees with the findings of Axelrad, 1979, that one works most frequently with this type of a topological vector space in the probabilistic micromechanics of solids. Returning to the chosen microscale, we have ${}^{\alpha}\underset{\sim}{\chi} \in L_{2}({}^{\alpha}\mathcal{D})$ representing the vector of measurable kinematic quantities and where ${}^{\alpha}\underset{\sim}{\chi}$ are actually the equivalence classes of functions over the ${}^{\alpha}\mathcal{D}$ domain. If we recall that $\{\Omega, \mathcal{F}, \mathcal{P}^{\chi}\}$ is a complete probability space, and let $\{\mathcal{K}, \mathcal{F}_{\mathcal{K}}\}$ be a measurable space where $\mathcal{F}_{\mathcal{K}}$ is the σ-algebra of all Borel subsets of $\mathcal{K}$, then following a formalism of Bharucha-Reid, 1972 we can give the following definition:

Definition 7:

A mapping ${}^{\alpha}\chi : \Omega \to \mathcal{K}$ is said to be a random variable with values in $\mathcal{K}$, if the inverse image under the mapping ${}^{\alpha}\chi$ of every Borel set E belongs to $\mathcal{F}_{\mathcal{K}}$; that is,

$${}^{\alpha}\underset{\sim}{\chi}^{-1}[E] \in \mathcal{F}_{\mathcal{K}} \text{ for all } E \in \mathcal{F}_{\mathcal{K}}.$$

This is equivalent to saying that ${}^{\alpha}\underset{\sim}{\chi}$ is a Banach space-valued Borel measurable function; the $\mathcal{K}$-space is separable.

The ${}^{\alpha}\underset{\sim}{\chi}$ mapping along with other associated transformations is presented in Fig. 2.7.

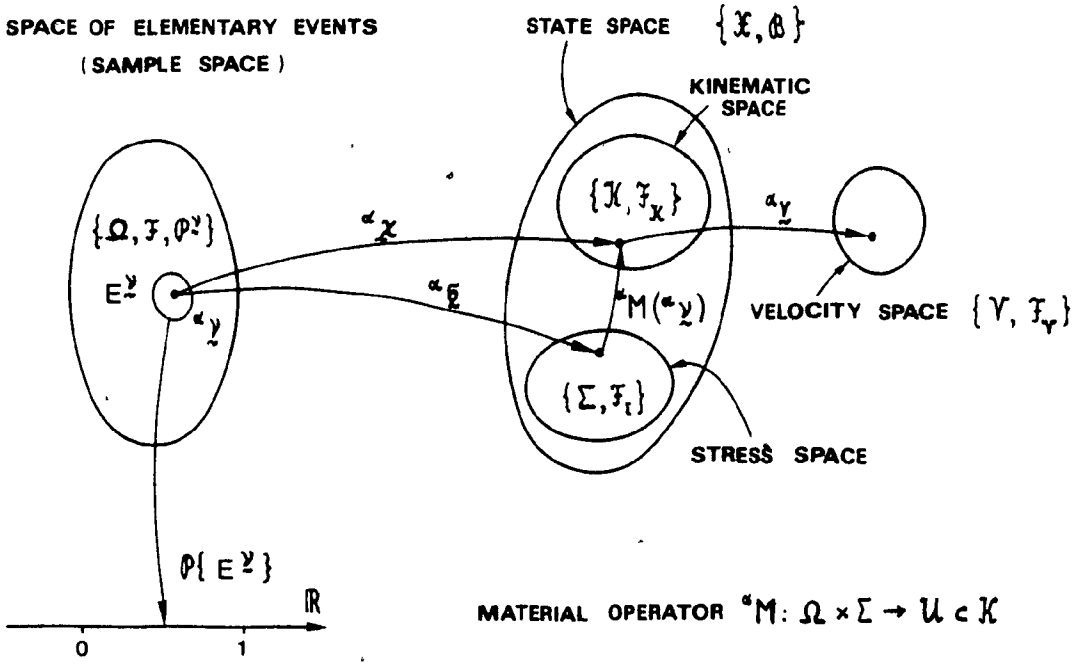

FIG. 2.7 STRUCTURE OF THE PROBABILISTIC FUNCTION SPACE EMPLOYED IN MICRODYNAMICS

CHAPTER III

MARKOV FIELD FORMULATION OF THE WAVE PROPAGATION

3.1 Introduction

3.1.1 Random field of the wave motion in the 3-D space-time

It has been pointed out in Postulate 2, that all the field variables in the mechanics of solids are of a random nature. This fact can be stated in a mathematical language by saying that the dynamic state vector as a function of space and time is a random field (R.F.), i.e.:

$$\underset{\sim}{y}(\underset{\sim}{X},t): \mathbb{R}^3 \times \mathcal{T} \times \Omega \rightarrow \Omega \equiv \mathfrak{X} \; ; \; \underset{\sim}{X} \in M \subset \mathbb{R}^3, \; t \in \mathcal{T} \qquad (3.1)$$

This kind of description of the mechanical behaviour of matter has been employed for the first time by Kolmogorov (1941), in his statistical theory of turbulence and later by Lévy (1956), in his studies of the Brownian motion. This gave an impetus to new developments, both in fluid mechanics and random field theory (see for instance Yaglom, 1957). It is important to note, that the random field theory of fluids had to be restricted to isotropic homogeneous turbulence and was usually confined to correlation studies. Generally speaking, this approach suffered from a lack of an evolution theory.

It was pointed out in Section 2.3 that an identification of a measure preserving transformation, if it can be done, permits the description of a stationary random process in terms of Markov theory. More generally, however, a causality relation pertaining to the state space leads to an arbitrary non-stationary Markov process, which in

turn, permits a very neat evolution relation by means of the Chapman-Kolmogorov relation.

At this point we recall from section 1.2, that the wave motion in an elastic continuum is governed by a differential equation of the second order with respect to time or:

$$\mu\, u_{i,jj} + (\lambda+\mu)\, u_{j,ji} + \rho f_i = \rho \ddot{u}_i \qquad (1.4)$$

where λ and μ are the well-known Lamé constants. This relation indicates that in order to ensure the Markovian character in a stochastic theory of wave propagation, we should consider a random process $\{{}^{\alpha}\underset{\sim}{u}(t), {}^{\alpha}\dot{\underset{\sim}{u}}(t)\}$. This means focusing the attention on the $\{{}^{\alpha}\dot{\underset{\sim}{u}}(t)\}$ process, whereby the deformation can always be obtained*. Thus, from now on we choose the deformation rate to be our intrinsic random variable, which we shall denote

$${}^{\alpha}\dot{\underset{\sim}{u}}(t) \equiv {}^{\alpha}\underset{\sim}{v}(t), \qquad (3.2)$$

and call the wave velocity vector.

Considering the dynamic motions in a discrete solid, unfortunately not much can be said about the probabilistic laws governing the evolution of a specific microelement in time. By this we mean, that for a random process:

$${}^{\alpha}\chi(t): \mathcal{T} \times \Omega \to \mathcal{K}, \quad \alpha \text{ - fixed} \qquad (3.3)$$

no meaningful equation can be established and integrated (see also Chapter XIV in Yosida, 1978), because the boundary $\partial^{\alpha}\mathcal{D}$ of the microelement α is not fixed in the $\mathbb{R}^3$ space.

However, we can consider the wave motion from another point of

---

* In our physical world the knowledge of positions and velocities determines the future, i.e. accelerations are not necessary for the determination of the future.

view, i.e. one which is analogous to the transport theory approach. The transport theory itself (see Ishimaru, 1978, and Uscinski, 1977) has been developed heuristically in that, it deals with the transport of energy through a medium via the averaged statistical quantities such as the specific intensity and energy flux. With reference to our discussion in Section 2.1 of the deterministic versus probabilistic approach, we shall construct here a rigorous probabilistic theory of the wave propagation in a random discrete solid.

3.1.2 Problem formulation for the wavefront propagation

We recall from Section 2.2.2 that the problem under consideration is one of plane waves propagating in the macroscopic body domain with a cubic microstructure, where the propagation vector is parallel to one of the axes of this lattice (Fig. 2.2). In this chapter we shall study the dynamic response of a macroscopic body M taken as a bar of an arbitrary uniform cross-section with a microstructure as defined earlier. Furthermore, we assume the pulses are applied uniformly to the front face of the bar. With reference to Fig. 3.1 we can now consider the bar to be composed of layers $\mathcal{U}(X_1)$ in the planes normal to the X_1 axis, or alternatively of sequences S_k lying parallel to the X_1 axis. It follows that there will be an equal number of grains in every layer $\mathcal{U}(X_1)$ as well as an equal number of grains in every sequence S_k. Hence, if we denote the entire bar by M we shall have:

$$\left.\begin{aligned} M &= \bigcup_{k=1}^{K} S_k \,, && \text{(a)} \\ M &= \bigcup_{n=1}^{N} \mathcal{U}_n \,. && \text{(b)} \end{aligned}\right\} \quad (3.4)$$

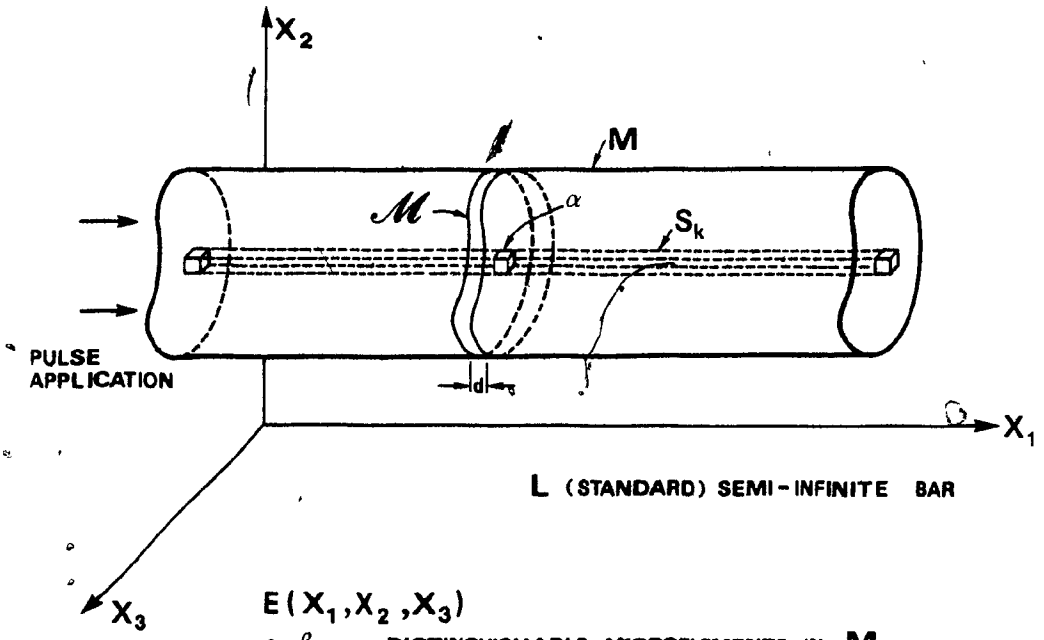

$E(X_1, X_2, X_3)$

$\alpha, \beta, \cdots$ - DISTINGUISHABLE MICROELEMENTS IN M

M - DOMAIN OF THE BAR (MACRO-MATERIAL BODY)

S_k - AN ARBITRARY SEQUENCE IN M ($k = 1, \ldots, K$)

$\mathcal{M}_n$ - AN ARBITRARY DOMAIN OF THICKNESS d (CRYSTAL SIZE) IN M

FIG. 3.1 MODEL FOR LONGITIDUNAL WAVE PROPAGATION IN A POLYCRYSTALLINE SOLID (CUBIC STRUCTURE).

The wave propagation is considered in this model of the semi-infinite bar up to a standard specified length L = 1m.

We study now the wave propagation due to a pulse at the front face, where:

$$\underset{\approx}{\sigma} \cdot \underset{\sim}{n} \Big|_{X_1=0} = P(t) \qquad (3.5)$$

Such an initial boundary value condition will give rise to a combination of longitudinal and transverse waves that will propagate in the X_1 direction independent of each other. We recognize however, that due to the multiple scattering, any single wave will soon evolve as a complicated macrodisturbance propagating in the X_1 direction and will also largely depend on the X_2 and X_3 position coordinates. However, since the medium is assumed to consist of microelements governed by the linear elastic law (recall Def. 1) thus excluding memory effects and long range forces, but admitting nonconservative effects in the grain boundaries, the wave propagation process can be characterized by the evolution of any single wavefront as it propagates through the microstructure. Thus, rather than studying response of the bar due to condition (3.5), we shall follow one wavefront due to a following initial boundary value condition:

$$\underset{\approx}{\sigma} \cdot \underset{\sim}{n} \Big|_{\substack{X_1=0 \\ t_0=0}} = P(t_0) \qquad (3.6)$$

3.2 Longitudinal Wave Propagation in the 1-D Model of the Solid

For the purpose of an initial formulation we consider a more simplified model here. Thus, we assume the microelements of the structure to interact with each other in the X_1 direction only. It follows, that the entire bar M may be considered as an ensemble of non-interacting sequences S_k. Hence, the only kind of wave, that can be realistically modelled here is a longitudinal wave. Thus the

stress boundary condition (3.6) simplifies to the following form:

$$\sigma_{11}(X_1,t)\big|_{X_1=0} = -P(t_0) \qquad (3.6')$$

It is obvious now, that a longitudinal wave generated at the front face of M will propagate independently through every sequence $S_k \in M$ and undergo a random evolution due to the random physical properties of the microelements. Considering that the statistics of these physical properties were assumed to be space homogeneous, it suffices to study the wavefront propagation in a typical sequence $S_k \in M$.

It is to be expected, that due to the variation of mechanical properties from one grain to another, the incident wave will result in a transmitted and a reflected part. However, since these variations are not large (vide Def. 1), already the primary reflected waves are at least one order of magnitude smaller, and thus the wave reflections at the internal grain boundaries can be taken as negligibly small.

It is illuminating to draw a space-time graph for the wavefront propagation process in a typical sequence $S_k \in M$, see Fig. 3.2. Such a pulse is represented by a so-called sample path, which in the 1-D model is a line composed of minute propagation paths in consecutive microelements (short straight lines). We distinguish two very important effects taking place in the model:

Effect I: the transmitted wave velocity ${}^{\beta}\underset{\sim}{V}$ is different from the incident wave velocity ${}^{\alpha}\underset{\sim}{V}$ due to the presence of the boundary $(\alpha\beta)$ (dam),

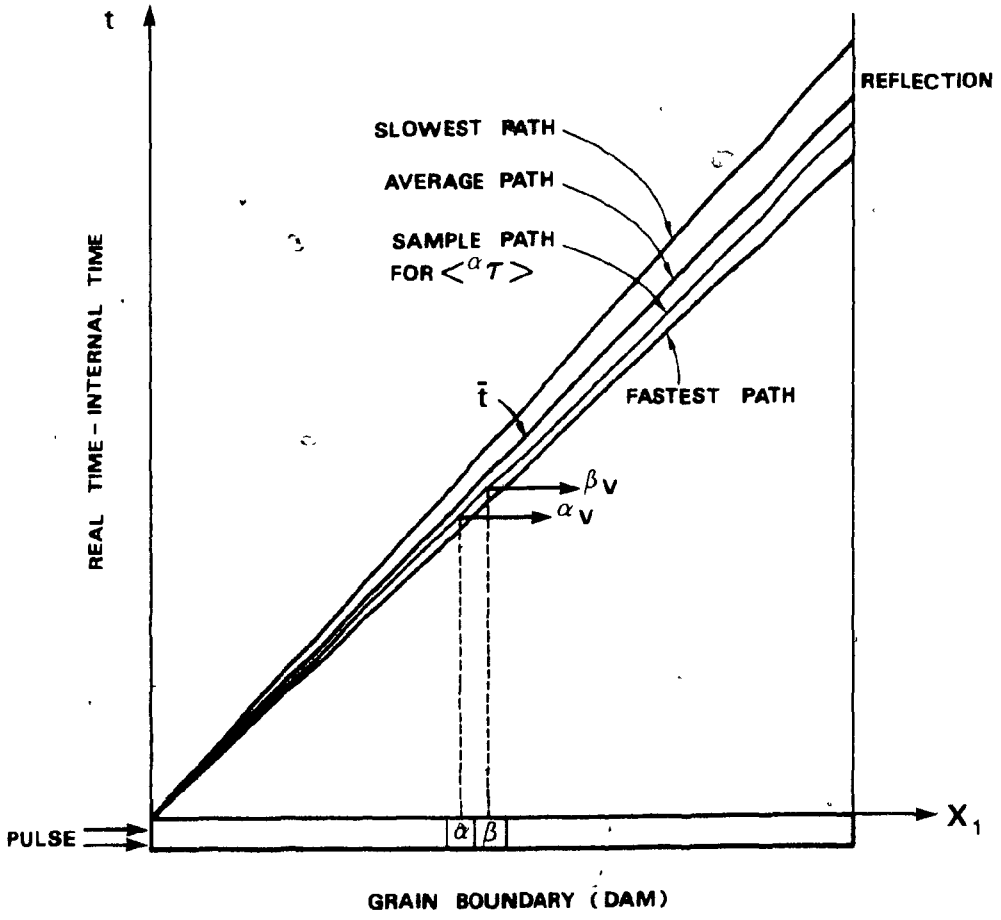

FIG. 3.2 TIME-SPACE GRAPH AND SAMPLE PATH OF L-WAVE IN 1-D MODEL.

Effect II: the wave propagation velocity ${}^{\alpha}C$ is random in every microelement*.

In order to precisely describe these two effects, we make use of the two random variables defined in Section 2.2.3 of this thesis (see Defs. 2 and 3). It is assumed that the probability distributions of C_{tr} and ${}^{\alpha}\tau$ can be obtained from appropriate experiments on single and/or bi-crystals, or derived analytically.

Returning to Fig. 3.2 we see, that the macroscopic disturbance must be viewed as the total of microdisturbances in any particular sequence. This is illustrated by the sample paths, contained between the slowest and the fastest paths, versus an average path. These microdisturbances evolve in their own internal times in contrast to the macrodisturbance, which occurs at an average pace. This observation leads us to give the following postulate:

Postulate 5:

> In dynamic phenomena pertaining to discrete media a multidimensional time is intrinsic. It encompasses an internal or micro-time and a macroscopic (average) time, where the micro-time is embedded in the internal time.+

---

* From the assumption that the neighbouring sequences are not interacting, it follows that the propagation velocity would be that of the one-dimensional stress model, i.e. ${}^{\alpha}C = \sqrt{{}^{\alpha}E/{}^{\alpha}\rho}$.

+ The expression "internal time" follows the terminology of Prigogine who uses the term "individual time" at this scale (see I. Prigogine, 1980, 1981).

Hence we can distinguish:

t : the internal time for a sample path of an L-wave, $t \in \mathcal{T}_2$.

$\bar{t}$: the macroscopic (average) time for the average path of an L-wave, $\bar{t} \in \mathcal{T}_1$.

If $\langle {}^{\alpha}\tau \rangle$ is an average passage time for an L-wave, then we have for an ensemble of $\alpha = 1, \ldots, n$ microelements:

$$\bar{t} = \sum_{\alpha=1}^{n} \langle {}^{\alpha}\tau \rangle , \quad \bar{t} \in \mathcal{T}_1 \tag{3.7}$$

indicating that $\bar{t}$ is related directly to the physical space X_1.

We also observe that due to the randomness of ${}^{\alpha}c_L$, the L-wave in any sequence S_k arrives anywhere in the time-space graph with an indeterminate time difference with respect to the macrodisturbance (average path). Hence, following the above definitions a special random variable can be identified as follows (see also Fig. 3.3):

Definition 8:

$\tau_L \stackrel{df}{=} t - \bar{t}$ is the dispersion time for the L-wave.

While τ_L is a random variable intrinsic in the $\underset{\sim}{v}(\bar{t}, t)$ random process, it is itself a random process with respect to the average time $\bar{t}$, i.e.:

$$\tau_L = \tau_L(\bar{t}) \tag{3.8}$$

Thus, we can write the following relation for the probabilities

$$P\{\underset{\sim}{v}(\bar{t}, t)\} = P\{\underset{\sim}{v}(t)\} \cdot P\{\tau_L(\bar{t})\} . \tag{3.9}$$

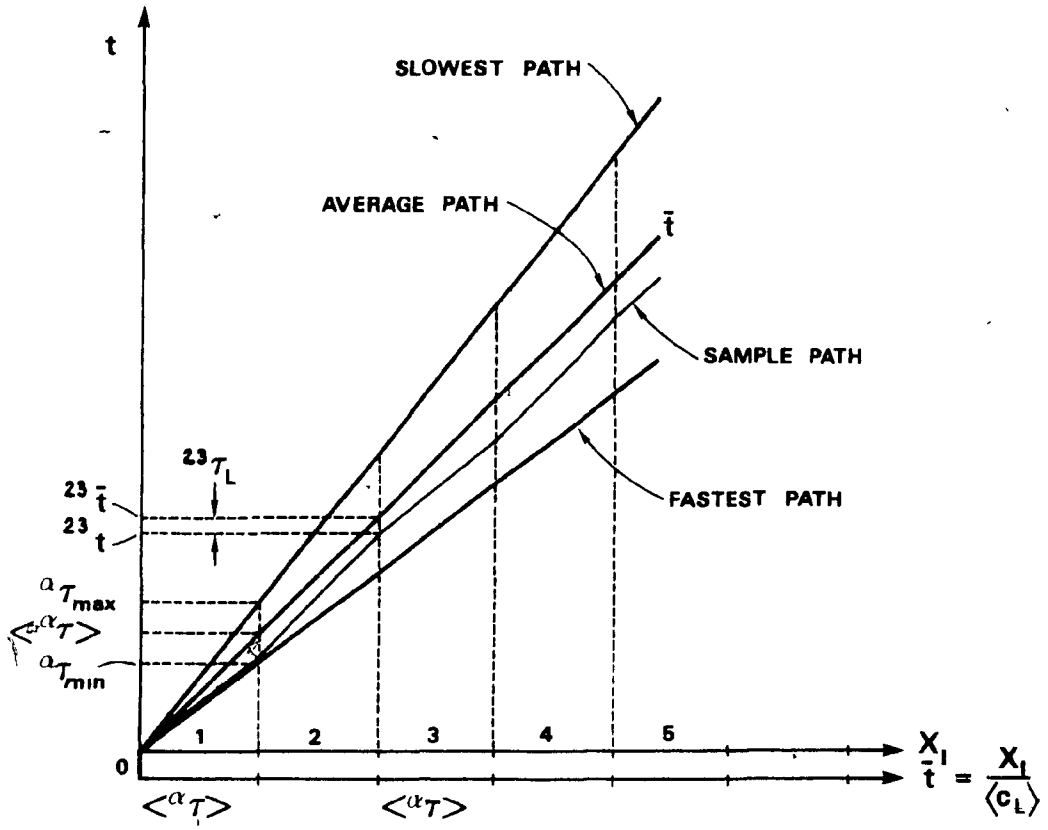

FIG.3.3 THE DISPERSION TIME PROCESS IN L-WAVE PROPAGATION.

It becomes apparent from the above relation that both effects I and II have been separated. This means the first term on the right hand side of (3.9) represents a modulation of the wave velocity vector $\underset{\sim}{v}(t)$ whilst the second term accounts for the dispersion of the wavefront in accordance with the time-space graph. Moreover, relation (3.9) indicates that $\underset{\sim}{v}$ will evolve independently with

regard to the internal and the average times. These evolutions can now be recognized as independent of their past histories and hence formulated in terms of Markov processes.

Let us first consider the L-wave evolution in terms of the internal time. Thus, using the conditional probability, we have:

$$P\{\underset{\sim}{y}(t) \in E\} = P\{\underset{\sim}{y}(t) \in E \mid \underset{\sim}{y}(t_0) = x\} \cdot P\{\underset{\sim}{y}(t_0)\}, \quad t_0 \leq t \tag{3.10}$$

expressing the Markov property of the $\underset{\sim}{y}(t)$ process and where the conditional probability is an explicit function of the probability distributions of the transmission coefficient and the passage time, viz:

$$P\{\underset{\sim}{y}(t) \in E \mid \underset{\sim}{y}(t_0) = x\} = P\{C_{tr} : \underset{\sim}{y}(t) = C_{tr} \cdot x\} \tag{3.11}$$

Recognizing this Markov process as a temporally homogeneous one and recalling from Section 2.4 that V is a subspace of $\mathcal{K}$ that is separable, we can, following Prohorov and Rozanov (1969), postulate the existence of a transition function as follows:

$$P(t, x, E) \stackrel{df}{=} P\{\underset{\sim}{y}(t) \in E \mid \underset{\sim}{y}(0) = x\}, \quad t \in T_2 = [0, \infty) \tag{3.12}$$

which will satisfy the following conditions:

a) for fixed t and $x \in V$, $P(t, x, E)$ is a probability measure on V,

b) for fixed t and $E \in \mathcal{F}_V$, $P(t, x, E)$ is a V-measurable function of $x \in V$,

c) $P(t, x, E) \leq 1$,

d) $P(0, x, V - \{x\}) = 0$

e) $P(t + t', x, E) = \int_V P(t, x, dy)\, P(t', y, E)$; $t, t' \geq 0$ (3.13)

The latter property (e) represents the well-known Chapman-Kolmogorov relation, which is a fundamental relation in the probability theory.

Considering this Markov process further we let $C(V)$ be a Banach space of all bounded continuous functions $f(\underset{\sim}{v})$ on the state space V, endowed with the norm $\|f\| = \sup_{x \in V} |f(x)|$. Then we can define an operator ${}^2T$ on V as follows:

$$ {}^2T(t)[f(x)] \stackrel{df}{=} \int f(y)\, P(t,x,dy) ; \quad f \in C(V). \tag{3.14} $$

It follows from properties c) and e) of the transition function that (3.14) defines an operator-valued function ${}^2T(t): [0,\infty) \to \mathcal{L}(C(V))$ such that $\{{}^2T(t); t \geq 0\}$ is a contraction semi-group of operators on $C(V)$ that is,

$$ \begin{aligned} &(i) \quad {}^2T(t+t')[f(\underset{\sim}{v})] = {}^2T(t)\,{}^2T(t')[f(\underset{\sim}{v})] \\ &(ii) \quad {}^2T(0) = I , \qquad I - \text{the identity operator} \\ &(iii) \quad \|{}^2T(t)\| \leq 1. \end{aligned} \tag{3.15} $$

We now turn to the analysis of the second stochastic process involved in the L-wave propagation, namely the evolution in terms of the average time $\bar{t}$. Hence, recalling Def. 8 we obtain:

$$ \underset{\sim}{v}(\bar{t}, t) = v(t) \quad \text{for a fixed} \tag{3.16} $$

and by following (3.9):

$$ P\{\underset{\sim}{v}(\bar{t}, t)\} = \text{const} \cdot P\{\tau_L(\bar{t})\} \tag{3.17} $$

The probability evolves analogously to a linear birth-death Markov process at regular $\langle {}^{\alpha}\tau \rangle$ intervals, i.e. the time dispersion process has no memory. Since the macroscopic time parameter $\bar{t}$ is discrete, whilst the internal time t is continuous, it may be inferred that τ_L is continuous. Thus in terms of a discrete-time Markov process

one can use the one-step transition function for such a process, which is given by:

$$P(\bar{t}_0, z, \bar{t}, D) \stackrel{df}{=} P\{\tau_L \in {}^{L}D \mid \tau_L(\bar{t}_0) = z\}, \quad \bar{t} \in \mathcal{T}_1 \tag{3.18}$$

which is a function of the distribution of the sojourn time $P({}^{\alpha}\tau)$:

$$P\{\tau_L(\bar{t}_1) \in {}^{L}D \mid \tau_L(\bar{t}_0) = z\} = P\{{}^{\alpha}\tau : {}^{\alpha}\tau - \langle {}^{\alpha}\tau \rangle = \tau_L(\bar{t}_1) - \tau_L(\bar{t}_0)\} \tag{3.19}$$

in which we have the following relations:

$\bar{t}_1 = \bar{t}_0 + \langle {}^{\alpha}\tau \rangle$, $\bar{t}_0$ being the initial time instant

and τ_L is an outcome in the sample space $\mathcal{D}_L$ of the dispersion times, ${}^{L}D$ is a Borel set in $\mathcal{D}_L$, belonging to the Borel field $\mathcal{F}_L$.

It is seen heuristically that this process is also temporally homogeneous, so that we can simplify the analysis by writing the transition function in the following manner:

$$P(\bar{t}, z, {}^{L}D) \equiv P(0, z, \bar{t}, {}^{L}D) \tag{3.20}$$

which satisfies the conditions below:

a') for fixed $\bar{t}$ and $z \in \mathcal{D}_L$, $P(\bar{t}, z, {}^{L}D)$ is a probability measure on $\mathcal{D}_L$,

b') for fixed $\bar{t}$ and ${}^{L}D \in \mathcal{F}_L$, $P(\bar{t}, z, {}^{L}D)$ is a $\mathcal{D}_L$-measurable function of z ,

c') $P(\bar{t}, z, \mathcal{D}_L) \leq 1$,

d') $P(0, z, \mathcal{D}_L - \{z\}) = 0$,

e') $P(\bar{t} + \bar{t}', z, {}^{L}D) = \int_{\mathcal{D}_L} P(\bar{t}, z, dw) \cdot P(\bar{t}', w, {}^{L}D)$; $\bar{t}, \bar{t}' \geq 0$. (3.21)

(Chapman-Kolmogorov relation)

Recalling that the $\tau_L(\bar{t})$ process is time-homogeneous (see eq. (3.20)), we can introduce a transition operator ${}^{1}T$ which is parametrized by

the average time $\bar{t}$ and defined as follows:

$$ {}^{1}T(\bar{t})[f(z)] \stackrel{df}{=} \int_{\mathcal{D}_L} f(w)\, P(\bar{t}, z, dw) \; ; \quad f \in C(\mathcal{D}_L). \tag{3.22} $$

Equation (3.22) indicates that the transition function defined through (3.18) and (3.20) is a kernel of the integral operator on the space of all continuous bounded fucntions $f(\tau_L)$ on $\mathcal{D}_L$; $C(\mathcal{D}_L)$ is a Banach space with a norm $\|f\| = \sup_{z \in \mathcal{D}_L} |f(z)|$. It follows from properties c') and e') above, that $\{{}^{1}T(\bar{t}), \bar{t} \geq 0\}$ is a contraction semi-group of operators on $C(\mathcal{D}_L)$, that is

$$ \begin{aligned} &\text{(i)} \quad {}^{1}T(\bar{t}+\bar{t}')[f(\tau_L)] = {}^{1}T(\bar{t})\,{}^{1}T(\bar{t}')[f(\tau_L)], \\ &\text{(ii)} \quad {}^{1}T(0) = I, \\ &\text{(iii)} \quad \|{}^{1}T(\bar{t})\| \leq 1, \end{aligned} \tag{3.23} $$

where I is the identity operator, and $f(\tau_L)$ may be given by (3.16) or (3.17).

Having identified both random processes that govern an L-wave propagation in the 1-D model of a discrete random medium we can generalize these results by proposing the following theorem:

Theorem 1

If $\{{}^{2}T(t), t \in \mathcal{T}_2 = [0, \infty)\}$ and $\{{}^{1}T(\bar{t}), \bar{t} \in \mathcal{T}_1\}$ are one-parameter semi-groups of contraction operators on $C(\mathcal{X})$ defined by (3.14) and (3.21), respectively, then there exists a two-parameter semi-group $\{T(\bar{t}, t), (\bar{t}, t) \in \mathcal{T}_1 \times \mathcal{T}_2\}$ such that:

(i) $T(\bar{t},t)$ is the direct product of two operators ${}^1T$ and ${}^2T$ so that $T(\bar{t},t) = {}^1T(t)\,{}^2T(t)$

(ii) $\lim_{(\bar{t},t)\to 0} T(\bar{t},t) = I$;

(iii) $T(\bar{t},t)$ is a contraction: $\| T(\bar{t},t)\| < 1$.

Proof

(i) Consider the Cartesian product space $V \times \mathcal{D}_L$, where $\{V, \mathcal{F}_V, P^{\underset{\sim}{v}}\}$ and $\{\mathcal{D}_L, \mathcal{F}_L, P^{\tau_L}\}$ are two probability spaces. Let $W = V \times \mathcal{D}_L$ denote the product of sets V and $\mathcal{D}_L$, and let $\mathcal{F}_W$ denote the least σ-algebra of subsets of W containing all sets $E \times {}^L D$, where $E \in \mathcal{F}_V$ and ${}^L D \in \mathcal{F}_L$. Then it follows from Theorem 3.4.1 of Rényi (1970), that there exists a unique measure P^W on W such that

$$P^W(E \times {}^L D) = P^{\underset{\sim}{v}}(E) \times P^{\tau_L}({}^L D) \tag{3.24}$$

It follows from Section 2.4 of Chapter II of this thesis that V must be a space of continuous functions on ${}^{\alpha}\bar{\mathcal{D}}$ (domain of α). Hence, according to the Imbedding Theorem of Sobolev (1963), the space V as a Sobolev space may be imbedded in the space $C({}^{\alpha}\bar{\mathcal{D}})$ of continuous functions on the domain ${}^{\alpha}\bar{\mathcal{D}}$. Of course, the space $C({}^{\alpha}\bar{\mathcal{D}})$ is separable and hence it is a countable union of sets $C_i \subset C({}^{\alpha}\bar{\mathcal{D}})$. Thus V is a σ-finite measure space. We note that $\mathcal{D}_L$ is a σ-finite measure space too.

We recognize $\underset{\sim}{v}(\bar{t},t)$ to be an element of the W space which is a more general state space than V ; $\underset{\sim}{v}(t) \in V$.

We can now introduce a function $f(\tau_L, \underset{\sim}{v})$ on the Cartesian product space $W = V \times \mathcal{D}_L$ such that:

- for each fixed $\tau_L \in \mathcal{D}_L$ we associate a function $f_{\tau_L}(\underset{\sim}{v})$ defined on $\mathcal{V}$ by $f_{\tau_L}(\underset{\sim}{v}) = f(\tau_L, \underset{\sim}{v})$,
- for each fixed $\underset{\sim}{v} \in \mathcal{V}$ we associate a function $f_{\underset{\sim}{v}}(\tau_L)$ defined on $\mathcal{D}_L$ by $f_{\underset{\sim}{v}}(\tau_L) = f(\tau_L, \underset{\sim}{v})$.

It is seen that the function $f_{\tau_L}(\underset{\sim}{v})$ is identical with the function $f(\underset{\sim}{v})$ employed in (3.14), and $f_{\underset{\sim}{v}}(\tau_L)$ is identical with the function $f(\tau_L)$ employed in (3.22). Evidently, $f(\tau_L, \underset{\sim}{v})$ is a measurable function on $\mathcal{D}_L \times \mathcal{V}$. It follows by Fubini's Theorem (Rudin, 1974) that:

$$\int_{\mathcal{D}_L \times \mathcal{V}} f(\tau_L, \underset{\sim}{v})\, d\rho^W = \int_{\mathcal{V}} \int_{\mathcal{D}_L} f_{\underset{\sim}{v}}(\tau_L)\, d\rho^{\tau_L} d\rho^{\underset{\sim}{v}} = \int_{\mathcal{D}_L} \int_{\mathcal{V}} f_{\tau_L}(\underset{\sim}{v})\, d\rho^{\underset{\sim}{v}} d\rho^{\tau_L} \qquad (3.25)$$

where $d\rho^W = d\left(\rho^{\tau_L} \times \rho^{\underset{\sim}{v}}\right)$ with ρ^W given by (3.24).

If we consider the integration with respect to $P(\bar{\tau}, z, D)$ and $P(t, x, E)$ which are the measures for fixed t,z and t,x, respectively (vide conditions a') and a)), then we get from (3.25):

$$\begin{aligned} {}^2T(t)\,{}^1T(\bar{t})[f(\tau_L, \underset{\sim}{v})] &= \int_{\mathcal{V}} \int_{\mathcal{D}_L} f_{\underset{\sim}{v}}(\tau_L)\, P(\bar{t}, z, dw)\; P(t, x, dy) \\ &= \int_{\mathcal{D}_L} \int_{\mathcal{V}} f_{\tau_L}(\underset{\sim}{v})\, P(t, x, dy)\, P(\bar{t}, z, dw) \\ &= {}^1T(\bar{t})\,{}^2T(t)[f(\tau_L, \underset{\sim}{v})] \\ &= T(\bar{t}, t)[f(\tau_L, \underset{\sim}{v})] \end{aligned} \qquad (3.26)$$

(ii) It follows from the point (i) and further from (3.15) and (3.23) that

$$\lim_{(\bar{t},t)\to 0} T(\bar{t},t) = \lim_{(\bar{t},t)\to 0} {}^{1}T(\bar{t})\,{}^{2}T(t) = I \cdot I = I .$$

(iii) Again from the point (i) and further from (3.15) and (3.23) it follows that

$$\| T(\bar{t},t) \| = \| {}^{1}T(\bar{t})\,{}^{2}T(t) \| \leq \| {}^{1}T(\bar{t}) \| \cdot \| {}^{2}T(t) \| \leq 1 . \qquad \square$$

The importance of the two-parameter semi-group operator shown above, is its ability to describe the evolution process of an L-wave pulse in terms of an abstract dynamical system $\{W, \mathcal{F}_W, \rho^W, T\}$. Thus with reference to Fig. 3.4 we see that given an initial

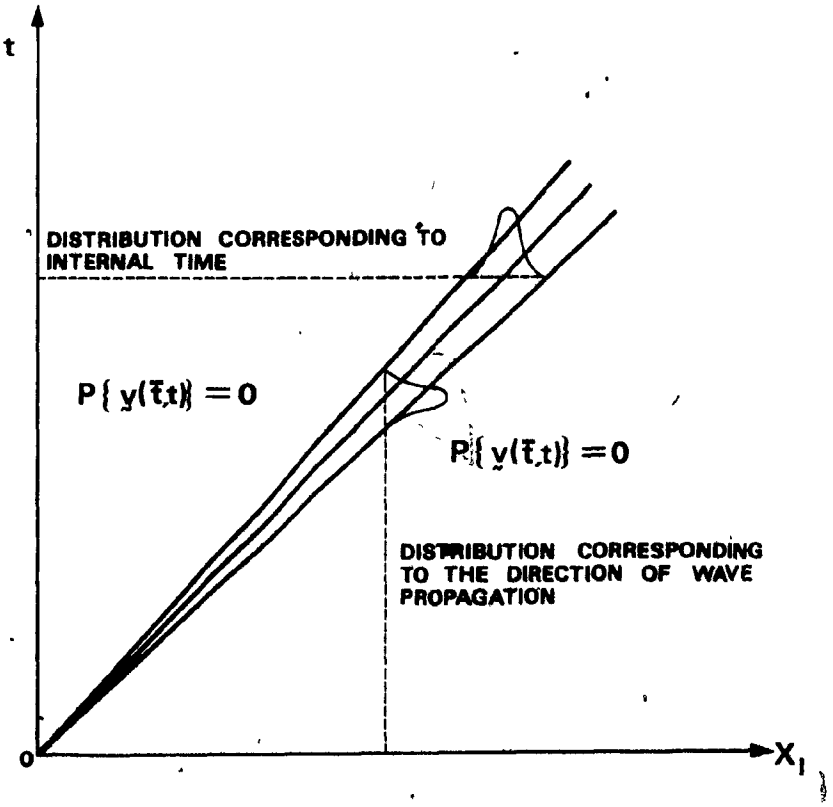

FIG.3.4 L-WAVE EVOLUTIONS IN THE SPACE-TIME GRAPH.

probability distribution:

$$P\{\underset{\sim}{v}(t=0)\} \qquad \text{and} \qquad P\{\tau_L(\bar{t}=0)=z\}$$

the probability distribution of $\underset{\sim}{v}$ at any later time $(\bar{t},t)$ can be obtained through an application of both the Chapman-Kolmogorov relations (3.13) and (3.21) in the following manner:

$$P\{\underset{\sim}{v}(\bar{t},t)\in F\} = P\{\underset{\sim}{v}(t)\in E\}\cdot P\{\tau_L(\bar{t})\in {}^{L}D\}, \quad F\in \mathcal{F}_{\mathbb{R}}$$

where

$$P\{\underset{\sim}{v}(\bar{t})\in E\} = P(t,x,E)\cdot P\{\underset{\sim}{v}(0)\},$$

and

$$P\{\tau_L(\bar{t})\in {}^{L}D\} = P\{\bar{t},z,{}^{L}D\}\cdot P\{\tau_L(0)=z\}.$$

We note that non-zero solutions will only be obtained within the dispersion time cone (Fig. 3.3), that is for:

$$P\{\underset{\sim}{v}(\bar{t},t)\}\neq 0 \quad \text{for} \quad P\{\tau_L(\bar{t})\}>0, \quad \tau_L \overset{df}{=} t-\bar{t}. \tag{3.27}$$

Again with reference to Fig. 3.4 we see that all non-zero solutions must be within this cone, illustrated by the lines of intersection with the plane corresponding to the fastest and shortest paths respectively. For a distribution $P\{\underset{\sim}{v}(t)\}$ there corresponds one obtained as a result of the evolution of all the microdisturbances propagating in the particular sequence and arriving at the particular position in the bar in their own internal time, i.e.:

$$P\{\underset{\sim}{v}(\bar{t})\} = P\{\underset{\sim}{v}(\bar{t},t), t\in \mathcal{T}_1\} = \begin{cases} \text{microdisturbance distribution} \\ \text{at } \bar{t} \\ 0 \text{ for } P\{\tau_L(\bar{t})\}=0 \end{cases} \tag{3.28}$$

Relation (3.28) represents an analytical analogue of a precise experimental observation at a particular station $X_1 \leftrightarrow \bar{t}$ for the response of the bar to a given dynamic excitation.

On the other hand taking a distribution $P\{\underset{\sim}{v}(t)\}$, i.e.

$$P\{\underset{\sim}{v}(t)\} = P\{\underset{\sim}{v}(\bar{t}, t), t \in \mathcal{T}_2\} = \begin{cases} \text{microdisturbance distribution at } t \\ 0 \text{ for } P\{\tau_L(\bar{t})\} = 0 \end{cases} \tag{3.29}$$

will correspond to considering a mesodomain distribution in the internal time. Hence, we se that this mesodomain represents a total of all pulses in the sequences $S_k \in M$, $k=1,\ldots,K$, which originated as a plane wave due to the initial impulse at the front face (see section 3.5).

It will be demonstrated in Appendix B of this thesis that the probability distributions $P\{\underset{\sim}{v}(t)\}$ and $P\{\tau_L(\bar{t})\}$ at a given time t and $\bar{t}$ respectively, are in fact approximately of the Gaussian type.

3.3 Longitudinal and Transverse Waves in the 1-D Model of the Solid

In this section we shall generalize the approach developed on the preceeding pages, to the case of an arbitrary plane wave in the one-dimensional model of the solid. Thus, the simplified model of the discrete random solid adopted in Section 3.2 and illustrated by Fig. 3.1 is assumed to hold here as well. As before, due to the assumed configuration discussed in Section 3.2, the disturbances will propagate independently in every sequence and remain a plane wave. Hence,

it is convenient for the following analysis to consider the process in a single typical sequence.

Assuming an arbitrary stress pulse is applied uniformly to the front face (see Section 3.1.2, equation (3.6)) so that:

$$\underset{\approx}{\sigma} \cdot \underset{\sim}{n} \Big|_{\substack{x_1=0 \\ t_0=0}} = P(t_0)$$

Two kinds of stress waves will be generated - a longitudinal and a transverse wave. It is obvious, that these waves will propagate independently of one another. The only qualitative difference between the longitudinal and transverse wave is that another kind of motion is involved, i.e.:

$$\underset{\sim}{u}(X_1, t) = f(X_1 - ct)\,\underset{\sim}{e} \qquad (3.30)$$

with the propagation vector $\underset{\sim}{p} \parallel X_1$, and a unit propagation vector $\underset{\sim}{e} \perp X_1$ and where $c = C_T$*. The same type of time-space graph can be drawn for the transverse wave as for the longitudinal wave (see Fig. 3.2) and exactly the same two effects previously discussed may be observed, i.e. the change of the wave velocity vector ${}^{\alpha}\underset{\sim}{v}$ from one microelement to the next due to the grain boundary effects, and the change of the propagation velocity ${}^{\alpha}C_T$. Thus, in accordance with the definitions 3 and 2 from before we proceed to introduce the transmission coefficient+ $C_{trT} = \frac{{}^{p}\underset{\sim}{v}}{{}^{\alpha}\underset{\sim}{v}}$ and the sojourn (passage) time ${}^{\alpha}\tau_T = \frac{{}^{\alpha}d}{{}^{\alpha}C_T}$, where the subscript "T" designates quantities pertaining to the transverse waves. Following Postulate 5 we will now have ${}^{T}t$ and ${}^{T}\bar{t}$ for the internal and average times, respectively so that:

$${}^{T}\bar{t} = \sum_{\alpha=1}^{n} \langle {}^{\alpha}\tau \rangle, \quad {}^{T}\bar{t} \in J_3 \qquad (3.31)$$

---

* ${}^{\alpha}C_T = \sqrt{{}^{\alpha}G/{}^{\alpha}\rho}$ in this one-dimensional model.

\+ C_{trT} here is the same as ${}^{\alpha}C_{tr}$ derived in Section 2.2.3.

showing that $\tau\bar{t}$ is again directly related to the physical space X_1.

In analogy with Definition 8 we introduce now a special random variable:

Definition 8'

$\tau_\tau \overset{df}{=} \tau t - \tau\bar{t}$ represents the dispersion time for the T-wave.

The above definition enables us to write the relation expressing the intrinsic character of the $\tau_\tau(\tau\bar{t})$ process in the $\underset{\sim}{\nu}(\tau\bar{t}, \tau t)$ process in terms of the probabilities as follows:

$$P\{\underset{\sim}{\nu}(\tau\bar{t}, \tau t)\} = P\{\underset{\sim}{\nu}(\tau t)\} \cdot P\{\tau_\tau(\tau\bar{t})\} \tag{3.32}$$

It is apparent that again two Markov processes can be identified for the transverse wave propagation, whereby a two-parameter semi-group of transition operators (with contraction) can be shown to model this kind of wave motion. Therefore, in order to present a general formulation of the combined case of longitudinal and transverse waves (see Fig. 3.5) we use a modified notation first. Thus, let us denote by:

$$\begin{aligned}
s_1 &= {}^{L}\bar{t} && \text{- average time of an L-wave,} && {}^{L}\bar{t} \in \mathcal{T}_1 \\
s_2 &= {}^{L}t && \text{- internal time of an L-wave,} && {}^{L}t \in \mathcal{T}_2 = [0, \infty) \\
s_3 &= \tau\bar{t} && \text{- average time of a T-wave,} && \tau\bar{t} \in \mathcal{T}_3 \\
s_4 &= \tau t && \text{- internal time of a T-wave,} && \tau t \in \mathcal{T}_4 = [0, \infty)
\end{aligned} \tag{3.33}$$

so that

$s = (s_1, s_2, s_3, s_4)$ becomes a generalized time, $s \in \mathcal{T} = \mathcal{T}_1 \times \mathcal{T}_2 \times \mathcal{T}_3 \times \mathcal{T}_4$

According to Definition 7, $\underset{\sim}{\nu}$ is a B-spaced-valued random variable. We can extend this notion by introducing the following

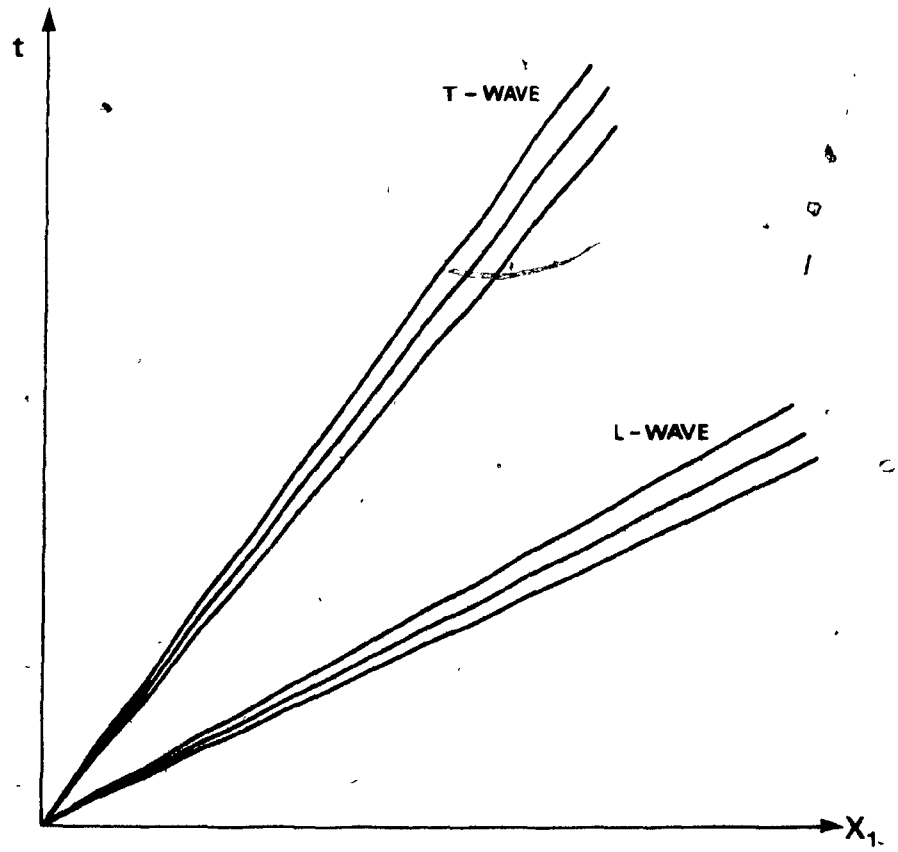

FIG.3.5 L-WAVE AND T-WAVE EVOLUTIONS IN THE SPACE-TIME GRAPH.

definition concerning a B-space-valued random field, i.e.:

Definition 9

A Banach space-valued random field on $\mathcal{T}$ is a mapping:

$\underset{\sim}{V}(s,\omega)$: $\mathcal{T} \times \Omega \rightarrow \mathcal{V}$ such that for every $s \in \mathcal{T}$, $\underset{\sim}{V}$ is

a Banach space-valued random variable: V is the wavefront subspace of the general state space $\mathfrak{X}$.

It was pointed out in Section 3.1.1 that the formulation of a random physical process by means of a random field is quite natural in many phenomena although it does not bring any results in itself. Thus, is is crucial for the further development of the theory to find some strong property which allows the characterization of such a random field. In view of the results of the preceding section (Theorem 1) we expect to arrive at a Markov random field in the present study. To avoid confusion we hasten to point out, that the notion of Markov random fields is not standardized, since this area of research is very new but expanding vigorously in several areas of science. We can generally distinguish two major trends of development of the Markov field theory: one in probability theory and one in statistical physics. Loosely speaking, the Markov field of probability theory is defined as a random field on an $\mathbb{R}^n$ parameter space in which past and future are independent given the present and where the present is identified with any smooth, closed (n-1) surface separating the parameter space into a bounded part (past) and an unbounded part (future) (see Lévy, 1956 and Wong, 1971). It is apparent, that this notion does not fit the microdynamics theory and we shall soon see that the wavefront random field as stated in Definition 9 is closely related to the Markov random fields encountered in statistical physics*.

---

* While the Lévy-type random field has connections with the multidimensional time domain of the microdynamics theory, the Ising-type formulation gives a basic framework for the random field interactions in the physical domain in the mechanics of solids. For the application of Markov random fields to discrete media see also Axelrad (1983).

We observe that the random field $\underset{\sim}{y}(s,\omega)$ can be characterized by the following four transition probabilites:

$P(s_1, z, {}^{L}D)$ defined in (3.18) and (3.20),

$P(s_3, z, {}^{T}D)$ defined analogously for the T-wave,

$P(s_2, x, E)$ defined in (3.12),

$P(s_4, x, E)$ defined analogously for the T-wave,

all of which are temporally homogeneous, i.e. this field has a homogeneity condition in the terminology of Spitzer (1971). Furthermore,

$$P^{\underset{\sim}{y}} > 0 \text{ for all } \underset{\sim}{y} \in V \tag{3.34}$$

hence a positivity condition.

However, this random field does not possess the so-called nearest neighbour condition, which physically expresses a coupling between the field parameters as in the case of the Ising models for instance (see also Dobrushin, 1968). Thus, we do not have a classical Markov random field in the sense of Spitzer and Dobrushin, but rather a "multiparameter Markov process" as a product of several one-parameter Markov processes.

It is important to note that the coupling between the space and time coordinates in the wave propagation process has been taken care of by introducing the dispersion time process parametrized by the average macroscopic time $\bar{t}$ and embedding it in the $\underset{\sim}{y}(\bar{t},t)$ process as expressed by relations (3.9) and (3.29). Hence this formulation enables use to introduce now a general evolution operator as a product of commuting suboperators, each parametrized by another time parameter. In this context, the noncommutativity of such suboperators

on the classical Markov fields prevents one from developing a general evolution operator. Thus, we are led to propose the following theorem :

Theorem 2:

If $\{V, \mathcal{F}_V, \rho^{\nu}\}$ is a Markov random field on $\mathcal{T}$, then the evolution is given through an abstract dynamical system $\{V, \mathcal{F}_V, \rho^{\nu}, T\}$, where $\{T(s), s \in \mathcal{T}\}$ is a 4-parameter semi-group such that:

(i) $T(s)$ is the direct product of the four one-parameter semi-groups, i.e.

$$T(s) \equiv T(s_1, s_2, s_3, s_4) = \prod_{i=1}^{4} {}^{i}T(s_i),$$

where the ${}^{i}T$ operators commute.

(ii) $\lim_{s \to 0} T(s) = I$,

(iii) $T(s)$ is a contraction operator, i.e. $\|T(s)\| \leq 1$.

Proof

Here V is a general velocity space of longitudinal and transverse wavefronts, i.e. $V = W_L \times W_T \equiv V_L \times \mathcal{D}_L \times V_T \times \mathcal{D}_T$

(i) If we introduce the general transition probability on V

$$P(s, x, V) = P(s_1, z_L, {}^{L}D)\, P(s_2, x_L, {}^{L}E)\, P(s_3, z_T, {}^{T}D)\, P(s_4, x_T, {}^{T}E)$$

we can define the transition operator on V by

$$T(s)[f(x)] \stackrel{df}{=} \int_V f(y) P(s, x, dy) \; ; \quad f \in C(V)$$

It follows now by induction from point (i) of Theorem 1 that

$$T(s) = \prod_{i=1}^{4} {}^{i}T(s_i), \quad \text{where} \quad s = (s_1, s_2, s_3, s_4)$$

(ii) Follows directly by induction from point (ii) of Theorem 1:

$$\lim_{s\to 0} T(s) = \lim_{(s_1,s_2,s_3,s_4)\to 0} {}^{1}T(s_1)^{2}T(s_2)^{3}T(s_3)^{4}T(s_4) = I\cdot I\cdot I\, I = I$$

(iii) Follows from point (iii) of Theorem 1, i.e.

$$\|T(s)\| = \|{}^{1}T(s_1)^{2}T(s_2)^{3}T(s_3)^{4}T(s_4)\| \leq$$

$$\leq \|{}^{1}T(s_1)\|\cdot\|{}^{2}T(s_2)\|\cdot\|{}^{3}T(s_3)\|\cdot\|{}^{4}T(s_4)\| \leq 1 . \qquad \square$$

It is important to note that although the above property of semi-group operators is known in classical functional analysis (see Hille and Phillips, 1957) it has never been proposed and proved for this kind of a Markov random field.

Time domain $\mathcal{T}$ being semi-infinite implies that this formulation is good for the wave propagation up to the point of reflection at the end face $x_1 = L$, see Fig. 3.2 (L being a standard length or specified length in a semi-infinite bar). However, this reflection can easily be introduced in the present formulation, as well as consecutive reflections.

The existence of a semi-group of transformations is the strongest property we can expect to find for the non-conservative system under consideration. This system is non-conservative because of the energy dissipation that enters the model through the transmission coefficients ${}^{\parallel}C_{tr}$ and ${}^{\perp}C_{tr}$, which sit in the random processes in the internal time parameters, ${}^{L}t$ and ${}^{T}t$, respectively. Certainly a non-conservative system is irreversible in time, and only its forward temporal evolution can be given; $s \longrightarrow +$, (see also (3.30)). It is important to note, however, that the process is irreversible also due to the existence of internal and average times which have been introduced in the present analysis. Consider for example an L-wave propagation where effect I is made to vanish due

to the assumption of perfect elastic grain boundaries. On the other hand, the effect II still exists and is modelled through the dispersion time process in the average time $\bar{t}$, which is naturally an irreversible phenomenon. Thus it is seen that even such an idealized fictitious process would be irreversible (compare Figs. 3.2 and 3.5). We can best put this observation in the words of Prigogine:

"irreversibility is the manifestation on a macroscopic scale of 'randomness' on a microscopic scale".

3.4 Plane Waves in the 3-D Solid

We now return to the general problem of the wave motion in the three-dimensional solid that we have already discussed at the beginning of this chapter. We shall concentrate only on the waves, which were initially plane waves and that are generated by a uniform pressure pulse at the front face (condition 3.6). Since the interactions between the elements of the microstructure are now allowed to occur generally in all the directions, there will be a weak coupling between the contiguous sequences $S_k \in M$. In particular, it is seen that for the cubic microstructure assumed here, a sequence not lying on the external boundary of the body domain M (see Fig. 3.1) will interact with four neighbouring sequences, while a sequence lying on the boundary will interact with either three, two or only one neighbour, depending on the specific configuration.

It is well known, that for waves propagating in a bar the effect of finite dimensions of the cross-section becomes important

for certain wavelengths and from a continuum point of view is usually modelled by the Pochhammer-Chree theory. Since our interest in this thesis lies in the theoretical formulation that accounts for the microstructural randomness and considers it as a key factor in the evolution laws of the field quantities, we shall presently consider these diameter-versus-wavelength effects to be of a secondary nature only and hence disregard them.

Assuming that there is no coupling between the longitudinal and transverse waves, we can then conclude that an analysis of wave propagation in a typical sequence S_k with interactions with four neighbours should be representative of plane wave in a 3-D cubic structural solid. Choosing to work with a pulse inducing a longitudinal wave, we can now employ the space-time graph of Fig. 3.2 as a representation of the wave propagation process in a discrete random medium. We note that similarly as in a 1-D model of the solid, two effects become significant, i.e.:

Effect I - transmitted wave velocity ${}^{\beta}\underset{\sim}{V}$ is different from the incident wave velocity ${}^{\alpha}\underset{\sim}{V}$ due to the grain boundary $\partial^{\alpha}\mathcal{D}$.

Effect II - wave propagation velocity ${}^{\alpha}c$ is random in every microelement α.

In this model the effect I comprises all possible interactions of the microelement α with its neighbours as opposed to the previous 1-D model. Although, it is seen on heuristic grounds that 3-D interactions on α will still be of a Markovian character, it becomes apparent that the effect I will, generally speaking, increase in

time as the sample paths continue to diverge in the space-time graph. Let us consider this process in detail.

It is seen that ${}^{\alpha}\underset{\sim}{V}$ goes into ${}^{\beta}\underset{\sim}{V}$ after a random passage time ${}^{\alpha}\tau$ such that the transmission process will depend on the neighbours on four sides of α (see Fig. 3.1). Thus the wave velocity vector also becomes a function of Y_2 and Y_3 coordinates and we need here a transmission operator rather than the transmission coefficient used earlier to describe this process. For this purpose we consider the following definition:

Definition 10

The transmission operator is a random mapping

$$C(\omega): {}^{\alpha}\underset{\sim}{V}(t) \rightarrow {}^{\beta}\underset{\sim}{V}(t+{}^{\alpha}\tau),$$

where ${}^{\alpha}\underset{\sim}{V}, {}^{\beta}\underset{\sim}{V} \in \mathcal{V}$.

Generally, this operator depends on the surface interactions at $\partial^{\alpha}\mathcal{D}$ (see Fig. 3.6) and the velocities in the four neighbouring grains, i.e.:

$$C = C(C_{tr} \text{ on } \partial^{\alpha}\mathcal{D}, {}^{r_i}\underset{\sim}{V}; i=1,\ldots,4) \tag{3.35}$$

Since the velocities ${}^{r_i}\underset{\sim}{V}$'s are themselves time-dependent random processes, relation (3.32) indicates that the operator C will also be time-dependent.

From our assumption of the wave motions in the elastic range (including acceleration waves), it follows that transmission operator is linear, i.e.:

$$C[a_1\underset{\sim}{V}_1 + a_2\underset{\sim}{V}_2] = a_1 C[\underset{\sim}{V}_1] + a_2 C[\underset{\sim}{V}_2] \text{ for all } \underset{\sim}{V}_1, \underset{\sim}{V}_2 \in \mathcal{V} \tag{3.36}$$

Hence, in view of Def. 10 it is evident that $C(\omega)$ is a random endomorphism of V, and since it is actually time-dependent we conclude that the transmission operator is an $\mathcal{L}(V)$-valued function such that:

$$C(s,\omega): \mathcal{T} \times \Omega \rightarrow \mathcal{L}(V). \tag{3.37}$$

In order to unify the present formulation and recalling Def. 9 of this chapter we can now introduce the definition below following the Bharucha-Reid's formalism:

Definition 11

A Banach space-valued random field on $\mathcal{T} = \mathcal{T}_1 \times \mathcal{T}_2$ and $\mathbb{R}^3$ is a mapping ${}^{\alpha}\underset{\sim}{v}(\bar{t}, t, {}^{\alpha}X, \omega) \equiv {}^{\alpha}\underset{\sim}{v}(s, {}^{\alpha}X, \omega)$: $\mathcal{T} \times \mathbb{R}^3 \times \Omega \rightarrow V$ such that for every $s \in \mathcal{T}$ and ${}^{\alpha}X \in M$, $\underset{\sim}{v}$ is a Banach space-valued random variable; V is the wavefront subspace of $\mathfrak{X}$ (${}^{\alpha}X$ is the centre of mass of α).

Now, for given distributions of the physical properties of a solid an explicit form of the $C(s,\omega)$ operator may be derived. Further a measure on $\mathcal{L}(V)$ may by introduced and a rigorous analysis of the evolution of the wavefront may be conducted in principle*. It becomes evident however, that working with this kind of random field is rather complicated considering the function space structure on $\mathcal{T} \times \mathbb{R}^3$ and hence it is convenient to reduce the analysis to a real-valued random field in terms of a power $\mathcal{P}: V \rightarrow \mathbb{R}^+$. Thus for a microelement we can write the following expression:

---

* See Section 4.4 for the explicit form of $C(s,\omega)$ operator and the corresponding numerical analysis.

$$ {}^{\alpha}\mathcal{P} = \int_{{}^{\alpha}v} \left[\left({}^{\alpha}\sigma_{ij}\, {}^{\alpha}\dot{u}_i \right)_{,j} + {}^{\alpha}\rho\, {}^{\alpha}f\, {}^{\alpha}\dot{u}_i \right] dv \quad ; \quad dv = dX_1 dX_2 dX_3 \tag{3.38} $$

where the second term of the integrand vanishes due to the assumed neglect of body forces. We note that from continuum theory ${}^{\alpha}\mathcal{P}$ is related to the time rate of change of the kinetic and potential energies of α through the energy identity, i.e.:

$$ {}^{\alpha}\mathcal{P} = \frac{d^{\alpha}K}{dt} + \frac{d^{\alpha}U}{dt} \tag{3.39} $$

It follows that ${}^{\alpha}\mathcal{P}$ may be taken as a linear functional on the $\mathcal{V}$ space so that we obtain a generalized random variable in the sense of Gel'fand and Vilenkin, 1964, i.e.:

$$ {}^{\alpha}\mathcal{P} : \mathcal{V} \rightarrow \mathbb{R}^{+} \tag{3.40} $$

Hence, in this sense the power ${}^{\alpha}\mathcal{P}$ in a given sequence is a function of the $\underset{\sim}{v}(\bar{t},t)$-process so that by Theorem 1 we obtain:

$$ \begin{aligned} T(\bar{t},t)\left[{}^{\alpha}\mathcal{P}(z,x)\right] &= T(\bar{t})^{2} T(t)\left[{}^{\alpha}\mathcal{P}(z,x)\right] = \\ &= \int_{\mathcal{V}} {}^{\alpha}\mathcal{P}(w,y)\, P(\bar{t},z,dw)\, P(t,x,dy) \end{aligned} \tag{3.41} $$

Furthermore, since $\underset{\sim}{v}(\bar{t},t)$ is Markovian we can write that:

$$ \begin{aligned} T(\bar{t},t)\left[{}^{\alpha}\mathcal{P}(z,x)\right] &= \int_{\mathcal{V}} {}^{\alpha}\mathcal{P}(w,y)\, P(\bar{t},z,dw)\, P(t,x,dy) = \\ &= E\left\{ {}^{\alpha}\mathcal{P}(\tau_L, \underset{\sim}{v})\ \text{at}\ (\bar{t},t) \,\middle|\, \tau_L(\bar{t}_0) = z\ ,\ \underset{\sim}{v}(t_0) = x \right\} = \\ &= E\left\{ {}^{\alpha}\mathcal{P}(\tau_L, \underset{\sim}{v})\ \text{at}\ (\bar{t},t) \,\middle|\, \mathcal{F}_L \times \mathcal{F}_{\mathcal{V}}\ \text{over}\ (0,\bar{t}_0)\times(0,t_0) \right\} \end{aligned} $$

It can be recognized now that depending on the interaction effects caused by the immediate neighbours of the single grain α, the expected value of the power flux may become smaller, equal or larger after the passage through α. This can be expressed by:

$$T(\langle {}^{\alpha}\tau\rangle, {}^{\alpha}\tau)[{}^{\alpha}\mathcal{P}(z,x)] =$$

$$= E\{{}^{\alpha}\mathcal{P}(\tau_L, \underset{\sim}{v}) \text{ at } (\langle {}^{\alpha}\tau\rangle, {}^{\alpha}\tau) \mid \mathcal{F}_L \times \mathcal{F}_V \text{ over } (0, \langle {}^{\alpha}\tau\rangle) \times (0, {}^{\alpha}\tau)\}$$

$$\gtreqless {}^{\alpha}\mathcal{P}(z,x) \text{ at } (0,0) \tag{3.42}$$

However, if we consider the power $\mathcal{P}$ of the total wavefront in all sequences $S_k \in M$, then evidently there is also some energy loss due to the reflections of the waves propagating backward (in the X_1-direction). Thus taking the evolution of $\mathcal{P}$ in terms of the passage time ${}^{\alpha}\tau$ we can give the following inequality:

$$T(\langle {}^{\alpha}\tau\rangle, {}^{\alpha}\tau)[\mathcal{P}(z)] = E\{\mathcal{P}(\tau_L, \underset{\sim}{v}) \text{ at } (\langle {}^{\alpha}\tau\rangle, {}^{\alpha}\tau) \mid \mathcal{F}_L \times \mathcal{F}_V\}$$

$$\leqslant \mathcal{P} \text{ at } (\bar{t}=0,\ t=0) \tag{3.43}$$

This clearly shows the super-harmonicity of the function $\mathcal{P}$ under the operator $T(\bar{t}, t)$. In order to establish a valuable connection of this probabilistic formulation with the abstract potential theory we have to simplify the analysis to the one-dimensional time*. Thus the evolution operator $T(\bar{t}, t)$ will henceforth be parametrized by $t=\bar{t}$ and hence it will be denoted simply by $T(\bar{t})$. This implies, that the time dispersion process $\tau_L(\bar{t})$ will be disregarded in the sequel, i.e.:

$$T(\bar{t}) = {}^{2}T(\bar{t}) \tag{3.44}$$

Extending now the result known for Markov chains (Lemma 5.3 in Syski, 1973) to the discrete parameter Markov process we propose the following lemma:

---

* The abstract potential theory, which has its origin in the studies of Brownian motion (Kac, 1951), is still suited only to the problems parametrized by the one-dimensional times.

Lemma 1:

If $\underset{\sim}{y}(\bar{t})$ is a discrete parameter Markov process representing the wavefront evolution in the macroscopic time t, with the transition operator ${}^{2}T(\bar{t})$ and the initial distribution $\underset{\sim}{y}(0)$, $\mathcal{P}$ is a bounded ${}^{2}T$-super-harmonic function on V; then the random process $\mathcal{P}(\underset{\sim}{y})$ on the σ-field $\mathcal{F}_V$ over $(0,\bar{t})$ is a super-martingale.

Proof

It follows from the Markov property of $\underset{\sim}{y}(\bar{t})$ that

$$E\{\mathcal{P}(\underset{\sim}{y} \text{ at } \bar{t} \mid \mathcal{F}_V \text{ over } (0,\bar{t})\} =$$
$$= E\{\mathcal{P}(\underset{\sim}{y}(\bar{t})) \mid \mathcal{P}(\underset{\sim}{y}(\bar{t} - \langle {}^{\alpha}\tau \rangle))\},$$

and further from the superhamonicity of $\mathcal{P}$ expressed by (3.43) that

$$E\{\mathcal{P}(\underset{\sim}{y}(\bar{t})) \mid \mathcal{P}(\underset{\sim}{y}(\bar{t} - \langle {}^{\alpha}\tau \rangle))\} =$$
$$= {}^{2}T(\langle {}^{\alpha}\tau \rangle)[\mathcal{P}(\underset{\sim}{y}(\bar{t} - \langle {}^{\alpha}\tau \rangle))] =$$
$$\int_V \mathcal{P}(\underset{\sim}{y}(\bar{t}))\, P(t,x,dy) \leq \mathcal{P}(\underset{\sim}{y}(\bar{t} - \langle {}^{\alpha}\tau \rangle)) \qquad \square$$

It is important to point out that even though the above result has been obtained for the case of a cubic structured solid (Fig. 2.2), it also applies to a polycrystalline solid with random internal geometry. However, in that case the Definition 10 of the transmission operator at a microscale would have to be modified. Furthermore, our formulation enables one to introduce some internal material parameters into the transition operator which could lead for example to the study of metastability (acceleration wave - shock

wave transition) on random fields. In general Lemma 1 opens up the microdynamics theory to the various techniques of the abstract potential theory which is currently experiencing a vigorous development (see for instance, Blumenthal and Getoor, 1968 and Fukushima, 1980).

It is of interest to point out that the averaging procedures employed in this section are with respect to the set of solutions of the random evolution equation and do not involve averaging this random equation itself. Thus in the light of the discussion in Section 2.1 we should obtain the "proper" expected values of the power flux in the wave propagation analysis.

3.5 Convergence of the Probabilistic Evolution Relation to the Generalized Wave Equation of Continuous Media

It has been stated in Section 2.1 that a probabilistic problem in mechanics may be stated through relation (2.1) in a very general way. In the case of the 1-D wave motion such a formulation has been given in accordance with Definition 9, whilst the laws of evolution of the random velocity field have been found in Theorem 2. It is of interest to check whether an averaging procedure as indicated by equation (2.2) will indeed yield a relation equivalent to the classical wave equation. We shall investigate this question in the present section.

In order to establish the convergence to continuum we work with the 1-D case of an L-wave (as discussed in Section 3.2) since

a more complex case would only make the analysis more cumbersome and complicated without bringing additional insight.

A point of fundamental importance in establishing the equivalence of physical theories constructed for various levels of approximation of natural phenomena, is the intermediate level where the agreement has to be found (see for instance H. Grad, 1962 and Yvon, 1969). Such an intermediate level between deterministic continuum mechanics and probabilistic microdynamics of structured solids is the infinitesimal element of continuum theory which corresponds to the microelement scale. Thus, we shall consider the wave motion in two continguous microelements of a typical sequence $S_k \in M$:

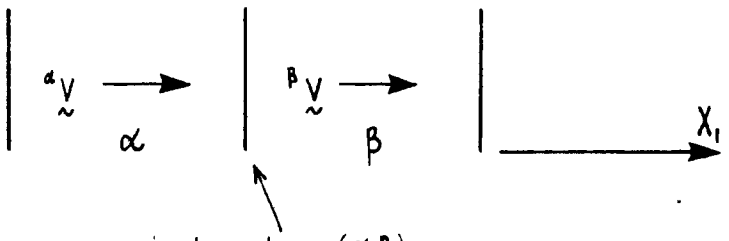

It is known from elastodynamics (see Achenbach, 1973), that for the pulse propagation the following relation holds:

$$\sigma = -\rho c_L \dot{u}$$

and hence the strain in the X_1-direction is given by:

$$\varepsilon_x = \frac{\partial u}{\partial x} = -\frac{1}{c_L}\frac{\partial u}{\partial t} \equiv -\frac{1}{c_L}\dot{u}$$

where we consider waves weaker than the acceleration wave, i.e. $\dot{u} \in H^m$, $m \geq 2$. In accordance with Definition 1, the above relations are taken to hold within an element α and β. Hence, we can write:

$$^{\beta}\underset{\sim}{V}(X_1 + d, t + {}^{\alpha}\tau) - {}^{\alpha}\underset{\sim}{V}(X_1, t + {}^{\alpha}\tau) = -{}^{\beta}c_L\,{}^{\beta}\varepsilon(X_1 + d, t + {}^{\alpha}\tau) + {}^{\alpha}c_L\,{}^{\alpha}\varepsilon(X_1, t + {}^{\alpha}\tau),$$

were $d = {}^{\alpha}d$ = constant. Taking the expectations of the above, we obtain:

$$\int_{\Omega} [\underset{\sim}{v}(X_1 + d, t + {}^{\alpha}\tau) - \underset{\sim}{v}(X_1, t + {}^{\alpha}\tau)]\, d\rho^{\underset{\sim}{v}} = \int_{\Omega} \frac{1}{{}^{\alpha}c_L} [\varepsilon(X_1, t + {}^{\alpha}\tau) - \varepsilon(X_1 + d, t + {}^{\alpha}\tau)]\, d\rho^{\underset{\sim}{v}} \quad (3.45)$$

where now the subscript α concerns random physical properties.

From the microdynamic model we know the following relation :

$$\rho\{\underset{\sim}{v}(X_1 + d, t + {}^{\alpha}\tau)\} = \rho\{\underset{\sim}{v}(\bar{t} + \langle {}^{\alpha}\tau \rangle, t + {}^{\alpha}\tau)\}, \quad (3.46)$$

which is due to the correspondence between the average time $\bar{t}$ and the physical space X_1 during the wave passage. Furthermore, we know from the Markovian formulation (see 3.19 nd 3.12) that:

$$\rho\{\underset{\sim}{v}(\bar{t} + \langle {}^{\alpha}\tau \rangle, t + {}^{\alpha}\tau)\} = P(\Delta\bar{t}, z, {}^{L}D)\, P(\Delta t, x, E)\, \rho\{\underset{\sim}{v}(\bar{t}, t)\}, \quad (3.47)$$

where $\Delta\bar{t} = \langle {}^{\alpha}\tau \rangle$ and $\Delta t = {}^{\alpha}\tau$.

Employing (3.46) and (3.47) on the left hand side (LHS) of (3.45) we obtain the following expression:

$$\begin{aligned} LHS &\equiv \int_{\Omega} [\underset{\sim}{v}(X_1 + d, t + {}^{\alpha}\tau) - \underset{\sim}{v}(X_1, t + {}^{\alpha}\tau)]\, d\rho^{\underset{\sim}{v}} = \\ &= \int_{\mathcal{D}_L} \int_{V} \underset{\sim}{v}(\bar{t} + \langle {}^{\alpha}\tau \rangle, t + {}^{\alpha}\tau) \cdot P(\langle {}^{\alpha}\tau \rangle, z, dw) \cdot P({}^{\alpha}\tau, x, dy)\, \rho\{\underset{\sim}{v}(\bar{t}, t)\} \\ &\qquad - \underset{\sim}{v}(X_1, t + {}^{\alpha}\tau)\, d\rho^{\underset{\sim}{v}}\, d\rho^{\tau_L} = \\ &= {}^{1}T(\langle {}^{\alpha}\tau \rangle)\, {}^{2}T({}^{\alpha}\tau)\, [\underset{\sim}{v}(\bar{t}, t)]\, \rho\{\underset{\sim}{v}(\bar{t}, t)\} - \langle \underset{\sim}{v}(X_1, t + \langle {}^{\alpha}\tau \rangle) \rangle, \end{aligned}$$

where ${}^{1}T$ and ${}^{2}T$ are the transition operators defined in (3.22) and (3.14), respectively. It follows now from the point (iii) of Theorem 1 that:

$$\begin{aligned} LHS &= (1-b)\langle \underset{\sim}{v}(\bar{t}, t) \rangle - \langle \underset{\sim}{v}(X_1, t + \langle {}^{\alpha}\tau \rangle) \rangle \quad (3.48) \\ &\equiv (1-b)\langle \underset{\sim}{v}(X_1, t) \rangle - \langle \underset{\sim}{v}(X_1, t + \langle {}^{\alpha}\tau \rangle) \rangle, \end{aligned}$$

where $0 < b \ll 1$ has been taken, and analogously to continuum mechanics the reflected wave has been omitted.

On the other hand, the right hand side (RHS) of (3.45) becomes

$$RHS \equiv \int_{\Omega} {}^{\alpha}c_L \left[\varepsilon(X_1, t+{}^{\alpha}\tau) - \varepsilon(X_1+d, t+{}^{\alpha}\tau)\right] d\rho^{\nu} =$$

$$= \langle {}^{\alpha}c_L \rangle \left[\langle \varepsilon(X_1, t+\langle {}^{\alpha}\tau \rangle) - \langle \varepsilon(X_1+d, t+\langle {}^{\alpha}\tau \rangle)\rangle\right]$$

Equating the above relation with (3.48) we obtain therefore:

$$(1-b)\langle \underset{\sim}{v}(X_1, t)\rangle - \langle \underset{\sim}{v}(X_1, t+\langle {}^{\alpha}\tau \rangle)\rangle =$$

$$= \langle {}^{\alpha}c_L \rangle \left[\langle \varepsilon(X_1, t+\langle {}^{\alpha}\tau \rangle)\rangle - \langle \varepsilon(X_1+d, t+\langle {}^{\alpha}\tau \rangle)\rangle\right.$$

which upon multiplying by $1/\langle {}^{\alpha}\tau \rangle$ becomes:

$$\frac{\langle \underset{\sim}{v}(X_1, t)\rangle - \langle \underset{\sim}{v}(X_1+\langle {}^{\alpha}\tau \rangle)\rangle}{\langle {}^{\alpha}\tau \rangle} - \frac{b}{\langle {}^{\alpha}\tau \rangle}\langle \underset{\sim}{v}(X_1, t)\rangle =$$

$$= \langle {}^{\alpha}c_L \rangle^2 \frac{\langle \varepsilon(X_1, t+\langle {}^{\alpha}\tau \rangle)\rangle - \langle \varepsilon(X_1+d, t+\langle {}^{\alpha}\tau \rangle)\rangle}{d} \qquad (3.49)$$

in which the assumption of ergodicity has been made, i.e.:

$$\frac{1}{\langle {}^{\alpha}\tau \rangle} = \frac{\langle {}^{\alpha}c_L \rangle}{d} \qquad (3.50)$$

We do not take a limit in (3.49) with $\langle {}^{\alpha}\tau \rangle \to 0$ and $d \to 0$, but consider this relation on the microelement scale rather to be equivalent to the partial differential equation of continuum, i.e.:

$$\frac{\partial^2 u}{\partial t'^2} + b' \frac{\partial u}{\partial t'} = c_L'^2 \frac{\partial^2 u}{\partial X_1^2} \qquad (3.51)$$

which is a generalized wave equation with dissipation. The coefficients c_L' and b' in (3.51) can be derived from the microstructural properties, that is:

$$\left.\begin{aligned} c_L' &= \langle c_L \rangle \\ b' &= \frac{b}{\langle {}^{\alpha}\tau \rangle} \end{aligned}\right\} \qquad (3.52)$$

Moreover, we observe that the time scale t' employed in (3.51) above is equivalent to the average time $\bar{t}$ of the probabilistic microdynamics model. Hence, it is seen that by taking the average over the internal times of microdisturbances in the particular sequences, only one time emerges, namely the average macroscopic time. Such a formulation has its parallel in statistical mechanics, where a time operator is introduced to account for the randomness at the microscopic scale and to allow a transition to the macroscopic scale via ensemble averages; see Prigogine (1980).

CHAPTER IV

COMPARISON OF THE CLASSICAL TO THE MICRODYNAMICS FORMULATION BY THE USE OF THE MONTE-CARLO SIMULATION TECHNIQUE

4.1 Introduction

In the two previous chapters the theory of probabilistic microdynamics has been presented. As pointed out in Section 3.1 the Markov field formulation is a porbabilistic analogue of the transport theory approach for the wave propagation, where the discrete microstructure is included in the formulation. In contrast to the deterministic elastodynamics theory where one can distinguish two quite separate stages, namely the formulation of the governing equations and the method of solution, in the present case these two stages are treated at the same time. By this we mean that Theorems 1, 2 and Lemma 1 of Chapter III provide a basis for the formulation of the problem as well as the solution of the problem. Thus, in order to determine the evolution of the system, which is the spatial-temporal evolution of a propagating wave, one has to calculate the Chapman-Kolmogorov relations in the internal and average times. Alhtough the probability kernels of the integral transition operators are derived explicitly as functions of the material properties (see (3.11) and (3.19)) such a calculation up to any instant of the generalized time $\mathbf{s}$ (Fig. 3.4) is possible but rather cumbersome. We therefore, due to the absence of actual laboratory tests, employ a simulation technique known as the Monte-Carlo method. This in addition permits a comparison of results of the present theory with the classical formulations. As we shall see

in Section 4.4, the Monte-Carlo simulation is based on the same considerations and assumptions concerning the wave propagation through a structured medium as the probabilistic model itself. In principle, it is developed from the same Markovian assumptions and hence, in view of the vast evidence in scientific literature of the success of this method, it is expected to furnish some indication as to the applicability of the probabilistic model.

On the other hand, the Monte-Carlo technique, representing simulation of the physical phenomenon is thought to replace an elaborate laboratory experiment, which could not be carried out within the present research program. Although the literature on experimental mechanics is very extensive no test procedure could be found by the author of this thesis that would recognize the effects of the rather complex material structure in the application of the stress waves. Hence for this reason the simulation technique had to be employed.

Thus the present chapter is devoted to the development of the Monte-Carlo simulation for the application to the wave propagation in discrete solids together with the comparison of known results of wave propagation in continuous media. It will be shown that the over-riding factors in this comparison were the relative strength of the fluctuations in the physical properties in a specific solid, the correlations range with respect to the existing grain size and the wavelength. Again, this will be illustrated for the case of a cubic structured solid. We start by giving a discussion of deterministic continuum and random continuum theories as applied to our problem.

4.2 Deterministic Continuum Formulation for Isotropic Homogeneous Elastic Solids

We recall from the section on the problem formulation, that the wave motion is generated by the application of a spatially uniform surface pressure at the bar's front face, i.e.:

$$\underset{\approx}{\sigma} \cdot \underset{\sim}{n} \Big|_{X_1 = 0} = P(t) \tag{3.5}$$

It is evident, that an initial boundary condition of such a general form will give rise to longitudinal and transverse waves in the bar. Assuming now the material of the bar to behave as an isotropic homogeneous linearly elastic continuum leads us to conclude that the two waves will travel independently at two constant propagation speeds c_L and c_T.

We can thus consider single type wave propagation and choose to analyze a longitudinal wavefront due to the following condition:

$$\sigma_{11}(X_1, t)\Big|_{\substack{X_1 = 0 \\ t = 0}} = -P \tag{4.1}$$

The motion of the medium is then governed by the standard wave equation:

$$\frac{\partial^2 u}{\partial X_1^2} = \frac{1}{c_L^2} \frac{\partial^2 u}{\partial t^2} \tag{4.2}$$

with the initial conditions:

$$\left.\begin{aligned} u &= 0 \quad \text{for} \quad t = 0\,, \; X_1 > 0 \qquad \text{(a)} \\ \dot{u} &= 0 \quad \text{for} \quad t = 0\,, \; X_1 > 0 \qquad \text{(b)} \end{aligned}\right\} \tag{4.3}$$

The general solution of the wave equation (4.2) is known to be:

$$u(X_1, t) = f\left(t - \frac{X_1}{c_L}\right) + g\left(t + \frac{X_1}{c_L}\right) \tag{4.4}$$

where f and g are forward and backward traveling waves, respectively. It is obvious that the pulse given in (4.1), will induce a forward traveling wave only, and hence (4.4) reduces to:

$$u(X_1, t) = f\left(t - \frac{X_1}{c_L}\right)$$

The boundary condition (4.1) yields then:

$-\rho c_L \dot{u} = -P$, since $\sigma_{11} = -\rho c_L \dot{u}$,

and hence

$$-\rho c_L f'\left(t - \frac{X_1}{c_L}\right) = -P$$

where upon integrating we obtain:

$$f\left(t - \frac{X_1}{c_L}\right) = \frac{1}{\rho c_L} \int_0^{t - \frac{X_1}{c_L}} P \, dt' + C_1 \qquad (4.5)$$

By employing condition (4.3a) we see that:

$$f\left(-\frac{X_1}{c_L}\right) = 0$$

and hence $C_1 = 0$ and (4.5) becomes therefore:

$$u(X_1, t) = \frac{1}{\rho c_L} \int_0^{t - \frac{X_1}{c_L}} P \, dt'$$

$$= \frac{1}{\rho c_L} P\left(t - \frac{X_1}{c_L}\right) = \frac{1}{\rho c_L} \begin{cases} P \text{ for } t > \frac{X_1}{c_L} \\ 0 \text{ for } t < \frac{X_1}{c_L} \end{cases} \qquad (4.6)$$

This solution shows that a plane longitudinal wavefront propagates through the bar with the constant velocity c_L. The pulse amplitude and shape remain unaltered.

4.3 Random Continuum Theory of Wave Propagation

This section aims to describe, in a comprehensive manner, the formulation and its consequences of wave analysis in random continuous

media. The general features of this macroscopic approach have already been outlined in Section 1.3 of this thesis.

In the classical theory (cf. Frisch, 1968) one replaces a single inhomogeneous medium M by an ensemble of media $\{M(\omega), \omega \in \Omega\}$, where ω is an outcome in the probability space Ω. If for each $\omega \in \Omega$ a certain random function $u(\underset{\sim}{X}, t, \omega)$ is introduced, which is said to describe the properties of the inhomogeneous medium, then $M(\omega)$ is called a random medium; the quantity $n(\underset{\sim}{X}, t, \omega)$ is a random variable and usually corresponds to the index of refraction.

For initial value problems, or propagation in time-dependent media, the random wave equation is of the form:

$$\frac{\partial \Psi}{\partial t} = (A + B(\omega))\,\Psi, \qquad (4.7)$$

where the unknown function Ψ (scalar or vector-valued) is the wave function (or field), A is a deterministic linear partial differential operator (usually with constant coefficients) and $B(\omega)$ is a linear partial differential operator with random coefficients which are centered random functions. In accordance with the elastodynamics formulation (see (1.5) and (1.6)) a more precise formulation of the radiation of waves in a lossless, homogeneous, isotropic, time-independent medium is given by the following wave equation:

$$\nabla^2 \Psi(\underset{\sim}{X}, \omega) - \frac{1}{c^2(\underset{\sim}{X}, \omega)} \cdot \frac{\partial^2}{\partial t^2}\, \Psi(\underset{\sim}{X}, \omega) = F(\underset{\sim}{X}_0, t) \qquad (4.8)$$

where $F(X_0, t)$ is a force function applied at position X_0. In the case of a harmonic point source excitation, we have the random Helmholtz equation expressed by:

$$\nabla^2 \Psi(\underset{\sim}{X},\omega) + k_0^2 n^2(\underset{\sim}{X},\omega)\,\Psi(\underset{\sim}{X},\omega) = \delta(\underset{\sim}{X}), \qquad (4.9)$$

where $k_0 > 0$ is the so-called free space wave number, n is the index of refraction with unit mean square value and $\delta(\underset{\sim}{X})$ is the Dirac-delta function. Obviously equations (4.8) and (4.9) have to be supplied with pertinent initial boundary conditions in order to render the problem well-set.

Since we are specifically looking at the propagation of initially plane waves in a long bar (semi-infinite), it is thought that the deliberate focus on the one-dimensional case at this stage will now permit a rather simple account of the mathematical development of the random continuum theory and its potential application to our problem. Thus the first thing to notice is the non-existence of dissipative terms in the equation (4.8), which reflects the smearing out of the medium in this macroscopic approach. The dissipation in structured media is thought to be, to a great extent, due to the presence of the internal boundaries and as evidenced by our analysis in Section 3.5. Hence the equation of the type (3.51) should be adopted as a more realistic model. However, to the best of the author's knowledge this is not the case, and thus according to the classical approach (e.g. Howe, 1971) a unidirectional wave motion obeys the following equation:

$$\frac{\partial^2 u(X,\omega)}{\partial X^2} - \frac{1}{c^2(X,\omega)} \frac{\partial^2 u(X,\omega)}{\partial t^2} = 0 \qquad (4.10)$$

where the exact deformation $u(X,\omega)$ is synthesized from the average value $\bar{u}$ of u and its fluctuating part u', i.e.:

$$u(X,t,\omega) = \bar{u}(X,t) + u'(X,t,\omega) \qquad (4.11)$$

The wave propagation velocity c is expressible in the following fashion:

$$c^2 = c_0^2 \left(1 + \eta(X)\right) \tag{4.12}$$

where C_0 is the average velocity.

Given the initial boundary condition it is possible, at least in principle, to solve the equation (4.10) for the mean and fluctuating parts of $u(X,\omega)$. However, since in our case c^2 is given by:

$$c^2 = \frac{E}{\rho} = \frac{\langle E \rangle + E'}{\langle \rho \rangle + \rho'}, \tag{4.13}$$

where it is assumed that E, ρ are Gaussian random variables, this does not allow a simple functional form of $\eta(\omega)$, and an explicit solution involving a Fourier synthesis for a sequence of successive approximations to $\bar{u}$ and u' (see also Levine, 1978) appeared unwieldy. In this context attention was also given to the simpler case of a harmonic excitation of (4.10). The governing relation now takes the form of a random Helmholtz equation in one dimension so that:

$$\frac{d^2}{dX^2} u(X) + k_0^2 \left(1 + \mu(X)\right) u(X) = 0 \tag{4.14}$$

which for nonrandom initial conditions of $u(0)$ and $\frac{\partial u(0)}{\partial t}$, becomes a linear random differential equation.

The classical approach is to assume that $\mu(X)$ is the Ornstein-Uhlenbeck process - represented by a centered, stationary, Gauss-Markovian random function with the correlation function

$$E\{\mu(X)\mu(X')\} = \varepsilon^2 \exp\left\{-\frac{|X - X'|}{\gamma}\right\}. \tag{4.15}$$

where ε is an arbitrary small non-dimensional parameter and γ is a

given correlation range.

In this case the solutions for the exact field $u(X,\omega)$ can be obtained as shown by Papanicolau (1971) and Morrison et al (1971). In these papers the reflection and transmission coefficients for the wave field in a finite interval of a random medium were introduced as random functions. Their probability density functions were then derived in the functional forms and these were subsequently used to calculate the mean of the square of the above coefficients.

In order to use these results, we must however determine two key parameters in the random continuum approach: the correlation range γ and the dimensionless parameter ε. The first of these is defined to be the minimum distance of two points at which simultaneous fluctuations are independent. Thus with respect to the discrete random medium formulation γ appears to be approximately d. The dimensionless parameter ε is a small number that characterizes the size of the fluctuations of the physical properties in the medium. One may take it as the ratio of the standard deviation of the most strongly fluctuating parameter and its mean value (Frisch, 1968). Thus ε in (4.15) is actually the standard deviation of the Gaussian distribution involved in the Ornstein-Uhlenbeck process $\mu(X)$. However, we note that the assumption of $\mu(X)$ in the form of such a process contradicts relation (4.13). The latter relation indicates that the square of the propagation velocity c^2, in form of the ratio of two Gaussian random variables will not be Gaussian, but will rather result in a Cauchy distribution. Noting that the mean and variance do not exist for such a distribution, we follow Frisch's argument stating that

the ratio of the standard deviation to the mean of the strongest fluctuating property should be considered as ε, and hence choose in the present case the fluctuations in ρ to determine the parameter ε (see Section 4.4 for details of physical properties of the adopted model).

Finally, with reference to the work of Morrison et al (1971) (see the equation (5.13) there) we have to choose the involved wave numbers. Thus we note that for wavelengths larger than the microelement size αd the frequency effect is small and becomes more important for wavelengths that are comparable to αd. We note however, that the latter case has been excluded from the present research program (see statements in Section 2.2.2).

For the purpose of the comparison of the continuum and discrete modelling the above considerations will be employed in Section 4.5 of this chapter.

4.4 Monte-Carlo Simulation of Wave Propagation in Polycrystalline Solids

We now return to the microdynamics formulation of wave propagation in a discrete random medium. As already pointed out in the introduction to this chapter, we aim at developing a Monte-Carlo simulation scheme which would replace a physical experiment on the one hand, and on the other shed some light on the characteristics of the results, that may be expected from the Markov field formulation.

The Monte-Carlo simulation method was developed in the late forties (see for instance Metropolis and Ulam, 1949 and Donsker and Kac, 1949) as a sampling procedure. The latter consisted of the production of models of complex combinational situations or of finding various distributions of particles in dynamics or other physical quantities. Such an experiment is performed on computing machines, whose high speed and large memory enable one to obtain approximate solutions of physical problems, where the exact mathematical solutions are unwieldy or prohibitively lengthy. A Monte-Carlo simulation, is thus naturally suited to problems of statistical physics where in general, one needs to specify the underlying mechanism of the phenomenon at the microscopic level in order to have the machine arrive at a global evolution of the entire physical system.

By analogy to statistical physics, for the Monte-Carlo simulation of the wave propagation in a discrete random medium, we have to specify the laws governing the wave process at the micro-scale and cast them in a computer language so that the rest, i.e. the evolution of the wave, can be done by the computer.

We consider wave propagation in a bar according to the general formulation given in Section 3.1.3 with a microstructure as discussed in Section 2.2. Thus we shall simulate the evolution of a wave as it propagates along the bar employing the wave velocity vector $\tilde{V}$ fixed to a given wavefront. Since the evolution of $\tilde{V}$ from grain to grain is governed by the transmission operator, which is a function of random physical properties of the medium (see relation (3.32)) we have to discuss this aspect first.

Values of elastic coefficients of crystals of various chemical compositions were obtained experimentally by Lazarus (1949) and Overton and Gaffney (1955). The absolute error of the measured c_{ij} elastic coefficients listed there is given by $\pm$ 0.25% for specially prepared crystal specimens of length $\sim$ 2 cm, which were considered to be single crystals. It is well known, that grains in polycrystalline solids may be assumed as single pure crystals (hence our Def. 1), however, to the best of the author's knowledge the statistical information about their elastic constants is not available. Therefore, we use the above mentioned information as a guideline for determination of two moduli ${}^{\alpha}E$ and ${}^{\alpha}G$ in this micromechanical model*. Thus we assume that the absolute variation in ${}^{\alpha}E$ and ${}^{\alpha}G$ is $\pm$ 0.3% about their respective average values. Furthermore, as in most cases in physics, we assume that the probability distributions $P({}^{\alpha}E)$ and $P({}^{\alpha}G)$ are of the simple Gaussian forms. We can thus establish the standard deviation σ in both cases by requiring that:

$$3\sigma = 0.3\% \tag{4.16}$$

whereby it is noted, that for a Gaussian random variate x we have:

$$\left.\begin{aligned} P\{x < \mu - 3\sigma\} &= 0.0013 \\ P\{x > \mu + 3\sigma\} &= 0.9987 \end{aligned}\right\} \tag{4.17}$$

---

* See also Hirth and Lothe (1968) for the average values of the Lamé constants in solids.

No statistical information is available about mass density variations in the single crystals or in the grains of the polycrystalline solids. Therefore, by a similar argument as in the case of elastic constants, the mass density ϱ is assumed to have a Gaussian distribution, where the mean mass density μ_ϱ is taken equal to the values given in the tables of material properties (Kolsky, 1963) and the standard deviation σ_ϱ is taken to vary from $\mu_\varrho/500$ to $\mu_\varrho/200$.

Since we have assumed a microstructure with the geometry of perfect cubic grains, we may choose copper as a typical metal, whose crystals display this kind of geometrical shape. Accordingly, the Gaussian statistics of the variables E, G and ϱ will be specified as follows:

$$\langle E \rangle \equiv \mu_E = 14.459 \cdot 10^{11}\ N/m^2 \tag{4.18}$$
$$\sigma_E = \mu_E/1000 = 14459\ 10^8\ N/m^2$$

$$\langle G \rangle \equiv \mu_G = 5.46 \cdot 10^{11}\ N/m^2 \tag{4.19}$$
$$\sigma_G = \mu_G/1000 = 5.46\ 10^8\ N/m^2$$

$$\langle \varrho \rangle \equiv \mu_\varrho = 8.9 \cdot 10^3\ kg/m^3 \tag{4.20}$$
$$\sigma_\varrho = \mu_\varrho \left(\frac{1}{500} \div \frac{1}{200}\right) = 17.8 \div 44.5\ kg/m^3$$

The crystal size is chosen to be 0.2 mm; this arbitrary choice is made in view of constraining computational costs and for the purpose of illustrating the application of the Monte-Carlo method to the problem of wave propagation in discrete solids. This grain size is employed for the construction of all subsequent diagrams. However, it corresponds to an average size of a fine grained metal structure.

Analogously to the development of the Markov field theory in Chapter III, three simulation models can be given here. One model

that corresponds to the longitudinal wave propagation in a 1-D solid, a second pertaining to a 2-D model of the solid and finally a third corresponding to the L- and T-wave propagation in a 3-D solid. We start by presenting the first model, which is considered as an ensemble of K non-interacting sequences; see Fig. 4.1. for the space-time graph of the process and the pertinent notations. At time t=0 and position $X_1=0$ (front face) a uniform pressure pulse p is applied. By assuming all first microelements of these K sequences to be characterized by ${}^0E = \mu_E$ and ${}^0\rho = \mu_\rho$ an initial velocity distribution ${}^0v = 1\ m/s$ in the first layer is postulated (0 denotes the first microelement). From now on the program takes the following steps:

- evaluate propagation velocity in the first crystal: ${}^0c_L = \sqrt{{}^0E/{}^0\rho}$
  evaluate the passage time: ${}^0\tau = d/{}^0c_L$
  evaluate the arrival time at (0,1) interface: $T = {}^0\tau$
  evaluate the wave velocity in the first crystal: ${}^0v = \dfrac{p}{{}^0\rho\ {}^0c_L} = 1$
- generate two random variables ${}^1\rho, {}^1E$ according to their Gaussian statistics*
  evaluate the propagation velocity: ${}^1c_L = \sqrt{{}^1E/{}^1\rho}$
  evaluate the passage time: ${}^1\tau = d/{}^1c_L$
  evaluate the arrival time at (1,2) interface: $T = {}^0\tau + {}^1\tau$
  evaluate the impedance ratio: ${}^{01}\chi = \dfrac{{}^1\rho\ {}^1c_L}{{}^0\rho\ {}^0c_L}$
  evaluate the transmission coefficient: ${}^{01}c_{tr} = \dfrac{2}{1+{}^{01}\chi}$
  evaluate the wave velocity in the second crystal: ${}^1v = {}^{01}c_{tr}\cdot {}^0v$

---

* The Gaussian variates are obtained using the Box-Muller method (Rubinstein, 1981).

- generate two random variables ${}^2\varrho$, ${}^2E$ for the crystal 2 and repeat the procedure.

This procedure is continued up to any desired grain so that we always know the following:

- the grain number N in the sequences, which corresponds to a definite position in space X_1 (line $0\text{-}X_1$)
- the arrival time $T = \sum_{\alpha=0}^{N} {}^{\alpha}\tau$ at the N/N+1 interface
- the pulse amplitude $V = \prod_{\alpha=0}^{N-1} {}^{\alpha,\alpha+1}C_{tr}$

Repetition of this procedure corresponds to the same initial pulse being propagated in another sequence $S_k \in M$ and gives another result. In the actual computer program the simulation has been conducted for K=100 sequences in parallel so that a read out of the arrival times $\{T_1, T_2, \ldots, T_{100}\}_N$ and of the pulse amplitudes $\{V_1, V_2, \ldots, V_{100}\}_N$ was possible (see Fig. 4.1).

Since it is known that any given random number generator gives rise to a sequence of pseudo-random numbers which has a distribution slightly deviating from a perfect uniform distribution, it was decided to combine two different generators in every simulation in order to even out the cumulative distribution of pseudo-random numbers. Thus the physical properties of the microelements in all odd-numbered sequences were generated with the seed 5^{13}, while those of all even-numbered sequences were generated with the number 7^{11}. Although a small difference in the obtained results was noticed when using these two generators separately it is assumed that the combination of these different generators leads ultimately to the acceptable pseudo-random results.

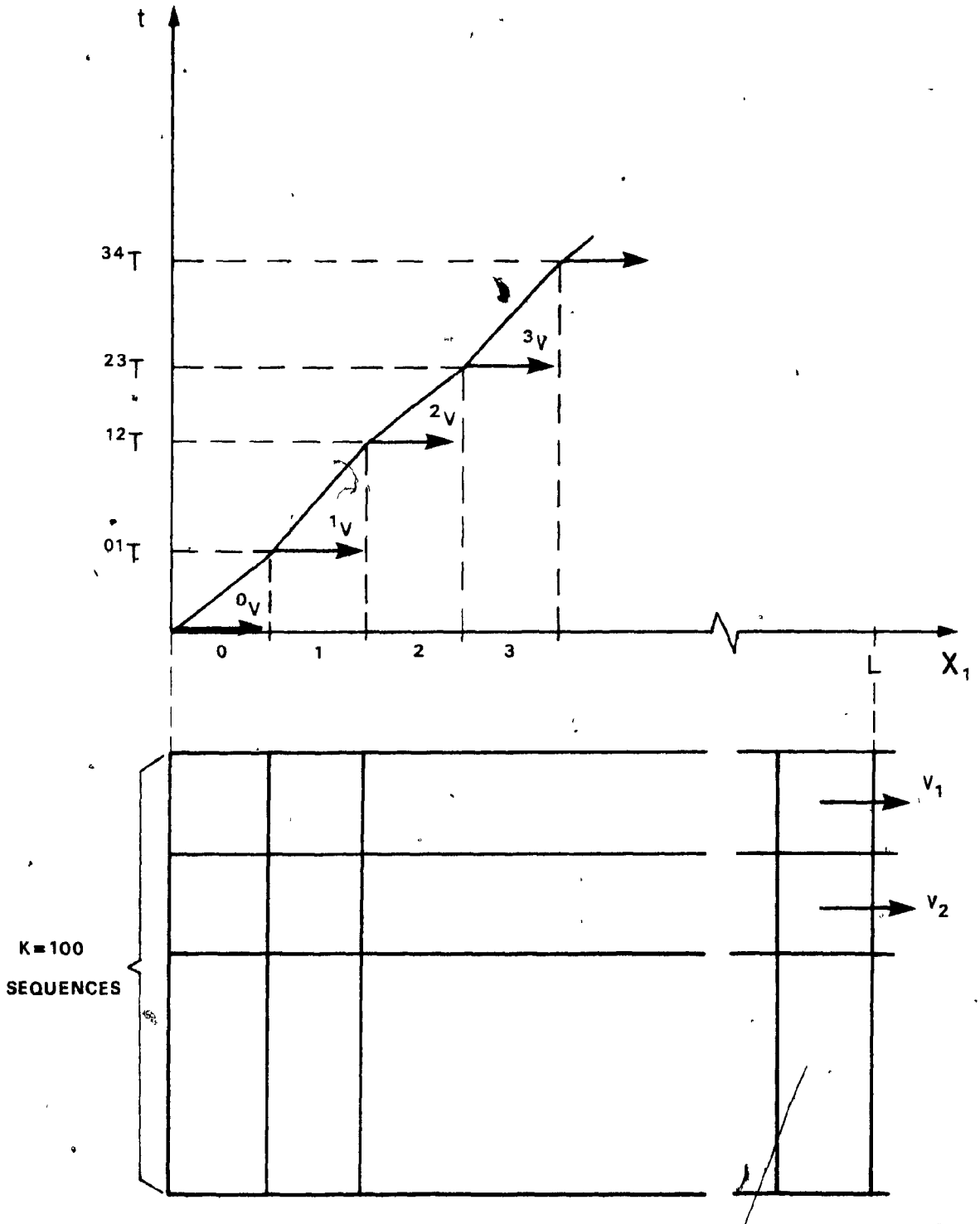

FIG 4 1 SIMULATION OF WAVE PROPAGATION IN SEMI-INFINITE BAR (1-D MODEL).

In the two-dimensional model we consider the bar to consist of 100 sequences arranged in a plane X_1X_2 (see Fig. 4.2a) and adopt the following model for the interaction of a microelement α with its two neighbours in the transverse direction. After the pulse ${}^{\alpha-1}\underset{\sim}{V}_i$ has been transmitted into α through the boundary $(\alpha-1,\alpha)$ perpendicular to the direction of propagation, the velocity ${}^{\alpha}\underset{\sim}{V}_{tr}$ undergoes a modulation at the two parallel grain boundaries $(\alpha\beta)$ and $(\alpha\gamma)$. It is evident that due to these interactions, the wave velocity vector ${}^{\alpha}\underset{\sim}{V}$, while representing the wave propagation in the X_1 direction, is also a function of the X_2 coordinate. This fact has forced us to introduce the transmission operator in Section 3.4. However, since on a computer we can only work with a number rather than a function, we choose to introduce a quantity which is an average of ${}^{\alpha}\underset{\sim}{V}$ taken over the cross-section of the grain α such that:

$$ {}^{\alpha}\bar{V}(X_1,t) \stackrel{df}{=} \underset{X_2}{E}\{{}^{\alpha}\underset{\sim}{V}(X_1,X_2,t)\}. \tag{4.21} $$

We know from the 1-D simulation, that the variations in the arrival times as well as in velocities $\underset{\sim}{V}$ are quite small for the specified Gaussian statistics in (4.18), (4.19) and (4.20). Thus instead of solving a rather complicated initial boundary value problem for the grain α, we can assume that the interactions at the boundaries $(\alpha\beta)$ and $(\alpha\gamma)$ are independent of each other and will involve the two halves of α separately (see Fig. 4.2b). This is an approximation since boundary effects usually do not occur deeper than 5÷10 atomic layers in the ideal lattice (Leibfried, 1955).

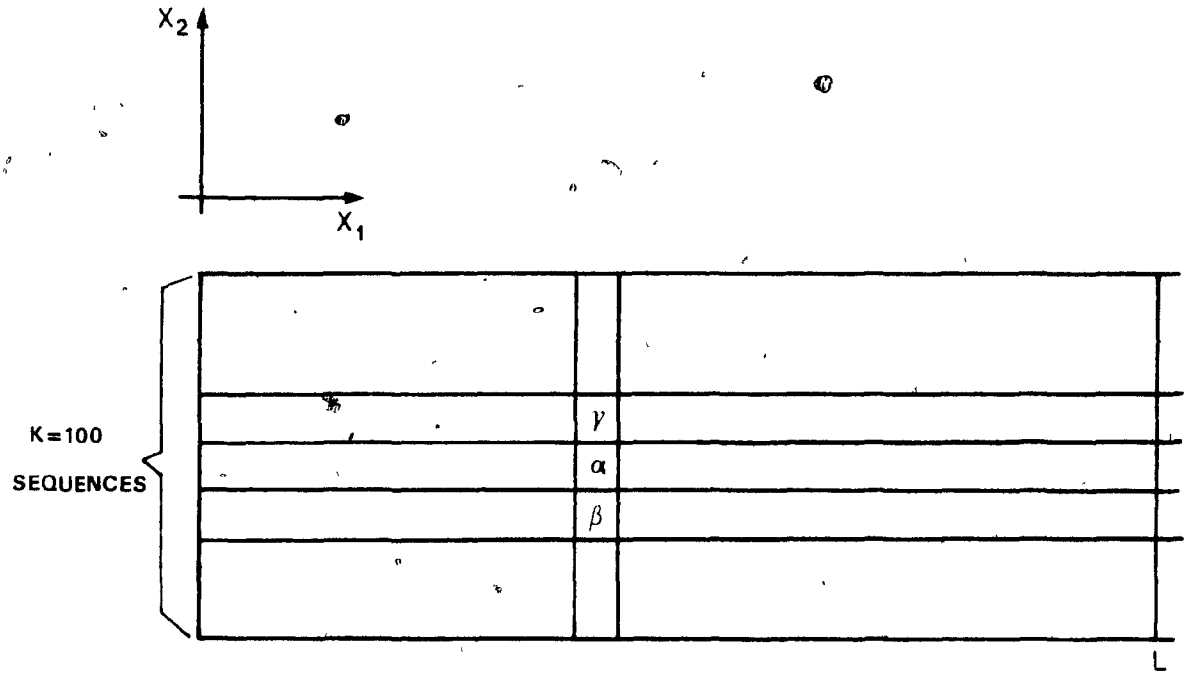

(a) INTERACTION NEIGHBOURS FOR THE CRYSTAL α.

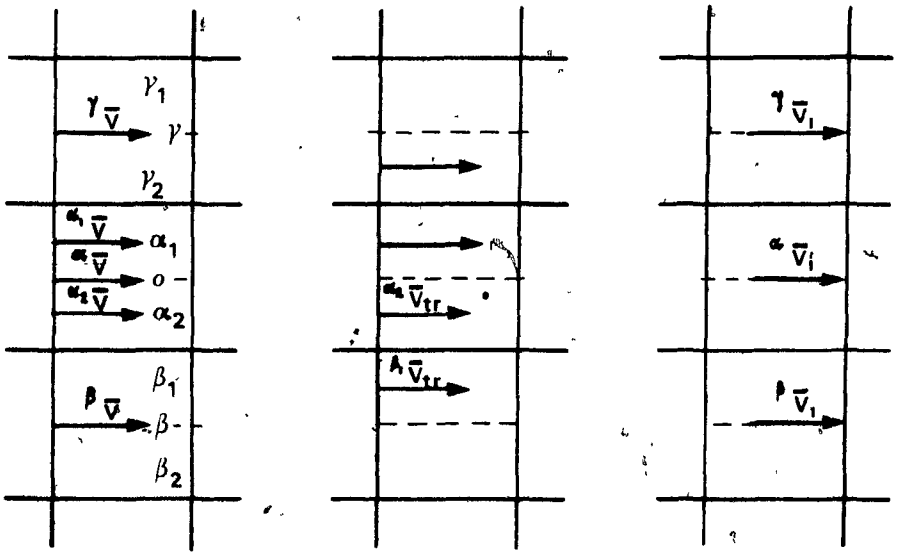

(b) THREE STAGES OF CALCULATION OF α_V DURING ITS PASSAGE THROUGH α.

FIG.4.2 INTERACTION IN 2-D MODEL OF THE SOLID.

It is to be noted that up to now considerable attention has been given to the derivation of an explicit form of the transmission operator and its dependence on the wavenumber involved. This attempt has shown to be rather complex and hence a simplified interaction law is adopted that permits the Monte-Carlo simulation. Hence with reference to Fig. 4.2b we see that in two neighbouring halves of the crystals α and β we will have initially a difference in wave velocities such that:

$$ {}^{\alpha\beta}\Delta \bar{V}_i = {}^{\alpha_2}\bar{V} - {}^{\beta_1}\bar{V}, \qquad (4.22) $$

where the bars indicate now quantities averaged over half the cross-section of a given grain. It may be recalled from Section 2.2.3 that the continuity of the wave velocity vector in the physical domain has been based on the continuity assumption for deformation and deformation rates at an intercrystalline boundary ($\alpha\beta$). It is more convenient however to use this continuity condition in conjunction with the condition of conservation of energy. Hence the following condition can be written:

$$ {}^{\alpha_2}P(t_0) + {}^{\beta_1}P(t_0) = {}^{\alpha_2}P(t_0 + \langle {}^{\alpha}\tau \rangle) + {}^{\beta_1}P(t_0 + \langle {}^{\alpha}\tau \rangle) \qquad (4.23) $$

It is further assumed that the resulting mean velocities in two half-grains are equal, i.e.:

$$ {}^{\alpha_2}\bar{V}_{tr}(t_0 + \langle {}^{\alpha}\tau \rangle) = {}^{\beta_1}\bar{V}_{tr}(t_0 + \langle {}^{\alpha}\tau \rangle) \qquad (4.24) $$

Hence, we get for the transmitted velocities the following expression:

$$ {}^{\alpha_2}\bar{V}_{tr} = {}^{\beta_1}\bar{V}_{tr} = \left[\frac{{}^{\alpha_2}\bar{V}^2 + {}^{\alpha\beta}\chi\, {}^{\beta_1}\bar{V}^2}{{}^{\alpha\beta}\chi + 1} \right]^{\frac{1}{2}} \qquad (4.25) $$

The transmitted wave velocities at the $(\alpha\gamma)$ interface of the grains α and γ can be similarly derived. Having determined the resulting velocities in the two halves of the grains α, i.e. ${}^{\alpha_1}\bar{V}_{tr}$ and ${}^{\alpha_2}\bar{V}_{tr}$ we can now replace these quantities by a single average velocity ${}^{\alpha}\bar{V}_i$, which is incident at the $(\alpha, \alpha+1)$ boundary. By using the conservation condition of the power flux, we obtain

$$ {}^{\alpha}\bar{V}_i = \sqrt{\frac{1}{2}\left({}^{\alpha_1}\bar{V}_{tr}^2 + {}^{\alpha_2}\bar{V}_{tr}^2\right)} \qquad (4.26) $$

We now see that the Monte-Carlo scheme for the wavefront propagation in a 2-D model of the solid should proceed as follows:

- postulate a uniform initial velocity distribution in the first layer:
  ${}^0V = 1\,m/s$
  evaluate the passage time: ${}^0\tau = d/{}^0c_L$
  evaluate the arrival time at (0,1) interface: $T = {}^0\tau$

- generate two random variables ${}^1\rho, {}^1E$ for every microelement of the next layer
  evaluate the propagation velocity: ${}^1c_L = \sqrt{{}^1E/{}^1\rho}$
  evaluate the passage time: ${}^1\tau$ $d/{}^1c_L$
  evaluate the arrival time at (1,2) interface: T ${}^0\tau + {}^1\tau$
  evaluate the transmitted wave velocity: ${}^1V$ ${}^{01}C_{tr}\,{}^0V$
  evaluate the velocities resulting from the interaction at all $(\alpha\beta)$ boundaries according to (4.24)
  evaluate the final velocities ${}^{\alpha}\bar{V}_i$ in all grains α of the second layer according to (4.26)

- generate two random variables ${}^{2}\rho, {}^{2}E$ for every microelement of the next layer and repeat the procedure.

Similarly as in the one-dimensional model the simulation is continued on the computer up to any desired number of grains in the sequence so that we obtain a set of arrival times $\{T_1, T_2, \ldots, T_{100}\}_N$ and wave amplitudes $\{V_1, V_2, \ldots, V_{100}\}_N$ at a given number N. In order to compromise the non-uniform trends in the generation of the pseudo-random numbers the physical properties of the odd-numbered sequences were generated with 5^{13} while those of the even-numbered sequences were generated with 7^{11}. Thus a simulation was run on the computer with these two seeds simultaneously.

In the three-dimensional model of the solid we have to account for the existence of four grain boundaries in the case of a cubic microelement α rather than only for two. Adopting the same model of interaction at any interface parallel to the direction of propagation we only have to modify the formula for the final velocity ${}^{\alpha}\bar{V}_i$, incident at the $(\alpha, \alpha+1)$ boundary. Thus we have instead of (4.26) the following relation:

$$ {}^{\alpha}\bar{V}_i = \sqrt{\frac{1}{4}\left(\alpha_1 \bar{V}_{tr}^{\,2} + \alpha_2 \bar{V}_{tr}^{\,2} + \alpha_3 \bar{V}_{tr}^{\,2} + \alpha_4 \bar{V}_{tr}^{\,2}\right)} \qquad (4.27) $$

The three-dimensional solid is now modelled as a rectangular (10x10) ensemble of 100 sequences of cubic microelements. Hence the development of the Monte-Carlo simulation scheme for the 3-D model of the cubic structured solid can be summarized as follows:

- postulate a uniform initial velocity distribution in the first layer: ${}^{1}V = 1\ m/s$.

evaluate the passage time: ${}^0\tau = d/{}^0c_L$

evaluate the arrival time at (0,1) interface: $T = {}^0\tau$

- generate two random variables ${}^1\rho, {}^1E$ for every microelement of the next layer

evaluate the propagation velocity: ${}^1c_L = {}^1E/{}^1\rho$

evaluate the passage time: ${}^1\tau = d/{}^1c_L$

evaluate the arrival time at (1,2) interface: $T = {}^0\tau + {}^1\tau$

evaluate the transmitted wave velocity: ${}^1V = {}^{01}C_{tr}\,{}^0V$

evaluate the velocities resulting from the interactions at all (α,β) boundaries in the layer according to (4.24)

evaluate the final velocities ${}^{\alpha}\bar{V}_i$ in all the grains α according to (4.27)

- generate two random variables ${}^2\rho, {}^2E$ for every microelement of the next layer and repeat the procedure.

Again this simulation is continued on the computer up to any desired number of grains so that we obtain a set of arrival times $\{T_1, T_2, \ldots, T_{100}\}_N$ and a set of wave amplitudes $\{V_1, V_2, \ldots, V_{100}\}_N$ at any given number N. In order to even out the pseudo-random number generation, the physical properties of the odd-numbered layers were generated with 5^{13} while those of the even-numbered layers were generated with 7^{11}.

The general flow chart of the simulation program is shown in Fig. 4.3 while the corresponding computer programs are attached in Appendix C of the thesis.

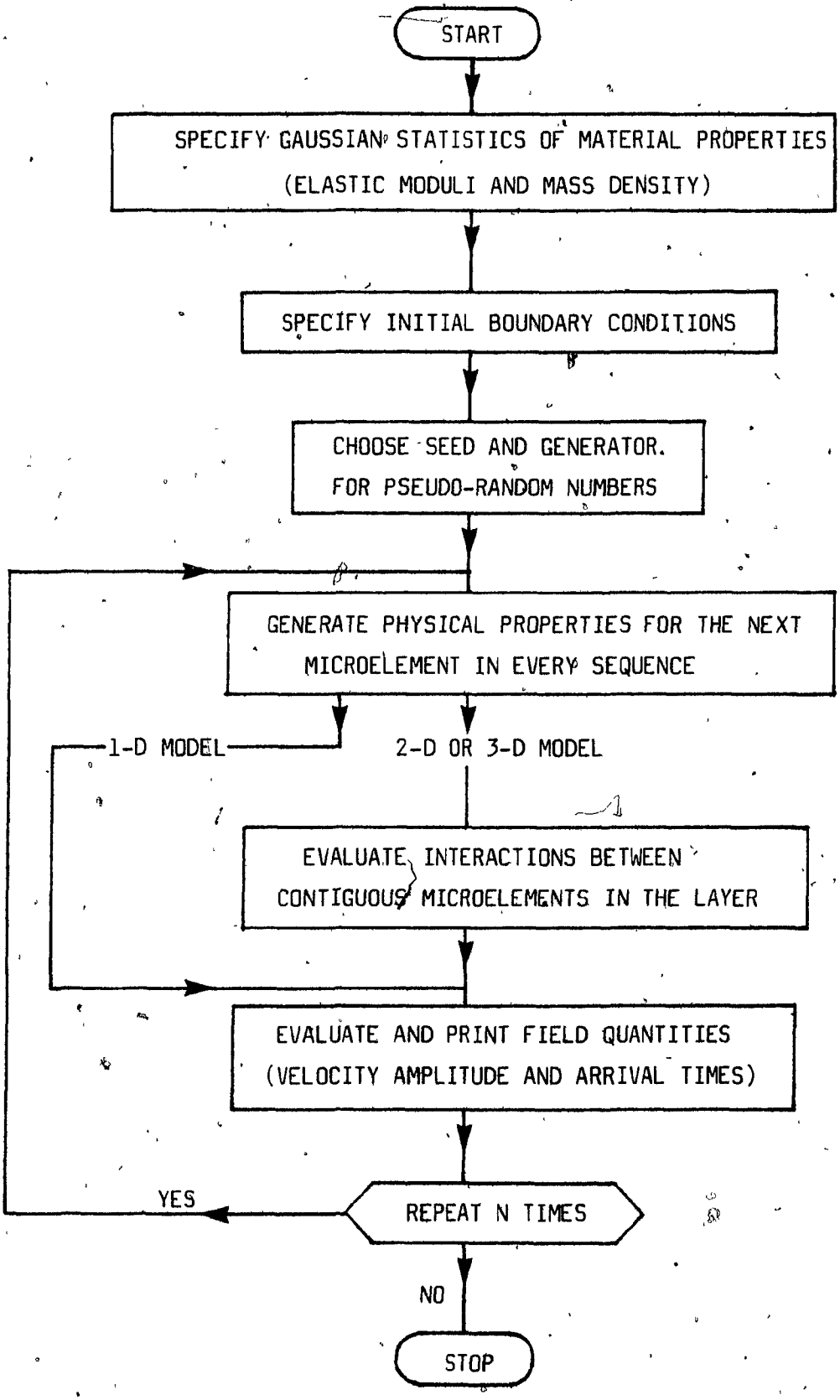

Fig. 4.3 Flow Chart of the Monte-Carlo Simulation Program

4.5 The Monte-Carlo Simulation Results and Discussion

In the previous section we have described the Monte-Carlo technique developed here for the purpose of simulating the wave propagation in a random discrete solid. Three cases of the discrete solid were dealt with, i.e. the one-dimensional, two-dimensional and three-dimensional model. In all cases the longitudinal wave propagation was simulated in terms of an arbitrarily chosen number of sequences and by inclusion of a proposed interaction mechanism. The particular number of sequences (K=100) was chosen as a compromise between a minimum number of pseudo-random results required to give meaningful probability distributions and the available computing time. Similarly, due to these constraints, the process of wave propagation was simulated for a standard distance L=1m only in the semi-infinite bar M. In accordance with the Markov-theoretic model developed in Chapter III the random evolution of this wavefront was characterized by two quantities, namely the wave velocity vector $\underset{\sim}{V}$ and the so-called arrival time T identical to the internal time of the Markov process $\underset{\sim}{V}(t)$; these two quantities were read out at every station in multiples of 10 cm. Recalling that the microstructure of the bar was assumed to be composed of perfectly cubic crystals of a constant size a_d = 0.2 mm, this model yields results ten times during the simulation process or at every 500-th grain. The statistics of the physical parameters involved in the longitudinal wave propagation (one-dimensional stress approximation) are specified through (4.18) and (4.20). It is to be noted that two cases of the mass density statistics were used, i.e. the case of $\sigma_\varrho = \mu_\varrho/200$ (a) and the case of $\sigma_\varrho = \mu_\varrho/500$ (b). We shall discuss case (a) first.

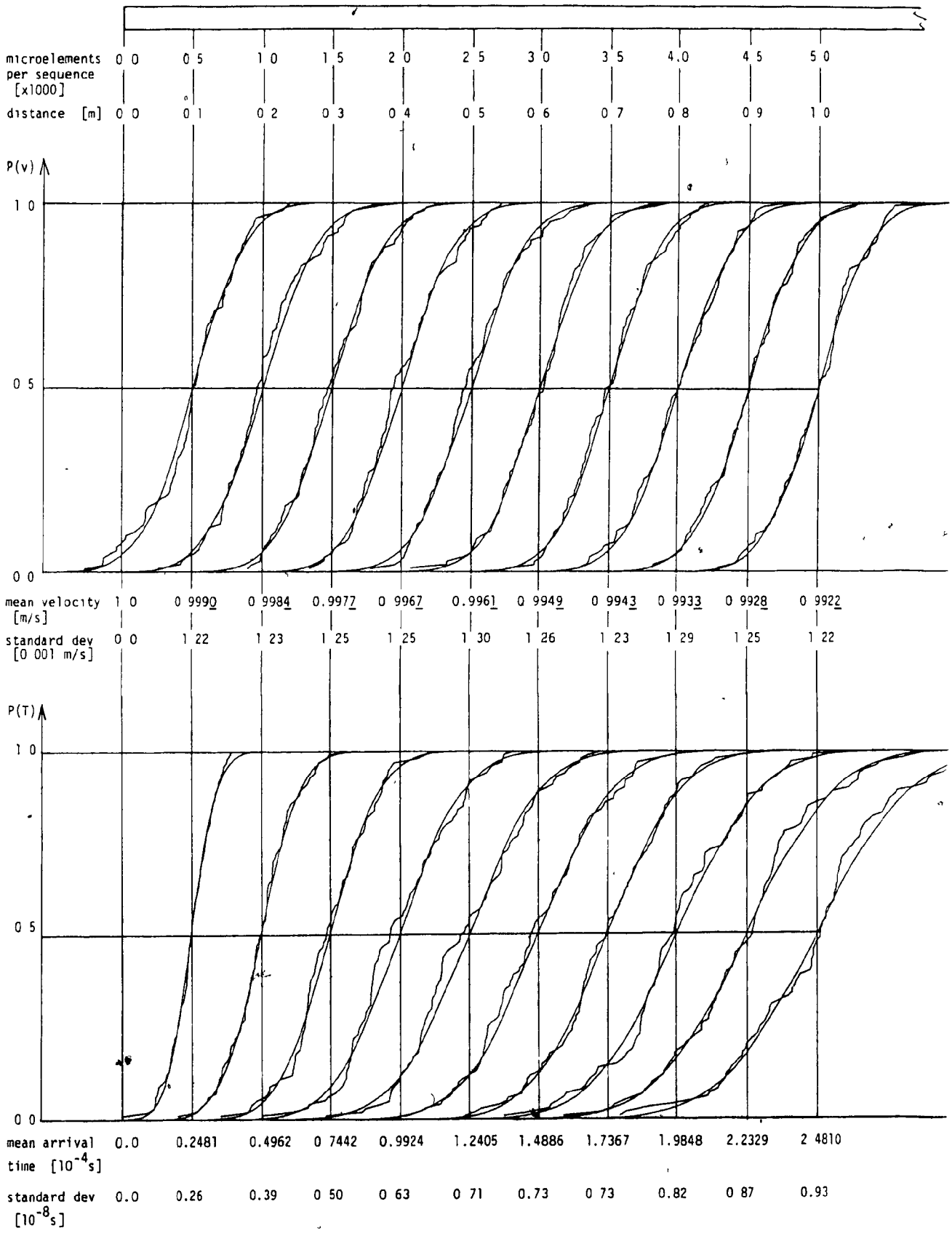

Fig. 4.4 Probability distribution of velocity and arrival time for a 1-D model, case (a)

The results of a simulation of an L-wave pulse propagating in the one-dimensional model of the solid are shown in Fig. 4.4. The evolution of the pulse given at $t = 0$ with the magnitude of $v = 1 m/s$ is shown in terms of the probability distributions $P(v)$ and $P(T)$, where $V \equiv |\dot{u}|$ and T is the arrival time. The cumulative distributions (frequency polygons) of these two quantities obtained by the simulation are plotted separately at every station or in multiples of 0.1 m, whereby the mean value and the standard deviation are illustrated by the abscissa. It is to be noted that while the scale of either random variable V or T is the same at every station the origin has been shifted appropriately so that the mean values coincide with the given read-out position on the X_1 axis of the bar. This convention along with the fixed scales is adopted for all the subsequent plots. Hence, an immediate visual comparison of various cases and models becomes possible. The velocity and the dispersion time distributions are approximated here by the Gaussian distributions, which display a very good fit. Indeed, this result confirms the theoretical formulation given in Appendix B of this thesis. Although the binomial- and Poisson-type fits have been tried, they proved less appropriate than the Gaussian fit. A closer analysis of the $P(v)$ graphs shows that the pulse falls off on the average, but the spread in magnitude as reflected by the standard deviation, remains fairly constant. On the other hand, the $P(T)$ graphs reflect the tendency of the pulse to spread within the dispersion time cone in the space-time graph (see Fig. 3.3). Thus we see that the entire Fig. 4.4 corresponds to the formulation given by (3.28), that is to the evolution of all the

microdisturbances (propagating in particular sequences) in terms of the postulated internal times. It is also interesting to note, that the dispersion time, or the deviation of the random arrival time from its mean is much smaller than expected, i.e. on the order of $\alpha\tau$ after one meter travelling distance. This indicates that the internal time fluctuations are very small. However, they may become significant in the case of strongly non-stationary (e.g. critical) phenomena. We also note that the one-dimensional model utilized in the computer simulation was also run for a larger distance L than one meter. It was revealed thereby that a slow (non-linear) increase in the arrival time spread (σ_T) occurs.

The results of the simulation of the same pulse in the two-dimensional and three-dimensional models of the solid are shown in Figs. 4.5 and 4.6, respectively. As before the simulation results are shown by the frequency polygons which are plotted for the velocity V and time T distributions at every station along the X_1-axis. It is seen that the Gaussian distributions are again giving a good approximation. This is rather an interesting result in view of the fact that there is a coupling between the contiguous sequences. However, this can be readily explained, if we note that the sums of weakly dependent random variables still converge to Gaussian distributions (due to the Central Limit Theorem). In general, we see, as before, the attenuation of the signal due to the minute reflections at the consecutive interfaces with the spread in the signal remaining fairly constant in both these models.

A global comparison of all three models for case (a) may best be conducted on the basis of Fig. 4.7. Here we present the

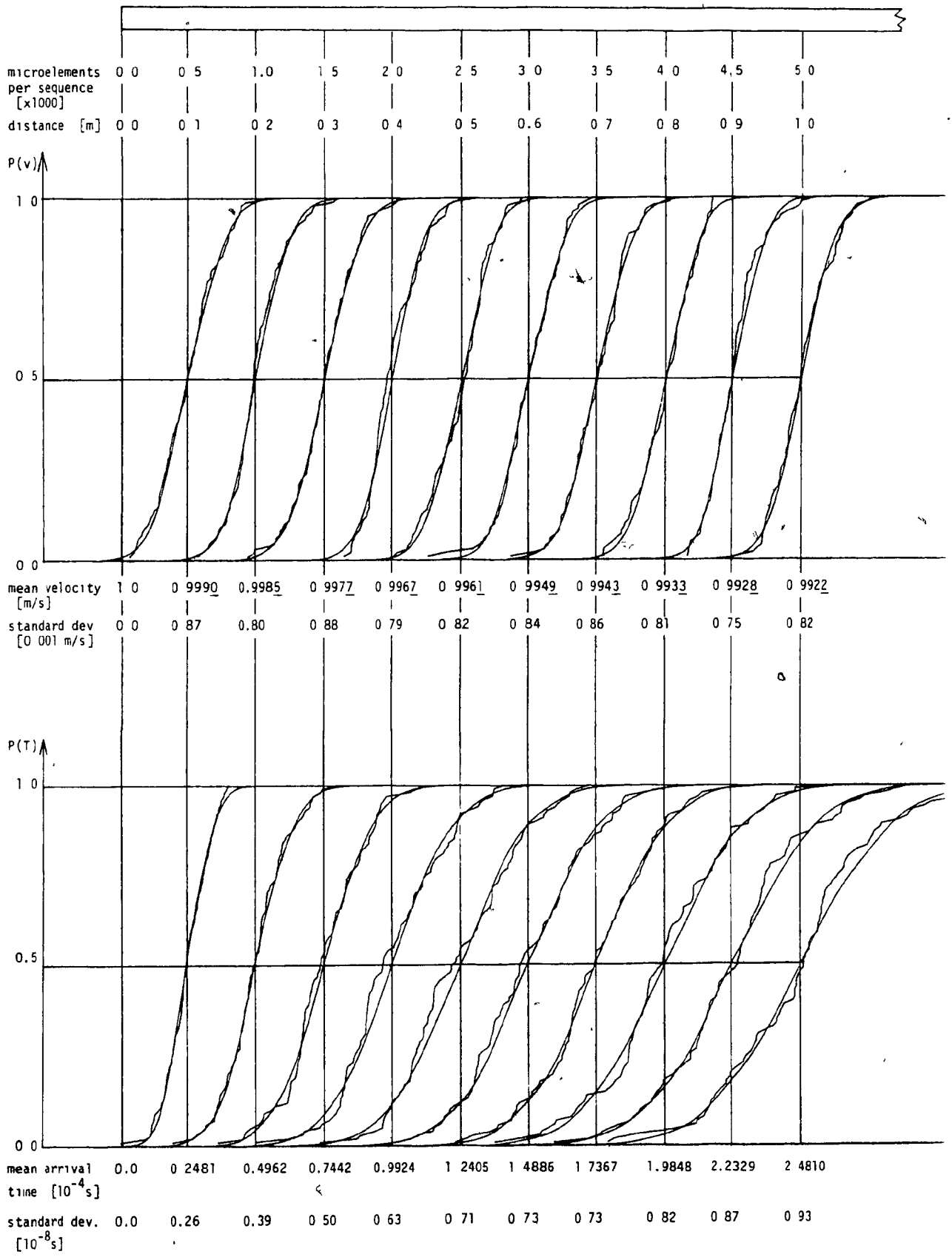

Fig. 4.5 Probability distributions of velocity and arrival time for a 2-D model, case (a)

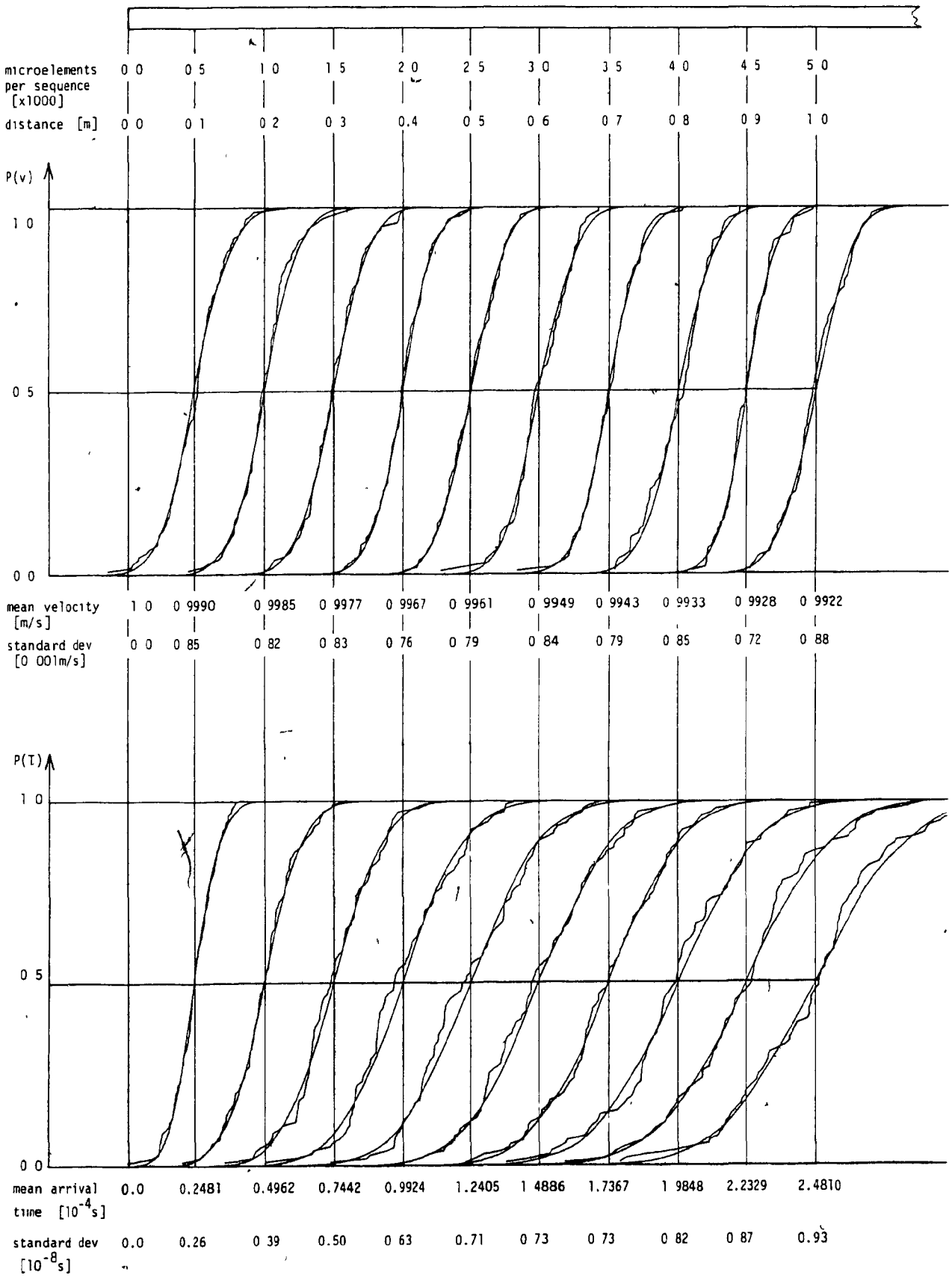

Fig. 4.6 Probability distributions of velocity and arrival time for a 3-D model, case (a)

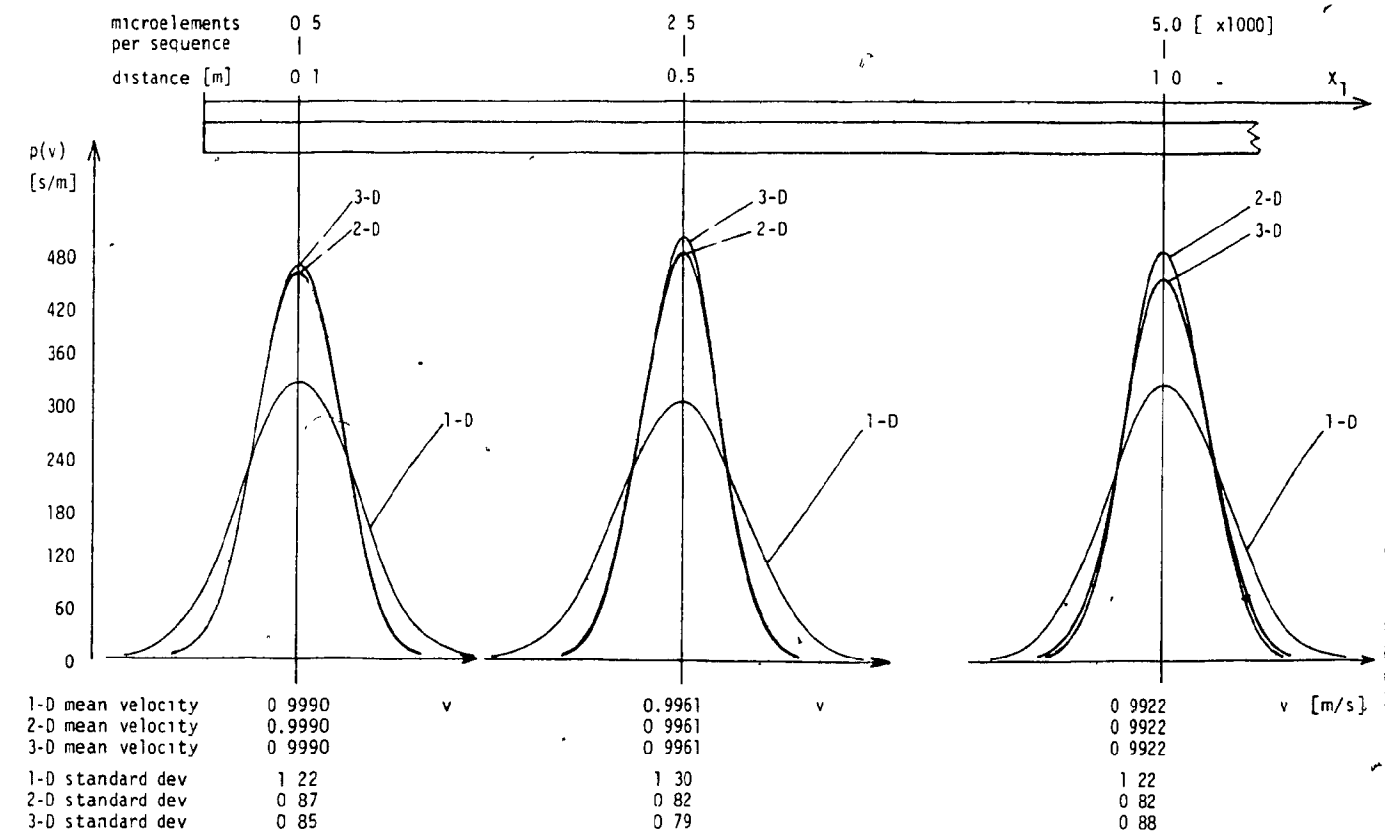

a)

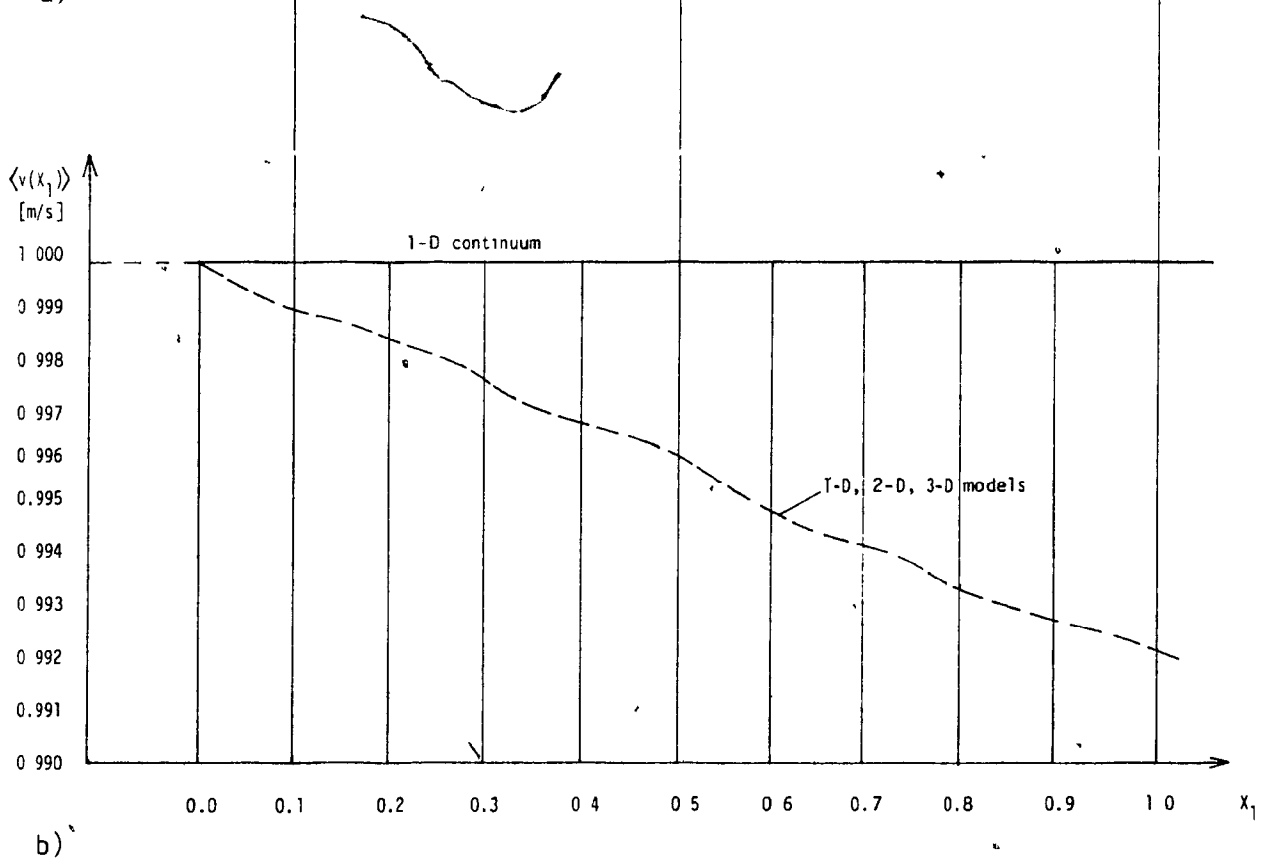

b)

Fig. 4.7 Comparison of 1-D, 2-D and 3-D Models, Case (a)

a) Evolution of probability densities
b) Evolution of the mean pulse

evolution of the velocity V in terms of the Gaussian density fits at three stations along the bar, i.e. at 0.1 m, 0.5 m and 1.0 m, as well as the mean pulse behaviour along X_1. The main observation here is that the mean velocity is of the same magnitude for all three models. It is seen that the standard deviation of the 1-D model is considerably larger than the standard deviations of both the 2-D and 3-D models. However, it is possible to note from the $P(v)$ distributions in Figs. 4.5 and 4.6 that the spread in velocity is slightly smaller in the three-dimensional model than that in the two-dimensional model. This further indicates that even the simple model of 3-D interactions as adopted in Section 4.4 leads to a somewhat smaller deviation in the magnitudes of the velocity.

It is to be noted from Fig. 4.7b) that the curves of the mean velocity in all three models coincide and show a certain amount of fluctuations between the chosen increments of distance. These fluctuations are due to the smoothing out of the actual numerical results obtained for the ten chosen stations. It is obvious that for a very large number of stations this smoothing procedure will lead to a more continuous appearance as depicted in Fig. 4.8. This figure has been obtained from a simulation of a pulse propagating in a single semi-infinite sequence using the 1-D model. The computer results were read out at every 2 m up to 400 m distance along the X_1 axis and show small fluctuations about the mean exponential attenuation. This observation is in accordance with the averaged wave equation (eq. (3.51)) obtained in Section 3.5, the solution of which is of the type $e^{-b't}$. It is important to note, that the results of the

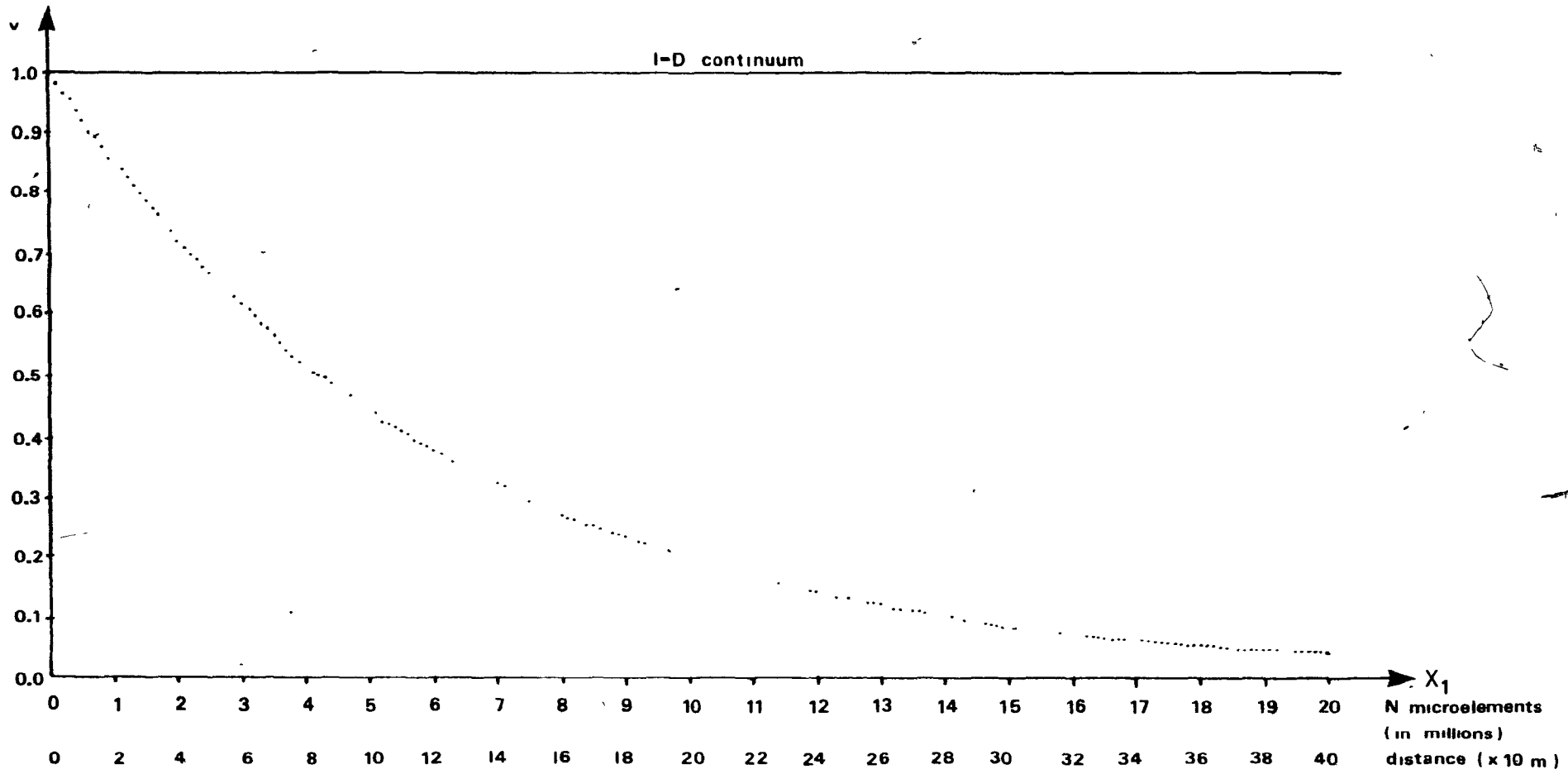

FIG. 4.8 PULSE PROPAGATION IN A SEMI-INFINITE SEQUENCE

one-dimensional deterministic continuum model are represented by a straight full line in Fig. 4.8, as well as in Fig. 4.7b). This is in accordance with our discussion in Section 4.2 dealing with the continuum formulation. However, such an analysis can be extended in a similar manner to the two- and three-dimensional case.

It is further of interest to note that no correlation between the pulse amplitudes and the arrival times in the one-dimensional simulation model was detected. This observation can be readily explained by the fact that the coefficient C_{tr} has, in general, a more complex form as a function of ϱ and E as opposed to that given by the definition of the passage time $^{\alpha}\tau$ (compare relation (2.41) and Def. 2). However, whilst one might generally expect this situation to change in the models with interactions between the contiguous sequences, this was not the case. In fact, the arrival time distribution $P(T)$ proved to be exactly the same in all three cases - compare Figs. 4.4, 4.5 and 4.6.

Finally, it is to be noted that the small variation in the arrival times as evidenced by these three figures justifies the assumption of our simplified interaction model of the previous section, where we disregarded the difference in the arrival times in the α and β grains for the coupling effect at their boundary.

Exactly the same type of simulation was conducted for case (b) i.e. $\sigma_{\varrho} = \mu_{\varrho}/500$ and all the other data remains the same. The results for the 1-D, 2-D and 3-D models are shown in Figs. 4.9, 4.10 and 4.11, respectively. They represent the same trends of attenuation of the pulse and its spread within the dispersion time cone, but less

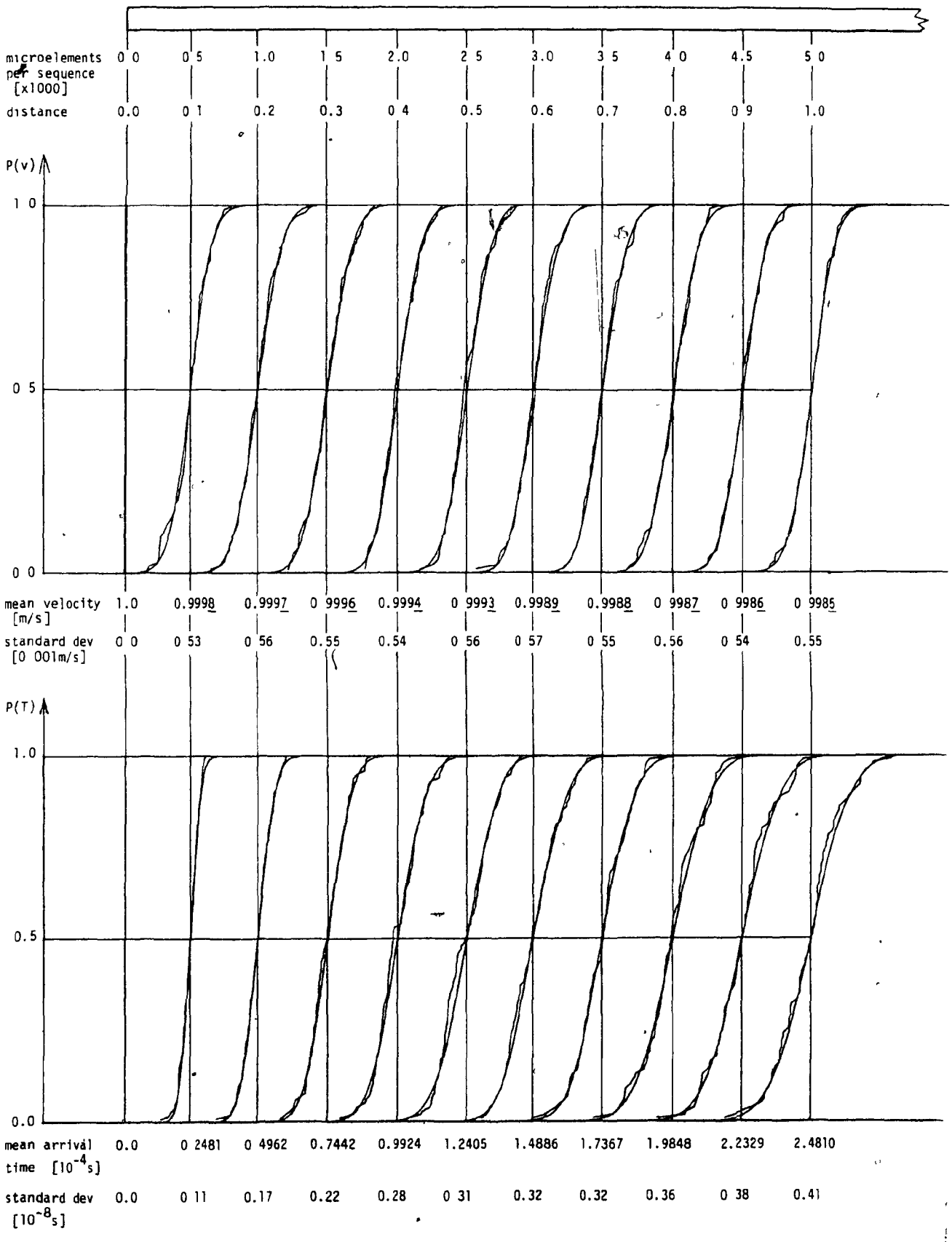

Fig. 4.9 Probability distributions of velocity and arrival time for a 1-D model, case (b)

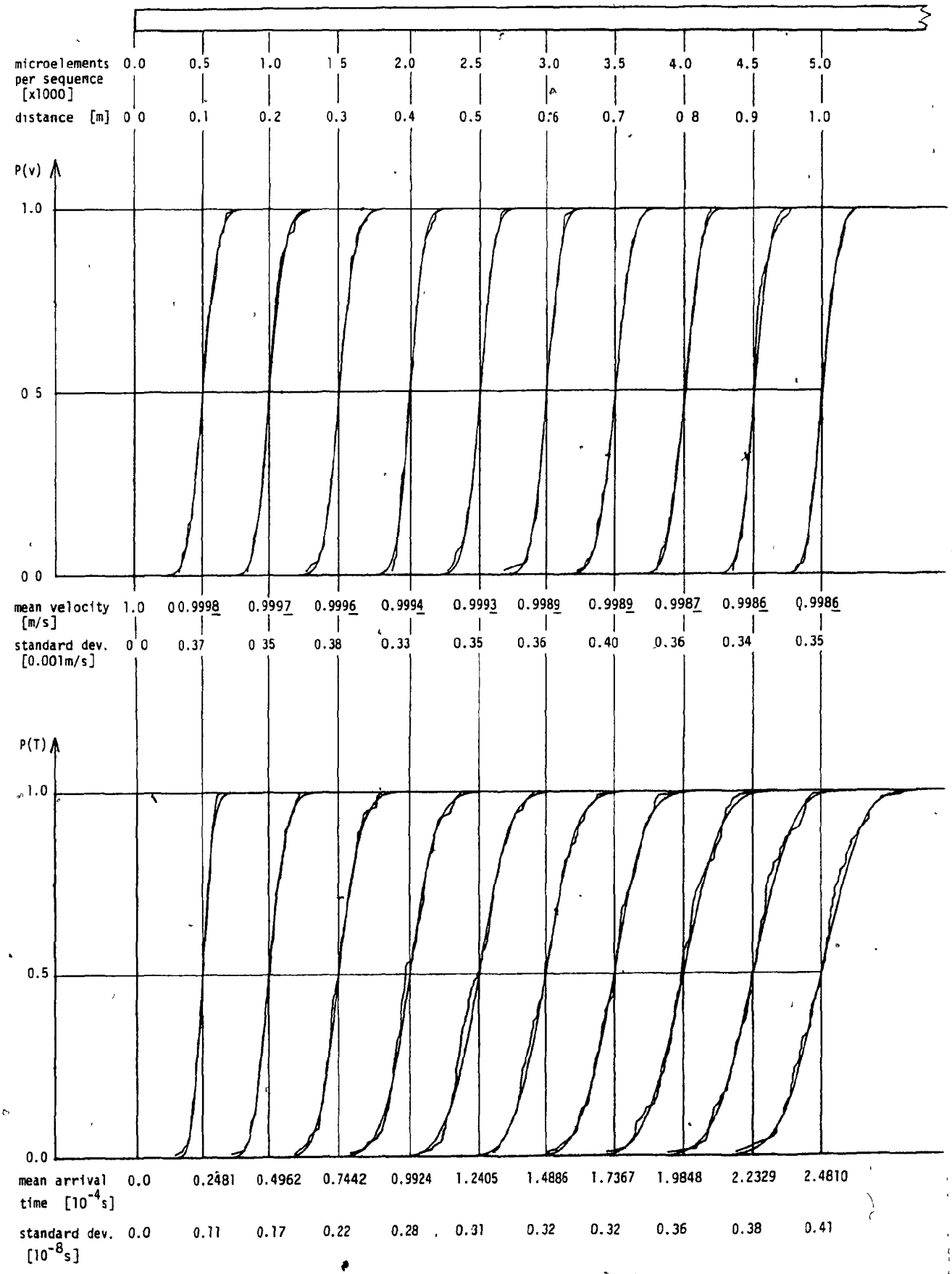

Fig. 4.10 Probability distributions of velocity and arrival time for a 2-D model, case (b)

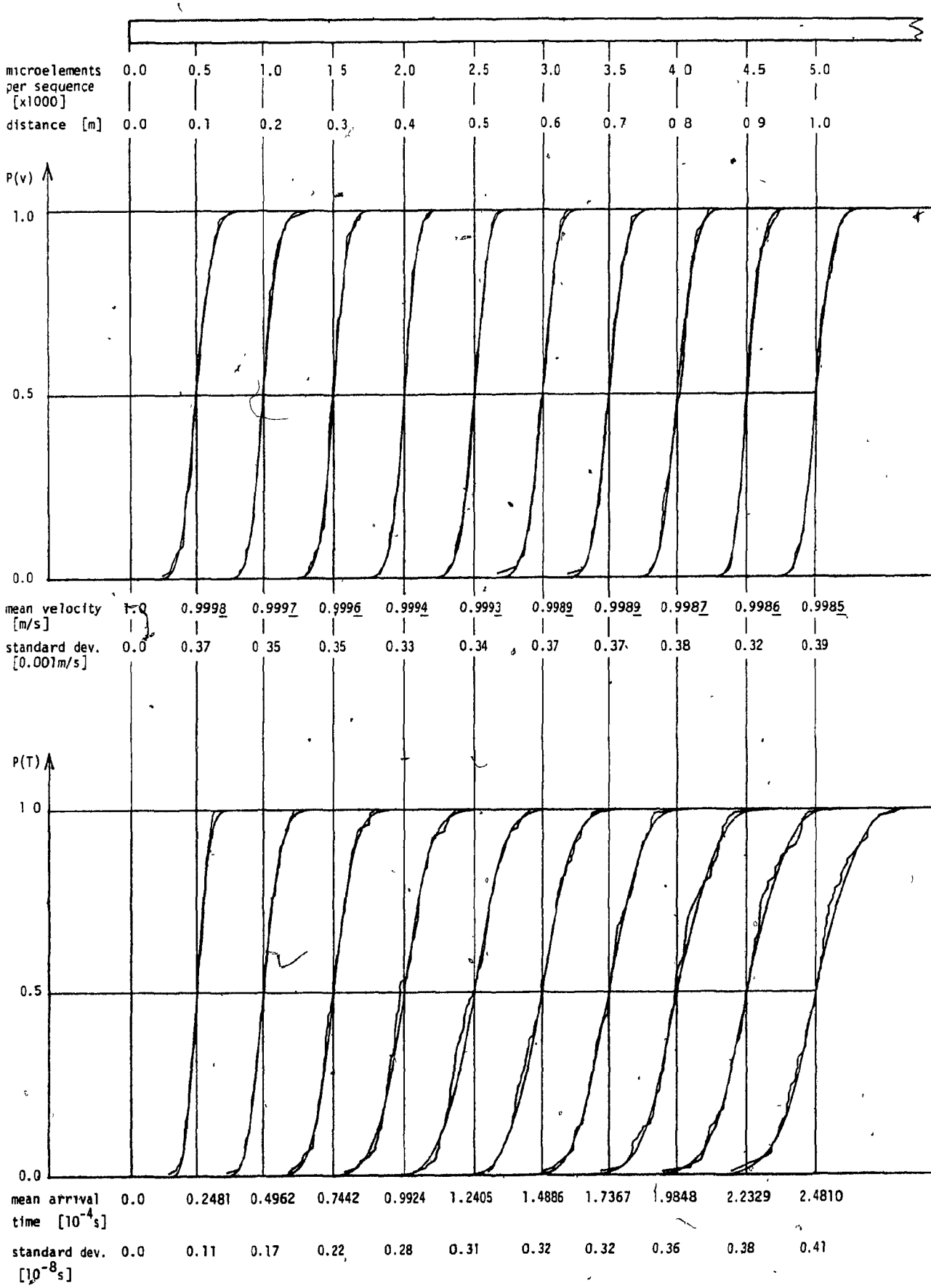

Fig. 4.11 Probability distributions of velocity and arrival time for a 3-D model, case (b)

pronounced than in case (a). This qualitative result has been expected, since smaller variations in the basic physical parameters (E and ρ) should result in smaller variations in the coefficients C_{tr} and C_r as well as the variable $\alpha\tau$. Hence, also smaller amounts of the energy losses at the internal surfaces could be expected. Thus, in either 1-D, 2-D or 3-D models the amplitudes of the micro-disturbances in particular sequences fluctuate about the mean but stay again within a certain band. In all these three models the decrease in the mean pulse is considerably slower than in case (a), while the band of fluctuations of the velocity V is much smaller. On the other hand, the mean of the arrival time is exactly the same as in case (a) but the dispersion quite smaller. Again, the entire arrival time process in all three models is the same - compare the $P(T)$ graphs of Figs. 4.9, 4.10 and 4.11. As expected, the Gaussian distributions give a very good fit for the $P(v)$ and $P(T)$ plots.

For reason of a possible comparison of the above results illustrating the developed microdynamics theory of wave propagation it may be appropriate to attempt at this stage to clarify the conceptual difference between the classical random continuum theory and the present theory. In the former the wave motion is described in terms of a stochastic differential equation the solution of which in the 1-D case has been discussed amongst others by Papanicolau (1971) and Morrison et al (1971). It has been shown in these papers that the solution of the equation of motion depends strongly on an abstract parameter which is related to the wave number of the pulse given to the random medium and an unspecified correlation length.

In contrast, the probabilistic microdynamics theory specifies from the onset a correlation length depending on a specific size of the chosen structure, i.e. the grain diameter ^{a}d . It has been mentioned in the introduction of Chapter II that the present study distinguishes the wave motion according to a chosen wavelength, either smaller or equal or bigger than ^{a}d . This in turn recognizes a specific correlation length for the present study of wave propagation to be at a minimum equal to ^{a}d . The other distinct feature of the works of Papanicolau and Morrison et al is the establishment of the mean power transmission coefficient which in their work also depends on the adopted wavelength. In the present theory, in accordance with the given definition of the transmission coefficient C_{tr} for the one-dimensional model, the mean power transmission coefficient results in a form which is independent of the wavelength but is equal to the square of the ratio of the amplitudes of the transmitted and incident waves pertaining to a single microelement of the discrete structure. It is evident therefore that the direct comparison between the random continuum approach and the microdynamics approach for the discrete media is not possible, unless the underlying parameters in both these approaches are matched. This statement is in accordance with the earlier discussion in Section 4.3 pointing out in particular the dependence on these parameters such as the correlation length, strength of fluctuations and the wavelength.

In order to clarify further the difference in the approach by means of random continuum theory and the present one, we consider the random continuum wave equation (Frisch, 1968 and Morrison et al, 1971) written for the one-dimensional model as follows:

$$\frac{\partial^2 u}{\partial X^2} - \frac{1}{\langle c\rangle^2}\left[1+\mu(X)\right]\frac{\partial^2 u}{\partial t^2} = 0 \tag{4.28}$$

which is another form of (4.10). It has to be recognized that in the above mentioned work the expression (4.28) is understood as a local relation. Hence, a macroscopic formulation is obtained by averaging (4.28) so that

$$\frac{\partial^2 \bar{u}}{\partial X^2} - \frac{1}{\langle c\rangle^2}\frac{\partial^2 \bar{u}}{\partial t^2} = 0 \quad \text{since} \quad \langle \mu(X)\rangle = 0 \tag{4.29}$$

This result clearly indicates that on the average the local disturbance due to the randomness of the medium vanishes and no dissipation is being allowed for. In contradistinction to the above we observe that the microdynamics theory yields for the same case (1-D model), by taking averages, the following telegraph equation (see Sec. 3.5):

$$\frac{\partial^2 \bar{u}}{\partial t^2} + b'\frac{\partial \bar{u}}{\partial t} = \langle c\rangle^2 \frac{\partial^2 \bar{u}}{\partial X^2} \quad , \quad b' > 0, \tag{3.51}$$

which may be cast in the following form:

$$D\frac{\partial \bar{u}}{\partial t} + \frac{\partial^2 \bar{u}}{\partial X^2} - \frac{1}{\langle c\rangle^2}\frac{\partial^2 \bar{u}}{\partial t^2} = 0 \quad , \quad \frac{-b'}{\langle c\rangle^2} = D \tag{4.30}$$

The above relation clearly shows the dissipation effects due to the presence of a parameter D. It is seen therefore that a comparison of (4.29) with (4.30) distinguishes the two approaches even if the same parameters concerning the wavelength and the correlation length are matched.

It may be useful for the purpose of a more comprehensive comparison between these two analytical approaches to return to the semi-group operational formulation and attempt a limit analysis. Thus, we recall from Def. 2 the passage time through a single crystal

(microelement) α of size ${}^{\alpha}d$ to be:

$$ {}^{\alpha}\tau \overset{df}{=} \frac{{}^{\alpha}d}{{}^{\alpha}c} , $$

whereby the average passage time is:

$$ \langle {}^{\alpha}\tau \rangle = \frac{\langle {}^{\alpha}d \rangle}{\langle {}^{\alpha}c \rangle} \tag{4.31} $$

since ${}^{\alpha}E$, ${}^{\alpha}\varrho$ and ${}^{\alpha}d$ have been taken as independent random variables. Further, using a macro-time $\bar{t}(n)$ in accordance with n steps in the propagation of the wavefront or

$$ \bar{t}(n) \overset{df}{=} \sum_{i=1}^{n} \langle {}^{\alpha_i}\tau \rangle = n \langle {}^{\alpha}\tau \rangle \tag{4.32} $$

gives the dispersion time for these n steps as

$$ \tau_L(n) = t - \bar{t}(n) , \tag{4.33} $$

in which t refers to the internal time as before. If we assume in the sense of continuum theory that

$$ \langle {}^{\alpha}\tau \rangle \cdot n = \text{const} = \frac{\bar{X}}{\langle c \rangle} , $$

$\bar{X}$ being an average distance travelled in time t, then we can take a limit of the dispersion time $\tau_L(n)$ in (4.33) as follows

$$ \lim_{\substack{\langle {}^{\alpha}\tau \rangle \to 0 \\ n \to \infty}} \tau_L(n) = \lim \left[t - \bar{t}(n) \right] = t - \frac{\bar{X}}{\langle c \rangle} = O(\tau_L) \tag{4.34} $$

Thus it is seen, that due to the loss in distinction of scales, the formal dispersion time of the random continuum theory (4.34) may only be treated as a small perturbation about the average time $\bar{t}$. This result becomes more evident if we consider the derivation of the infinitesimal generators of both evolution operators ${}^{1}T(\bar{t})$ and ${}^{2}T(t)$, that is

$$ {}^1A = \lim_{\langle {}^\alpha\tau\rangle \to 0} \frac{{}^1T(\langle {}^\alpha\tau\rangle) - I}{\langle {}^\alpha\tau\rangle} \tag{4.35a} $$

$$ {}^2A = \lim_{{}^\alpha\tau \to 0} \frac{{}^2T({}^\alpha\tau) - I}{{}^\alpha\tau} \tag{4.35b} $$

A strict limit analysis should yield the ${}^1A$ and ${}^2A$ generators as being equivalent to the infinitesimal generator of the random continuum theory (eq. (4.7)):

$$ \frac{\partial \Psi}{\partial t} = (A + B(\omega))\,\Psi , $$

where

$$ A + B(\omega) = \begin{bmatrix} 0 & , I \\ c^2(\omega)\nabla^2 & , 0 \end{bmatrix} , \quad \omega \in \Omega \tag{4.36} $$

Thus it becomes clear why $c(\omega)$ in that approach can be treated as a random perturbation only.

CHAPTER V

CONCLUDING REMARKS

5.1 General Remarks

As it was pointed out in the introduction to this thesis and further evidenced in Sections 3.5, 4.3 and 4.5 the available theories of continuum mechanics fail to bring out the discreteness and randomness of the structured media in the relations governing the evolution of the field quantities. Thus the main aim of this research program has been to develop a rigorous mathematical basis for the dynamics and especially for the wave propagation in such media. In order to evaluate the success of this attempt it is appropriate to review in this chapter the basic and important features of the theory presented in this thesis. Thus, it is to be noted that:

(i) the proposed theory introduces for the first time the distinct discreteness of the real solid media in the wave propagation analysis,

(ii) the microdynamics theory permits the formulation of the dispersion and dissipation effects in a more realistic sense than the phenomenological one,

(iii) the formulation of the dynamic analysis in terms of an abstract dynamical system shows on the basis of the discreteness assumption that the kinematic quantities belong to the kinematic space with a Hilbertian-Sobolev topology for the mesoscale,

(iv) a new parameter has been introduced, the passage time through a single element of the microstructure, which permits the scaling of the wave phenomena on this level spatially and temporally,

(v) by using the rigorous probabilistic functional analysis and on the basis of the Markov assumption, one can derive a semi-group operator parametrized by the internal (real) time and the macroscopic (average) time, which formally describes the evolution of the wave motion (Theorems 1 and 2),

(vi) for a three-dimensional medium, one can formulate the wavefront propagation in terms of the total power flux which becomes a super-martingale on a random field (Lemma 1),

(vii) a very simplified model for the grain boundary behaviour in structured solids has been introduced as a first approximation to the more complex interaction effects in the wave motion at the intercrystalline boundaries,

(viii) in order to verify, to a certain extent, the analytical approach, the computer experiments by the Monte-Carlo simulation have been suggested for all three models of the solid discussed in the thesis, i.e. for one-, two- and three-dimensional models; the results have been shown in Figs. 4.4 to 4.11,

(ix) by taking the averages in the probabilisitc microdynamics theory the generalized wave equation with a dissipative

term may be obtained. Although such a dissipative term is usually assumed in continuum theories, the present approach permits an exact formulation and derivation of this quantity in terms of the physical characteristics of the given solid. On the other hand, it is indicated that by taking the averages of the important parameters (such as average passage time and average grain size) tending to zero, a convergence to the standard wave equation could be obtained.

5.2 Remarks on Further Research

On the basis of the work presented in this thesis it is suggested that the following items should be considered for future research.

(i) The present work could be extended to the formulation of the wave propagation in solids with a random geometric structure. This could be significant in the extension of the present theory to non-crystalline solids and/or its application to rock mechanics.

(ii) Further consideration could be given to the newly introduced notion of temporal scales together with the application of spatial scales other than those dealt with in the present theory. Such an extension would encompass the wave motion on either an atomistic or molecular scale, or the analysis of large scale phenomena which are encountered in geophysics.

(iii) For the global representation of the wave motion in a discrete random medium in terms of the complete set of governing equations, the set of solutions and their stability should be investigated. This would ultimately lead to a rigorous random field analysis.

(iv) Finally, the extension of the proposed theory to the description of wave motion including critical phenomena in random media should be pursued, e.g. waves in multi-phase media, shock waves, etc.

STATEMENT OF ORIGINALITY

AND

CONTRIBUTION TO KNOWLEDGE

The author of this thesis claims to have made the following original contributions to the knowledge of theoretical mechanics:

(i) On the basis of the probabilistic micromechanics theory of Axelrad, a rigorous mathematical theory has been developed in this thesis to permit a probabilistic functional analysis of the dynamics of structured solids.

(ii) The model for the wave propagation across the inter-crystalline boundaries has been formulated on the basis of interatomic interactions.

(iii) The representation of the wave motion has been given in terms of an abstract dynamical system where the underlying probabilistic function space has been identified with the kinematic space with a Hilbertian-Sobolev topology.

(iv) For the first time, the multidimensional time (comprising the macroscopic and internal times of the physical process) has been introduced for the wave propagation analysis enabling the formulation of:

a) evolution of the combined longitudinal and transverse waves in a one-dimensional model of the solid in terms of a four-parametric semi-group of Markov transition operators.

b) evolution of the combined longitudinal and transverse waves in a three-dimensional model of the solid in terms of a supermartingale on a generalized random field.

(v) The equivalence of the Markov-theoretic formulation with the continuum theory has been established by averaging over the state space in terms of the semi-group evolution operators.

(vi) A Monte-Carlo technique has been developed for the simulation of the wave propagation in the discrete solid for the specified cubic structure.

REFERENCES

J.D. Achenbach, "Wave Propagation in Elastic Solids", North Holland Publ. Co., Amsterdam, 1973

D.R. Axelrad, "On the Deformation of 2-phase Systems at High Temperature", J. Soc. Mat. Sci., Japan, 12, p. 322, 1963

D.R. Axelrad and J.W. Provan, "Probabilistic Micromechanics of Structured Solids", in Symp. Stat. Cont. Mech., Polish Acad. Sci., Jabtonna, Poland, 1972

D.R. Axelrad, "Micromechanics of Solids", PWN-Elsevier Publ. Co., Amsterdam, 1978

D.R. Axelrad, "The Mechanics of Discrete Media", General Lecture, 3-rd International Symposium on Continuum Models of Discrete Systems, Freudenstadt, West Germany, Waterloo University Press, Canada, June 24-30, 1979

D.R. Axelrad, "Probabilisitc Mechanics of Solids", Lecture Notes, Leoben, Austria, 1980

D.R. Axelrad, "Foundations of the Probabilistic Mechanics of Discrete Media", Pergamon Press, Oxford, 1983

R. Balescu, "Equilibrium and Nonequilibrium Statistical Mechanics", John Wiley and Sons, New York, 1975

S. Basu, "On a General Deformation Theory of Structured Solids", Ph.D. Thesis, Dept. of Mechanical Engineering, McGill University, 1975

R.T. Bharucha-Reid, "Random Integral Equations", Academic Press, 1972

D.R. Bland, "Nonlinear Dynamic Elasticity", Blaisdell Publishing Co., 1969

R.M. Blumenthal and R.K. Getoor, "Markov Processes and Potential Theory", Academic Press, New York and London, 1968

W. Bollman, "Crystal Defects and Crystalline Interfaces", Springer-Verlag, 1970

L. Brillouin, "Wave Propagation in Periodic Structures", Dover, New York, 1953

L.A. Chernov, "Wave Propagation in a Random Medium", McGraw-Hill, New York, 1960

P.L. Chow and J.B. Keller, "Wave Propagation in a Random Lattice. I", Journal of Mathematical Physics, 13, No. 9, 1972

J.W. Christian, "The Theory of Transformations in Metals and Alloys", Pergamon Press, Oxford, 1965

S.K. Datta, "Scattering by a Randon Distribution of Inclusions and Effective Elastic Properties", in Continuum Models of Discrete Systems, Mont Gabriel, Quebec, 1977

R.L. Dobrushin, "Description of a Random Field by Means of Conditional Probabilities and the Conditions Governing its Regularity", Theory of Probability and its Applications, 13, pp. 197-224, 1968

D.M. Donsker and M. Kac, "The Monte Carlo Method and its Applications", Proc. Computation Seminar, IBM Corp., New York, 1949

A.C. Eringen, "Non-Local Polar Elastic Continua", Int. J. Engineering Science, 10, pp. 1-16, 1972

A.C. Eringen and E.S. Suhubi, "Elastodynamics", Vol. I and II, Academic Press, New York and London, 1974

U. Frisch, "Wave Propagation in Random Media", in "Probabilisitc Methods in Applied Mathematics" (A.T. Bharucha-Reid, ed.) Vol. 1, pp. 75-198, Academic Press, New York, 1968

M. Fukushima, "Dirichlet Forms and Markov Processes", North Holland Publ. Co., Amsterdam, 1980

I.M. Gel'fand and N. Ya. Vilenkin, "Generalized Functions", Vol. IV, Academic Press, New York, 1964

H. Grad, "Asymptotic Equivalence of the Navier-Stokes and Nonlinear Boltzmann Equations", Symp. Appl. Math., Providence, R.I., 1962

E. Hille and R. Phillips, "Functional Analysis and Semi-Groups", Amer. Math. Soc. Colloq. Publ., Vol. 31, Rev. Ed., 1957

J.P. Hirth and J. Lothe, "Theory of Dislocations", McGraw-Hill, New York, 1968

M. Howe, "Wave Propagation in Random Media", J. of Fluid Mechanics, 45, pp. 769-783, 1971

A. Ishimaru, "Wave Propagation and Scattering in Random Media", Academic Press, New York, 1978

M. Kac, "On Some Connections Between Probability Theory and Differential and Integral Equations" (Proc. Second Berkeley Symp. on Math. Stat. and Probability), University of California Press, Berkeley, 1951

J. Kampé de Fériet, "Statistical Mechanics of Continuous Media", Proc. Symp. Appl. Math., 13, pp. 165-198, Amer. Math. Soc., Providence, Rhode Island, 1962

J. Kampé de Fériet, "Statistical Fluid Mechanics: Two-Dimensional Gravity Waves", in "Partial Differential Equations and Continuum Mechanis" (R.E.Langer, Ed.), pp. 107-136, Univ. of Wisconsin Press, Madison, Wisconsin, 1966

J.B. Keller, "Wave Propagation in Random Media", Proc. Symp. Appl. Math., 13, pp. 227-246, Amer. Math. Soc., Providence, R.I., 1962

C. Kittel, "Introduction to Solid State Physics", John Wiley and Sons Inc., New York, 1968

A.N. Kolmogorov, "The Local Structure of Turbulence in an Incompressible Fluid at Very Large Reynolds Numbers", Dok. Akad. Nank SSSR, 30, 1941, pp. 229-303

H. Kolsky, "Stress Waves in Solids", Dover Publ. Inc., New York, 1963

R.J. Knops and E.W. Wilkes, "Theory of Elastic Stability", in Encyclopedia of Physics, Springer-Verlag, 1973

I.A. Kunin, "Theories of Elastic Media with Microstructures", Proc. Vibr. Probl., Vol. 9, p. 323, 1968

D. Lazarus, "The Variation of the Adiabatic Elastic Constants of KCL, NcCl, CuZu, Cu and Al with Pressure to 10,000 Bars", Physical Review, 76, No. 4, pp. 545-553, 1949

G. Leibfried, "Gittertheorie der Mechanischen und Thermischen Eigenschaften der Kristalle", Handbuch der Physik, Band VII/1, Springer-Verlag, Berlin, 1955

H. Levine, "Unidirectional Wave Motion", Amsterdam, North-Holland, 1978

P. Lévy, "A Special Problem of Brownian Motion, and a General Theory of Gaussian Random Function", Proc. 3-rd Berkeley Symp. Math. Stat. and Prob., 2, pp. 133-175, 1956

U.S. Lindholm (editor), "Symposium on Mechanical Behaviour of Materials Under Dynamic Loads", Springer-Verlag, New York, 1968

A.E.H. Love, "A Treatise on the Mathematical Theory of Elasticity", Dover, N.Y., 1926

J.W. Martin and R.D. Doherty, "Stability of Microstructure in Metallic Systems", Cambridge University Press, 1976

W.P. Mason, "Physical Acoustics and the Properties of Solids", D. Van Nostrand Co. Inc., Princeton, New Jersey, 1958

N. Metropolis and S. Ulam, "The Monte Carlo Method", J. Am. Stat. Assoc., Vol. 44, pp. 335-341, 1949

J. Miklowitz, "Recent Developments in Elastic Wave Propagation", Appl. Mech. Rev., 13, pp. 865-78, 1966

J.A. Morrison, G.C. Papanicolau and J.B. Keller, "Mean Power Transmission Through a Slab of Random Medium", Comm. Pure and Appl. Math., Vol. 24, pp. 473-489, 1971

J.T. Oden, "Applied Functional Analysis", Prentice-Hall, Englewood Cliffs, N.J., 1979

W.C. Overton and J. Gaffney, "Temperature Variation of the Elastic Constants of Cubic Elements I. Copper", Physical Review, 98, No. 4, pp. 969-977, 1955

J.C. Oxtoby and S. Ulam, "Measure Preserving Homeomorphisms and Metrical Transitivity", Annals of Mathematics, Vol. 42, No. 4, 1941, pp. 874-920

G.C. Papanicolau, "Wave Propagation in a One-Dimensional Random Medium", SIAM J. Appl. Math., Vol. 21, No. 1, pp. 13-18, 1971

H. Poincaré, "Mémoire sur les Courbes Définies par les Equations Différentielles", J. Math. Pures et Applique, (3) 7, pp. 375-422, 1881

I. Prigogine, "From Being to Becoming", W.H. Freeman and Co., San Francisco, 1980

I. Prigogine, "Entropy, Time and Kinetic Description", in "Order and Fluctuations in Equilibrium and Nonequilibrium Statistical Mechanics", 17-th Int. Solvay Conf. on Physics, ed. G. Nicolis, G. Dewell and J.W. Turner, John Wiley and Sons, New York, 1981

Yu. V. Prohorov and Yu. A. Rozanov, "Probability Theory", Springer-Verlag, New York, 1969

J.W. Provan, "A Model for Fatigue Crack Initiation in Polycrystalline Solids", 4-th Int. Conf. Fracture, University of Waterloo, Canada, 1977

A. Rényi, "Foundations of Probability", Holden-Day Inc., San Francisco, 1970

R.Y. Rubinstein, "Simulation and the Monte-Carlo Method", Wiley, New York, 1981

W. Rudin, "Functional Analysis", McGraw-Hill, New York, 1973

W. Rudin, "Real and Complex Analysis", McGraw-Hill, New York, 1974

R.A. Smith, "Wave Mechanics of Crystalline Solids", London, Chapman and Hall Ltd., 1961

I.N. Sneddon and D.S. Berry, Chapter on "Dynamical Problems", in "The Classical Theory of Elasticity" in Encyclopedia of Physics, Springer-Verlag, 1958

I.N. Sneddon and R. Hill, "Progress in Solid Mechanics", Vol. I, II, III and IV, North-Holland Publ. Co., Amsterdam, 1960

K. Sobczyk, "Elastic Wave Propagation in a Discrete Random Medium", Acta Mechanica, 25, pp. 13-28, 1976

S.L. Sobolev, "Applications of Functional Analysis in Mathematical Physics", Amer. Math. Soc., Providence, R.I., 1963

F. Spitzer, "Markov Random Fields and Gibbs Ensembles", Advances in Mathematics, 3, pp. 142-154, 1971

I. Stakgold, "Green's Function and Boundary Value Problems", John Wiley and Sons, New York, 1979

B.J. Uscinski, "The Elements of Wave Propagation in Random Media", McGraw-Hill, 1977

E. Wong, "Stochastic Processes in Information and Dynamical Systems", McGraw-Hill, New York, 1971

A.M. Yaglom, "Some Classes of Random Fields in n-Dimensional Space Related to Stationary Random Processes", Theory of Probability and its Applications, II, No. 3, pp. 273-320, 1957

K. Yosida, "Functional Analysis", Springer-Verlag, New York, 1978

J. Yvon, "Correlation and Entropy in Classical Statistical Mechanics", Pergamon Press, London, 1969

APPENDIX A

NUMERICAL MODEL OF THE BOND BEHAVIOUR

A.1 Function of the Program

The program calculates the evolution of the bond distance r in time t_m. It is written in a general form, so that the response of the bond can be studied either in motion perpendicular or parallel to the grain boundary ($\alpha\beta$). This is done by exchanging several cards according to the equations (2.38) or (2.45).

A.2 Program Structure and Computation Procedure

The entire program is written in Fortran IV (Watfiv) language. The program has the following structure:

MAIN PROGRAM

SUBROUTINE DVERK*

SUBROUTINE FCN1

All calculations are carried out with double precision on an Amdahl V7 digital computer.

Given all the necessary data, the Main Program transfers the task of computing the specific values of the bond distance r at the consecutive time steps onto the subroutine DVERK. The subroutine FCN1 provides the specific functional form as the right hand side of equations (2.38) or (2.45) depending on the case studied. The subroutine DVERK is based on the Runge-Kutta method; it iterates to

---

* From the International Mathematical Subroutine Library

find the value of r and upon achieving the specified accuracy it proceeds one time step forward and repeats the procedure.

The program is shown in Fig. A-1.

A.3 Input Data and Output Results

The input data are fed into the computer through the Main Program.

The velocity of the incident wave is taken to be equal 1 m/s. In view of the fact that the Monte-Carlo simulation of the wave propagation is done for copper (see Chapter IV) the pertinent physical constants are chosen as follows:

$$C_L = 4030.641 \text{ m/s}$$

$$C_T = 2476.859 \text{ m/s}$$

$$\rho = 8900 \text{ kg/m}^3$$

Furthermore, the relative impedance χ is taken equal to 1.0, since only the general character of the bond motion is sought. The initial bond distance r (t=0) was taken equal to that of the lattice spacing for copper (see Kittel, 1968).

Samples of the output results that correspond to the longitudinal wave incident upon the perpendicular grain boundary, are shown in Fig. A-2. In general it was found that for the motion perpendicular and parallel to the boundary the bond distance r tended within 10^{-13}s asymptotically to a certian equilibrium value, which did not exceed r_0 by more than 10%. This clearly justifies the assumptions (2.40) and (2.47) of Chapter II.

```
*EATCH WATFIV CXDD (90,90)
*********************************************************************
      $WATFIV ,TIME=90,PAGES=90,NOWARN,NOEXT
    1         IMPLICIT REAL*8(A-Z)
    2         INTEGER N,INC,IER,K,NW
    3         DIMENSION Y(1),C(24),W(1,9)
    4         EXTERNAL FCN1
    5         NW=1
    6         N=1
    7         X=0.D0
    8         Y(1)=2.55D-1(
    9         TOL=0.00005
   10         IND=1
   11         XEND=0.D0
   12         DO 10 K=1,100
   13         XEND=XEND+1D-15
   14         CALL DVERK(N,FCN1,X,Y,XEND,TOL,IND,C,NW,W,IER)
   15         IF(IND.LT.0.OR.IER.GT.0)GO TO 20
   16         WRITE(6,35)X,Y(1)
   17   35    FORMAT(/,20X,2D22.12)
   18   10    CONTINUE
   19         STOP
   20   20    CONTINUE
   21         STOP
   22         END
      C
      C
      C
      C


   23         SUBROUTINE FCN1(N,X,Y,YPRIME)
   24         IMPLICIT REAL*8(A-Z)
   25         INTEGER N,N1
   26         DIMENSION Y(N),YPRIME(N)
   27         S=(2.55D-10)/Y(1)
   28         YP=4*(0.6519766D-19)*(6*(S**6)/Y(1)-12*(S**12)/Y(1))
   29         V=1.D0
   30         C=4030.6410D0
   31         RO=8900.D0
   32         G=1.D0
   33         B=-(G+1)/V/RO/C
   34         N1=1
   35         DN=0.153787D20/N1**2
   36         YPRIME(1)=V*(B*DN*YP-2)
   37         RETURN
   38         END
```

Fig. A-1

0.100000000000D-14	0.259425354478D-09
0.200000000000D-14	0.262701045175D-09
0.300000000000D-14	0.265271779939D-09
0.400000000000D-14	0.267366622317D-09
0.500000000000D-14	0.269119141330D-09
0.600000000000D-14	0.270614026181D-09
0.700000000000D-14	0.271908332516D-09
0.800000000000D-14	0.273042312529D-09
0.900000000000D-14	0.274045412635D-09
0.100000000000D-13	0.274939815020D-09
0.110000000000D-13	0.275742638856D-09
0.120000000000D-13	0.276467367048D-09
0.130000000000D-13	0.277124803954D-09
0.140000000000D-13	0.277723737627D-09
0.150000000000D-13	0.278271409577D-09
0.160000000000D-13	0.278773855448D-09
0.170000000000D-13	0.279236156938D-09
0.180000000000D-13	0.279662631316D-09
0.190000000000D-13	0.280056976180D-09
0.200000000000D-13	0.280422381573D-09
0.210000000000D-13	0.280761617887D-09
0.220000000000D-13	0.281077105569D-09
0.230000000000D-13	0.281370970960D-09
0.240000000000D-13	0.281645091449D-09
0.250000000000D-13	0.281901132301D-09
0.260000000000D-13	0.282140576935D-09
0.270000000000D-13	0.282364751997D-09
0.280000000000D-13	0.282574848265D-09
0.290000000000D-13	0.282771938193D-09
0.300000000000D-13	0.282956990717D-09
0.310000000000D-13	0.283130838822D-09
0.320000000000D-13	0.283294415266D-09
0.330000000000D-13	0.283448311765D-09
0.340000000000D-13	0.283593236917D-09
0.350000000000D-13	0.283729798041D-09
0.360000000000D-13	0.283858552129D-09

Fig, A-2

APPENDIX B

CONVERGENCE OF THE VELOCITY AND DISPERSION TIME DISTRIBUTIONS TO THE GAUSSIAN DISTRIBUTIONS

First we prove that the distribution $P\{v(t)\}$ at any given t is Gaussian. For simplicity we consider v to be a real-valued random variable. Consider the transmission of a wave from grain α to the neighbouring $\alpha+1$. We have:

$$ {}^{\alpha+1}v = {}^{\alpha,\alpha+1}C_{tr}\ {}^{\alpha}v, \tag{B.1} $$

where ${}^{\alpha,\alpha+1}C_{tr}$ fluctuates around the value 1.0 depending on the physical properties of both grains. Thus, we can write

$$ {}^{\alpha,\alpha+1}C_{tr} = 1 + {}^{\alpha,\alpha+1}\delta \tag{B.2} $$

where we assume for a structured solid:

$$ |{}^{\alpha,\alpha+1}\delta| \ll 1 \tag{B.3} $$

If we consider wave propagation in a one-dimensional model starting from an initial value ${}^{0}v$ in the first grain 0 we shall have:

$$ {}^{1}v = {}^{01}C_{tr}\ {}^{0}v = (1 + {}^{01}\delta)\,{}^{0}v $$

$$ {}^{2}v = {}^{12}C_{tr}\,{}^{1}v = {}^{12}C_{tr}\,{}^{01}C_{tr}\,{}^{0}v = (1+{}^{12}\delta)(1+{}^{01}\delta)\,{}^{0}v = (1+{}^{01}\delta+{}^{12}\delta+{}^{01}\delta\,{}^{12}\delta)\,{}^{0}v $$

$$ {}^{3}v = {}^{23}C_{tr}\,{}^{2}v = {}^{23}C_{tr}\,{}^{12}C_{tr}\,{}^{01}C_{tr}\,{}^{0}v = (1+{}^{23}\delta)(1+{}^{12}\delta)(1+{}^{01}\delta)\,{}^{0}v $$

$$ = (1+{}^{01}\delta+{}^{12}\delta+{}^{23}\delta+{}^{01}\delta\,{}^{12}\delta+{}^{01}\delta\,{}^{23}\delta+{}^{12}\delta\,{}^{23}\delta+{}^{01}\delta\,{}^{12}\delta\,{}^{23}\delta)\,{}^{0}v $$

$$ \vdots $$

$$ {}^{n}V = \prod_{\alpha=0}^{\alpha=n-1} {}^{\alpha,\alpha+1}C_{tr}\, {}^{0}V = \left(1+ {}^{n-1,n}\delta\right)\left(1+ {}^{n-2,n-1}\delta\right)\cdot\ldots\cdot\left(1+ {}^{01}\delta\right){}^{0}V $$

$$ = \left[1 + {}^{01}\delta + {}^{12}\delta + \ldots + {}^{n-1,n}\delta + 0(\delta^2) + 0(\delta^3) + \ldots + 0(\delta^n)\right] \quad (B.4) $$

It follows from the assumption (B.3) that we can write:

$$ \langle {}^{n}V \rangle = \left[1 + n\langle {}^{\alpha,\alpha+1}\delta \rangle\right]{}^{0}V \quad (B.5) $$

where $\langle {}^{\alpha,\alpha+1}\delta \rangle$ is the average of ${}^{\alpha,\alpha+1}\delta$. It is seen on the heuristic grounds (energy loss) that

$$ \langle {}^{\alpha,\alpha+1}\delta \rangle < 0 \quad (B.6) $$

Of course, ${}^{\alpha,\alpha+1}\delta$ has a finite variance.

If we disregard higher order terms in (B.4) we can write

$$ {}^{n}V = {}^{0}V + \sum_{\alpha=0}^{n-1} {}^{0}V\, {}^{\alpha,\alpha+1}\delta = \sum_{\alpha=0}^{n-1}\left[\frac{{}^{0}V}{n} + {}^{0}V\, {}^{\alpha,\alpha+1}\delta\right] \quad (B.7) $$

Consider now another random variable

$$ \xi_i \quad D\sqrt{n}\, {}^{0}V\, {}^{\alpha,\alpha+1}\delta + E \quad (B.8) $$

where

$$ E = \langle \xi_i \rangle \quad (B.9) $$

and D is a standard deviation of ξ_i . It is important to note that (B.9) is satisfied in view of (B.5). If we now consider the sum

$$ \zeta_n \stackrel{df}{=} \frac{1}{\sqrt{n}\,D} \sum_{i=1}^{n} \xi_i \quad (B.10) $$

and recognize that ${}^{\alpha,\alpha+1}\delta$ and hence ξ_i are independent and identically distributed random variables we will obtain:

$$ \lim_{n\to\infty} P\{\zeta_n < x\} = \Phi(x) \quad (B.11) $$

where $\Phi(x)$ is a standard normal distribution. In the above the Central Limit Theorem has been involved. If we consider a new random variable $\tilde{v}$ defined as follows:

$$\tilde{v} = {}^{0}v - \langle {}^{n}v \rangle + \sum_{\alpha=1}^{n-1} {}^{0}v^{\alpha,\alpha+1}\delta$$

it will also converge to the standard normal distribution as implied jointly by (B.8) and (B.10). This result leads us to conclude that ${}^{n}v$ as given in (B.7) will converge to the general normal distribution with a non-zero mean. Indeed it is seen from (B.5) that the mean of ${}^{n}v$ is dependent on n, that is on the number of microelements the wave has passed. This is equivalent to saying that v converges weakly to the non-standard normal distribution for $t \to \infty$ and thus it is approximately Gaussian for all large but finite t with the mean $\langle v \rangle$ decreasing for t increasing.

Let us now consider the dispersion time process $\tau_L(\bar{t})$. It follows from the Definition 8 that

$$\tau_L(\bar{t} + \langle {}^{\alpha}\tau \rangle) = \tau_L(\bar{t}) + {}^{\alpha}\tau - \langle {}^{\alpha}\tau \rangle \qquad (B.12)$$

If we introduce an integral-valued parameter

$$n = \bar{t} / \langle {}^{\alpha}\tau \rangle$$

then we can write (B.12) as follows:

$$\tau_L(n+1) = \tau_L(n) + {}^{\alpha}\tau - \langle {}^{\alpha}\tau \rangle$$

Thus in general we have

$$\tau_L(n) = \sum_{\alpha=1}^{n} [{}^{\alpha}\tau - \langle {}^{\alpha}\tau \rangle] \qquad (B.13)$$

The passage time ${}^{\alpha}\tau$ has a finite standard deviation D which depends on the physical properties of the given solid. If we recognize ${}^{\alpha}\tau$ to

be independent identically distributed random variables it will follow from the Central Limit Theorem (see Corollary to Theorem 4.7.1 of Rényi, 1970) that:

$$\lim_{n\to\infty} P\left\{ \frac{\tau_L(n) - n\langle^{\alpha}\tau\rangle}{D\sqrt{n}} < x \right\} = \Phi(x) \qquad (B.14)$$

The above result indicates that for a fixed large n the distribution

$$P\{\tau_L(n) - n\langle^{\alpha}\tau\rangle < x D\sqrt{n}\} \qquad (B.15)$$

will be close to the standard normal distribution $\Phi(xD\sqrt{n})$. Thus, we can conclude that $P\{\tau_L(n)\}$ will be close to a general normal distribution which will evidently depend on $\bar{t}$ as $\sqrt{n}$.

APPENDIX C

MONTE-CARLO SIMULATION PROGRAMS

```
$WATFIV ,TIME=599,PAGES=99,NOEXT
      IMPLICIT REAL*8(A-Z)
      DIMENSION V(10),T(10)
      INTEGER I,J,IR,K,Y
      IR=1
      K=5**13
      MURO=8900.D0
      MUE=14.459D10
      SGRO=0.D0
      SGE=MUE/1000
      DO 2 J=1,10
      V(J)=1.D0
      T(J)=0.D0
      Y=0
      RO0=MURO
      E0=MUE
      C0=DSQRT(E0/RO0)
      T0=0.0001D0/C0
      DO 1 I=1,10000
      CALL ODDS(K,IR,N1,N2)
      RO1=MURO+SGRO*N1
      E1=MUE+SGE*N2
      C1=DSQRT(E1/RO1)
      T1=0.0001D0/C1
      KAPA=RO1*C1/RO0/C0
      CTR=2/(1+KAPA)
      V(J)=V(J)*CTR
      T(J)=T(J)+T0
      T0=T1
      Y=Y+1
      RO0=RO1
      C0=C1
      IF((I/1000)*1000.EQ.I) GO TO 5
      GO TO 1
5     WRITE(6,10) Y,T(J),V(J)
10    FORMAT(/,5X,I7,2D22.12)
1     CONTINUE
2     CONTINUE
      WRITE(6,7) K,IR
7     FORMAT(/,5X,'K=',I11,5X,'IR=',I11)
      STOP
      END

      SUBROUTINE ODDS(K,IR,N1,N2)
      IMPLICIT REAL*8(A-Z)
      INTEGER K,IR
      PI=3.14159265358979D0
      IR=IR*K
      IF(IR.LT.0) IR=IR+2*(2**30-1)+2
      R=DFLOAT(IR)/2.D0**31
      R1=R
      IR=IR*K
      IF(IR.LT.0) IR=IR+2*(2**30-1)+2
      R=DFLOAT(IR)/2.D0**31
      R2=R
      N1=DSQRT(-2*DLOG(R1))*DCOS(2*PI*R2)
      N2=DSQRT(-2*DLOG(R1))*DSIN(2*PI*R2)
      RETURN
      END
```

Fig. C-1 Simulation Program for a 1-D Model

```
C**************
C
C FILE NAME IS 'RUMA' FILE OPENED ON 14-1-83
C**********************************************************************
C ***********************************************************************
C *  MONTE-CARLO SIMULATION FOR 2-D MODEL WITH CONSTANT LENGTH **
C *  PGM FOR 100 INTER ACTING SEQUENCES WITH MIXED R.N. OF SEED **
C *  5**13 AND 7**11  DIFFERS FROM 'M2D' FILE IN ENERGY EXCHANGE
C *  IN TRANSVERSE DIRECTION
C ***********************************************************************
CCC
C
0001          IMPLICIT REAL*8(A-Z)
0002          REAL RANGE(4),RANGET(4),RANGE1(4),RANGE2(4)
0003          DIMENSION E(150),V(150),T(150),C(150),RO(150),FV(150),V1(150,10),
             $T1(150,10),YFV(150,1),CR(150),CR1(150),DS(150),
             $ RO1(150),E1(150),FT(150)
             $,VG(150,10),C1(150),V2(150),T2(150),PT(150),VC(150),FP(150,1)
             $,VB(150),VU(150),VBAR(150),P(150),P1(150),
             $ P12(150),P2(150),Y(165),YT(165)
0004          INTEGER I,J,IR,K,X,N,IK,JK,L,M,NJ,NC,IC,NI,IR1,K1,L1,LC,ICT
0005          DATA RANGE/0.981,1.001,0.0,1.0/
0006          DATA RANGE2/0.0,1.0,0.981,1.001/
C***   INITIALISING MEAN AND STD. DEV. OF DENSITY AND YOUNG'S MODULAS****
0007          MURO=8900.D0
0008          MUE=14.459D10
0009          SGRO=MURO/500
0010          SGE=MUE/1000
C ++++LENGTH OF MICRO ELENENT ASSIGNED++++
0011          D=0.0002D0
0012          L1=10
0013          L=100
0014          DO 63 I=1,L
0015          DO 63 J=1,L1
0016          V1(I,J)=0.D0
0017          T1(I,J)=0.D0
0018     63   CONTINUE
C ==========================================================
C ****   MAIN PGM STARTS(IN FIRST CASE  SIMULATION WITH SEED
C        5**13 WILL BE DONE ,NEXT WITH 7**11
C ==========================================================
0019          IR=1
0020          IR1=1
0021          K=5**13
0022          K1=7**11
0023          IK=0
0024          DO 2 I=1,L
0025          VC(I)=1.D0
0026          RO(I)=MURO
0027          E(I)=MUE
0028          C(I)=DSQRT(MUE/MURO)
0029          T(I)=D/C(I)
0030     2    CONTINUE
0031          NJ=1
```

Fig. C-2 Simulation Program for a 2-D Model

```
FORTRAN IV G1  RELEASE 2.0            MAIN              DATE = 83045          22/57/44

0069              79    CONTINUE
0070              77    CONTINUE
                  C ***********************************************************
                  C MAIN PART OF MAIN PGM. FINISHED
                  C ***********************************************************
0071                    WRITE(6,205)
0072              205   FORMAT(1H1,20X,'VELOCITY METRIX')
0073                    WRITE(6,25)((V1(I,J),J=1,5),I=1,L)
0074                    WRITE(6,203)
0075              203   FORMAT(1H1,20X,'CONTINUATION')
0076                    WRITE(6,25)((V1(I,J),J=6,10),I=1,L)
0077              25    FORMAT(/,5X,5D22.12)
0078                    WRITE(6,26)
0079                    WRITE(6,25)((T1(I,J),J=1,5),I=1,L)
0080                    WRITE(6,203)
0081                    WRITE(6,25)((T1(I,J),J=6,10),I=1,L)
0082              26    FORMAT(1H1,20X,'TIME MATRIX')
                  C ***********************************************************
                  C CLCULATION OF MEAN AND STD. DEV. OF VEL. AND TIME AT EACH SIN.
                  C ***********************************************************
0083                    M=0
0084                    DO 667 JK=1,L1
0085                    M=M+1
0086                    S=0.D0
0087                    S1=0.D0
0088                    S12=0.D0
0089                    S2=0.D0
0090                    DO 83 J=1,L
0091                    FV(J)=V1(J,M)
0092              83    FT(J)=T1(J,M)
0093                    DO 81 I=1,L
0094                    S=S+FV(I)
0095                    S1=S1+FT(I)
0096                    S12=S12+(FV(I))**2
0097                    S2=S2+(FT(I))**2
0098              81    CONTINUE
0099                    XR=L
0100                    P(JK)=S/XR
0101                    P1(JK)=S1/XR
0102                    P12(JK)=DSQRT(S12/XR-P(JK)**2)
0103                    P2(JK)=DSQRT(S2/XR-P1(JK)**2)
0104              667   CONTINUE
0105                    WRITE(6,456)
0106                    WRITE(6,676)(P(I),P12(I),P1(I),P2(I),I=1,L1)
0107              456   FORMAT(1H1,///,24X,'MEAN-VELOCITY',8X,'SIGMA-VELOCITY',3X,'MEAN-
                     $TIME',8X,'SIGMA-TIME',///)
0108              676   FORMAT(//,20X,4D22.12)
                  C
                  C ***********************************************************
                  C     INTODUCING DISTANCE ROW & AND PLOT OF VEL. AT DIFF. SIN.
                  C ***********************************************************
                  C
0109                    SC=0.D0
0110                    DO 88 I=1,L1
```

Fig. C-2 Continued

```
FORTRAN IV G1  RELEASE 2.0              MAIN                DATE = 83045          22/57/44

0111                    DS(I)=SC+(1.D0/L1)
0112               88   SC=DS(I)
0113                    DO 22 I=1,L1
0114                    DO 22 J=1,L
0115               22   VG(J,I)=V1(I,J)
                   C ****** PLOT OF VEL. AT EACH 0.1MTR DIT OF BAR TILL 1MTR *********
0116                    CALL GRP3(DS,VG,L)
                   C **** PLOT OF V(T),P(V),P(T) GRAPHS AT EACH 1000 MICRO-ELEMENTS *****
0117                    M=0
0118                    DO 66 JK=1,L1
0119                    M=M+1
0120                    DO 813 J=1,L
0121                    YFV(J,1)=V1(J,M)
0122                    FV(J)=YFV(J,1)
0123               813  FT(J)=T1(J,M)
0124                    READ(5,*) (RANGE1(I),I=1,4)
                   C ********  TIME VS. VELOCITY GRAPH  AT EACH 0.1MTR. LENGTH OF BAR ****
0125                    CALL GRP2(FT,YFV,RANGE1,L)
0126                    J=L
0127                    CALL SORT(J,FV)
0128                    CALL SORT(J,FT)
0129                    WRITE (6,104)
0130               104  FORMAT(1H1,///,40X,'VELOCITY',9X,'P(V)')
                   C *********        P(V) GRAPH AT EACH STATION      **********************
0131                    CALL GRP1(FV,RANGE,L)
0132                    WRITE(6,105)
0133               105  FORMAT(1H1,///,42X,'TIME',9X,'P(T)')
0134                    READ(5,*) (RANGET(I),I=1,4)
                   C    **********     P(T) GRAPH AT EACH STN.  ********************
0135                    CALL GRP1(FT,RANGET,L)
0136               66   CONTINUE
0137                    DO 12 I=1,L1
0138               12   YP(I,1)=P(I)
                   C ==========================================================
                   C PLOT OF DISTANCE VS  MEAN VELOCITY
0139                    CALL GRRP2(DS,YP,RANGE2,L1)
                   C ==========================================================
0140                    READ(5,*) (Y(I),I=1,61)
                   C ----------------------------------------------------------
                   C PLOT OF P(V) GRAPH IN ZETA PLOTTER
0141                    CALL GV(P,P12,V1,Y,L,L1)
                   C----------------------------------------------------------
                   C PLOT OF P(T) GRAPH IN ZETA PLOTTER
0142                    READ(5,*) (YT(I),I=1,61)
                   C ..........................................................
0143                    CALL GT(P1,P2,T1,YT,L,L1)
0144                    WRITE(6,478) K,K1,IR,IR1
0145               478  FORMAT(/,5X,'K=',I11,5X,'K1',I11,5X,'IR=',I11,5X,'IR1=',I11)
0146                    STOP
0147                    END

 *OPTIONS IN EFFECT*  NOTERM,ID,EBCDIC,SOURCE,NOLIST,NODECK,LOAD,NOMAP,NOTEST
 *OPTIONS IN EFFECT*  NAME = MAIN     , LINECNT =       56
 *STATISTICS*    SOURCE STATEMENTS =       147,PROGRAM SIZE =     74650
```

Fig. C-2 Continued

```
ORTRAN IV G1  RELEASE 2.0              MAIN              DATE = 83064          13/35/41

                C MONTE-CARLO SIMULATION FOR THREE DIMENSIONAL MODEL WITH
                C CONST. LENGTH
                C
                C
0001                  IMPLICIT REAL*8(A-Z)
0002                  DIMENSION VIN(20,20),RO1(20,20),E1(20,20),C1(20,20),
                     $ T(20,20),RO2(20,20),E2(20,20),C2(20,20),VTR(20,20),
                     $ VE(20,20),VW(20,20),VN(20,20),VS(20,20),VST(20,20,2),
                     $ TST(20,20,20),AVS(20),SVS(20),ATS(20),STS(20),Y(65),YT(65)
0003                  INTEGER I,J,K,L,M,N,L1,IR,IR1,K1,IK,I1,J1,IN,M1,M2,Z,IJ,IL,JK,IC
                C
                C (1) INITIALISING PHYSICAL PROPERTIES OF M.E.
                C
0004                  MURO=8900.D0
0005                  MUE=14.459D10
0006                  SGRO=MURO/200.D0
0007                  SGE=MUE/1000.D0
0008                  D=0.0002D0
                C
                C (2) SIZE OF BAR IS INTRODUCED. BAR IS MADE OF SEVERAL BLOCKS OF M.E.
                C     L=ROW DIMENSION & M=COLUMN DIMENSION OF EACH BLOCK. N=NO OF BLOCKS
                C     OF MICRO ELEMENTS. L1= PRINT OUT REQ). AFTER CERTAIN BLOCKS OF M.E
                C
0009                  L=10
0010                  M=10
0011                  N=5000
0012                  L1=N/10
                C
                C (3)  GENERATOR & SEED VALYES ASSIGNED. 2 GEN. USED FOR GENERATING TWO
                C      DIFFERENT TYPES OF R.N. SO THAT TRAINS OF R.N. GENERATED
                C      BY DIFF. SEED & GENERATOR COMPENSATE EACH OTHER
                C
0013                   IR=1
0014                   IR1=1
0015                   K=5**13
0016                   K1=7**11
                C
                C (4) IK IS USED TO FILL UP VELOCITY & TIME STORAGE MATRIX AT DIFF. STN.
                C
0017                  IK=0
                C
                C (5) ASSIGNING PHYSICAL PROPERTIES TO 1ST BLOCK OF M.E.
                C
0018                  DO 1 I=1,L
0019                  DO 1 J=1,M
0020                  VIN(I,J)=1.D0
0021                  RO1(I,J)=MURO
0022                  E1(I,J)=MUE
0023                  C1(I,J)=DSQRT(MUE/MURO)
0024                  T(I,J)=D/C1(I,J)
0025             1    CONTINUE
                C
                C (6)  SIMULATION STARTS FROM HERE I.E.FROM 2ND BLOCK OF M.E.
                C
```

Fig. C-3 Simulation Program for a 3-D Model

```
FORTRAN IV G1  RELEASE 2.0              MAIN                DATE = 83064          13/35/41

0026                  DO 2 I1=2,N
                    C ..........  LOOP #2 GIVES NO OF BLOCKS OF M.E.INVOLVED
                    C
                    C ----------  THE RANDOM PHYSICAL PROPERTIES (RO2 & E2)
                    C ----------  ARE GENERATED FROM 5**13 SEED FOR ODD NO. OF BLOCKS
                    C ----------  AND FROM 7**11 SEED FOR EVEN NO. OF BLOCKS
                    C
0027                  DO 3 I=1,L
0028                  DO 3 J=1,M
0029                  IF(I1/2*2.NE.I1) GO TO 4
0030                  CALL RAND(K1,IR1,N1,N2)
0031                  IF(I1/2*2.EQ.I1) GO TO 5
0032                4 CALL RAND (K,IR,N1,N2)
0033                5 RO2(I,J)=MURO+SGRO*N1
0034                  E2(I,J)=MUE+SGE*N2
0035                  C2(I,J)=DSQRT(E2(I,J)/RO2(I,J))
0036                  T(I,J)=T(I,J)+(D/C2(I,J))
0037                  KAPA=RO2(I,J)*C2(I,J)/RO1(I,J)/C1(I,J)
0038                  CTR=2/(1+KAPA)
0039                  VTR(I,J)=VIN(I,J)*CTR
0040                3 CONTINUE
                    C
                    C (7) ENERGY EXCHANGE AMONG MICRO ELEMENTS IN A BLOCK
                    C
                    C  *********  ASSIGNING VELOCITIES, TO OUTER M.E. OR SAY THE
                    C  *********  M.E. AT THE BOUNDARIES
                    C
0041                  DO 6 J=1,M
0042                  VN(1,J)=VTR(1,J)
0043                  VS(L,J)=VTR(L,J)
0044                6 CONTINUE
0045                  DO 7 I=1,L
0046                  VW(I,1)=VTR(I,1)
0047                  VE(I,M)=VTR(I,M)
0048                7 CONTINUE
                    C  ==========  CALCULTION OF VELOCITIES FOR INNER M.E. AFTER INTERACTION
0049                  DO 8 I=1,L
0050                  DO 8 J=1,M
0051                  IF((I.EQ.L).AND.(J.EQ.M)) GO TO 14
0052                  IF(J.EQ.M) GO TO 9
0053                  KAPAE=RO2(I,J+1)*C2(I,J+1)/RO2(I,J)/C2(I,J)
0054                  IF(I.EQ.L) GO TO 10
0055                9 KAPAS=RO2(I+1,J)*C2(I+1,J)/RO2(I,J)/C2(I,J)
0056                  IF(J.EQ.M) GO TO 11
0057               10 VE(I,J)=DSQRT(((VTR(I,J))**2)+(KAPAE*(VTR(I,J+1))**2))/(KAPAE+1))
0058                  IF(I.EQ.L) GO TO 12
0059               11 VS(I,J)=DSQRT(((VTR(I,J))**2)+(KAPAS*(VTR(I+1,J))**2))/(KAPAS+1))
0060                  IF(J.EQ.M) GO TO 13
0061               12 VW(I,J+1)=VE(I,J)
0062                  IF(I.EQ.L) GO TO 81
0063               13 VN(I+1,J)=VS(I,J)
0064               81 CONTINUE
0065                8 CONTINUE
                    C
```

Fig. C-3 Continued

```
FORTRAN IV G1  RELEASE 2.0              MAIN                    DATE = 83064          13/35/41

                      C  @@@@@2 INCIDENT VELOCITY CALCULATED FOR 2ND BLOCK OF M.E.
                      C
0066                  14      DO 15 I=1,L
0067                          DO 15 J=1,M
0068                          VIN(I,J)=DSQRT((VE(I,J)**2+VW(I,J)**2+VN(I,J)**2+VS(I,J)**2)/4.00)
0069                  15      CONTINUE
                      C
                      C (8)  UPDATING OF PHYSICAL PROPERTIES
                      C
0070                          DO 16 I=1,L
0071                          DO 16 J=1,M
0072                          RO1(I,J)=RO2(I,J)
0073                          C1(I,J)=C2(I,J)
0074                  16      CONTINUE
                      C
                      C   STORING OF VELOCITY AND TIME MATRIX(2DMATRIX) AFTER
                      C   EACH REQD. NO. OF BLOCKS
                      C
0075                          IF(I1/L1*L1.NE.I1) GO TO 2
0076                          IK=IK+1
0077                          DO 17 I=1,L
0078                          DO 17 J=1,M
0079                          VST(I,J,IK)=VIN(I,J)
0080                          TST(I,J,IK)=T(I,J)
0081                  17      CONTINUE
                      C  -------- LOOP #2 ENDS HERE ALSO MAIN PGM ENDS
0082                  2       CONTINUE
                      C
                      C(10) PRINTING OF VST & TST MATRIX
                      C
0083                          J1=M/5
0084                          IN=0
0085                          DO 18 IJ=1,IK
0086                          M1=0
0087                          M2=0
0088                          IN=IN+1
0089                          Z=IN
0090                  19      FORMAT(1H1,///,50X,'VELOCITY MATRIX AT STATION=',I2)
0091                  20      FORMAT(1H1,///,50X,'TIME MATRIX AT STATION=',I2)
0092                          DO 21 IL=1,J1
0093                          WRITE(6,19)IN
0094                          M1=M2+1
0095                          M2=M2+5
0096                          WRITE(6,22)((VST(I,J,Z),J=M1,M2),I=1,L)
0097                  21      CONTINUE
0098                          M1=0
0099                          M2=0
0100                          DO 23 IL=1,J1
0101                          M1=M2+1
0102                          M2=M2+5
0103                          WRITE(6,20) IN
0104                          WRITE(6,22)((TST(I,J,Z),J=M1,M2),I=1,L)
0105                  23      CONTINUE
0106                  18      CONTINUE
```

Fig. C-3 Continued

```
FORTRAN IV G1  RELEASE 2.0              MAIN                    DATE = 83064          13/35/41

0107          22    FORMAT(/,5X,5D22.12)
              C
              C  (11)  CALCULATION OF MEAN AND STD. DEV. OF VELOCITY
              C          AND TIME AT DIFF. STN.
              C
0108                IC=0
0109                DO 24 JK=1,IK
0110                IC=IC+1
0111                AV=0.D0
0112                SV=0.D0
0113                AT=0.D0
0114                ST=0.D0
0115                DO 25 I=1,L
0116                DO 25 J=1,M
0117                AV=AV+VST(I,J,IC)
0118                SV=SV+(VST(I,J,IC))**2
0119                AT=AT+TST(I,J,IC)
0120                ST=ST+(TST(I,J,IC))**2
0121          25    CONTINUE
0122                X1=L
0123                X2=M
0124                X=X1*X2
0125                AVS(JK)=AV/X
0126                SVS(JK)=DSQRT(SV/X-AVS(JK)**2)
0127                ATS(JK)=AT/X
0128                STS(JK)=DSQRT(ST/X-ATS(JK)**2)
0129          24    CONTINUE
0130                WRITE(6,26)
0131                WRITE(6,27)(AVS(I),SVS(I),ATS(I),STS(I),I=1,IK)
0132          26    FORMAT(1H1,///,26X,'MEAN VELOCITY',8X,'SIGMA VELOCITY',9X,'
             $MEAN TIME',8X,'SIGMA TIME',///)
0133          27    FORMAT(//,20X,4D22.12)
              C*****************************************************************
              C  PLOT OF P(V) & P(T) GRAPH
              C*****************************************************************
0134                READ(5,*) (Y(I),I=1,61)
0135                CALL GV(AVS,SVS,VST,Y,L,M)
0136                READ(5,*) (YT(I),I=1,61)
0137                CALL GT(ATS,STS,TST,YT,L,M)
0138                STOP
0139                END

 *OPTIONS IN EFFECT*  NOTERM,ID,EBCDIC,SOURCE,NOLIST,NODECK,LOAD,NOMAP,NOTEST
 *OPTIONS IN EFFECT*  NAME = MAIN     , LINECNT =       56
 *STATISTICS*    SOURCE STATEMENTS =      139,PROGRAM SIZE =   175904
 *STATISTICS*  NO DIAGNOSTICS GENERATED
```

Fig. C-3 Continued